

ACTIONS OF ISOVALINE AND ENDOGENOUS AMINO ACIDS ON INHIBITORY  
RECEPTORS IN VENTROBASAL THALAMUS

by

JAMES EDWARD COOKE

BSc, Carleton University, 2002  
MSc, Carleton University, 2004

A THESIS SUBMITTED IN PARTIAL FULFILMENT OF THE REQUIREMENTS  
FOR THE DEGREE OF

DOCTOR OF PHILOSOPHY

in

THE FACULTY OF GRADUATE STUDIES

(Pharmacology)

THE UNIVERSITY OF BRITISH COLUMBIA  
(Vancouver)

August, 2010

© James Edward Cooke, 2010

## ABSTRACT

This thesis consists of three manuscripts that examine the effects of amino acids and inhibitory neurotransmission in ventrobasal thalamus, a region of the brain responsible for processing nociceptive information. In the first manuscript we examined the possibility that a proposed antagonist of receptors for endogenous amino acids was selective for  $\beta$ -amino acids. In the second manuscript, we determined the ionic mechanism of action of isovaline, a non-biogenic amino acid with chemical similarity to glycine and GABA. In the third manuscript, we determined that the inhibitory action of isovaline is mediated by metabotropic receptors, likely GABA<sub>B</sub>.

In the first manuscript we used whole-cell patch clamp electrophysiology and immunohistochemistry to examine the differential antagonism of GABA<sub>A</sub>ergic IPSCs by a proposed  $\beta$ -amino acid antagonist, TAG. In IPSCs that were attributable to both GABAergic and glycinergic stimulation, TAG significantly reduced both components. TAG had no effect in purely GABA<sub>A</sub>ergic IPSCs. Our data supports the hypothesis that a specific GABA<sub>A</sub> subunit,  $\alpha 4$ , is sensitive to the  $\beta$ -amino acid antagonist, TAG.

The second manuscript examines the ionic mechanism of action of isovaline, demonstrated to have analgesic properties in animal models. Isovaline inhibited action potential firing of thalamocortical neurons by activating a long-lasting potassium conductance that was insensitive to the glycine antagonist, strychnine. The sensitivity of isovaline currents to K<sup>+</sup> channel blockers, their reversal near  $E_K$  and Nernstian behavior

on changing the extracellular  $[K^+]$  confirmed  $K^+$  current involvement in isovaline inhibition.

Since glycine receptors were not apparently involved in isovaline action, we proceeded to determine whether the actions of isovaline were mediated by a metabotropic receptor. In the third manuscript we showed that the long-lasting inhibition of isovaline was eliminated by preventing activation of G-proteins and by antagonism of  $GABA_B$  receptors. Alteration of  $GABA_B$  receptor function by CGP7930, an allosteric  $GABA_B$  modulator, resulted in a potentiation of isovaline's actions, and the current-voltage relationship of isovaline was similar to that of baclofen, a  $GABA_B$  agonist. However isovaline also had actions that were different from baclofen. For example, isovaline increased a transient 'A-type' potassium current and did not activate some neurons that responded to baclofen.

## TABLE OF CONTENTS

ABSTRACT .....	ii
TABLE OF CONTENTS .....	iv
LIST OF TABLES .....	viii
LIST OF FIGURES .....	ix
LIST OF ABBREVIATIONS .....	x
ACKNOWLEDGEMENTS .....	xii
DEDICATION .....	xiii
CO-AUTHORSHIP STATEMENT .....	xiv
1. GENERAL INTRODUCTION .....	1
1.1 Scope of thesis .....	1
1.2 Background.....	3
1.2.1. Ventrobasal thalamic nuclei .....	3
1.2.2. Inhibitory neurotransmitter receptors .....	5
1.2.2.1. GABA <sub>A</sub> receptors .....	5
1.2.2.2. Glycine receptors .....	9
1.2.2.3. GABA <sub>B</sub> receptors.....	11
1.2.3. Isovaline.....	15
1.3. Overview and objectives.....	16
1.4 References.....	22
2. FIRST MANUSCRIPT: EFFECTS OF THE $\beta$ -AMINO ACID ANTAGONIST TAG ON THALAMOCORTICAL INHIBITION .....	36
2.1. Introduction.....	36
2.2. Methods .....	39
2.2.1. Animals and slice preparation .....	39
2.2.2. Tissue preparation and immunocytochemistry.....	39
2.2.3. Imaging and quantification .....	40
2.2.4. Electrophysiological recording .....	41
2.2.5. Current clamp data analysis.....	42
2.2.6. IPSC classification and analysis .....	42
2.2.7. Drugs.....	43
2.2.8. Statistical analysis.....	44
2.3. Results .....	44
2.3.1. Co-localization of GABA <sub>A</sub> $\alpha_4$ subunits and glycine receptors with inhibitory nerve terminals.....	44
2.3.2. TAG effects on membrane properties.....	46
2.3.3. Effects on mixed IPSCs .....	46
2.3.4. Concentration-response relationship .....	48
2.3.5. Effects on mixed IPSC components with isolated decay kinetics .....	49
2.3.6. Effects on pure GABA <sub>A</sub> ergic and glycinergic IPSCs.....	50
2.4. Discussion .....	51
2.5. References.....	66

3. SECOND MANUSCRIPT: ISOVALINE CAUSES INHIBITION BY INCREASING POTASSIUM CONDUCTANCE IN THALAMIC NEURONS .....	73
3.1 Introduction.....	73
3.2 Experimental procedures .....	74
3.2.1. Tissue preparation for immunohistochemistry .....	74
3.2.2. Slice preparation for electrophysiology.....	75
3.2.3. Electrophysiology.....	76
3.2.4. Drugs.....	77
3.2.5. Data analysis.....	77
3.3. Results .....	78
3.3.1. Effects of R-isovaline on evoked firing in ventroposterolateral neurons .....	78
3.3.2. Mechanism of inhibitory action on evoked firing .....	79
3.3.3. Effects on membrane properties .....	79
3.3.4. Dose-response relationship.....	80
3.3.5. Current-voltage (I-V) relationship for isovaline action .....	80
3.3.6. Identifying the ionic basis for isovaline inhibition.....	81
3.3.7. Effects of altering extracellular $K^+$ concentration on $E_{R-Iva}$ .....	82
3.4. Discussion.....	84
3.5. References.....	100
4. THIRD MANUSCRIPT: METABOTROPIC RECEPTORS FOR THE NOVEL AMINO ACID ISOVALINE .....	103
4.1. Introduction.....	103
4.2. Methods .....	105
4.2.1. Slice preparation .....	105
4.2.2. Electrophysiology .....	105
4.2.3. Drugs.....	106
4.2.4 Data analysis .....	107
4.2.5. Tissue preparation for immunohistochemistry .....	108
4.3. Results .....	109
4.3.1. Immunocytochemistry in ventrobasal thalamus .....	109
4.3.2. Isovaline effects on bath and local applications .....	110
4.3.3. Isomer-specific actions of isovaline .....	111
4.3.4 Comparison to baclofen, GABA <sub>B</sub> agonist .....	111
4.3.5. Outward currents are activated by isovaline, not baclofen.....	112
4.3.6. Absence of extracellular $Ca^{2+}$ does not alter isovaline action .....	113
4.3.7. Potential involvement of GABA <sub>B</sub> receptors .....	113
4.3.8. Dissimilarities to baclofen .....	115
4.4. Discussion.....	115
4.4.1. GABA <sub>B</sub> agonist-like actions .....	116
4.4.2. Pharmacological properties consistent with GABA <sub>B</sub> agonism.....	116
4.4.3. G-protein dependency and role of GIRK channels.....	117
4.4.4. Unique actions of isovaline .....	118
4.5. References.....	136

5. GENERAL DISCUSSION.....	142
5.1. TAG actions on IPSCs of VB thalamus: GABA <sub>A</sub> $\alpha$ 4 and glycine receptor co-localization.....	142
5.1.1. Implications of GABA <sub>A</sub> $\alpha$ 4-glycine co-localization .....	145
5.1.2. Future studies.....	145
5.1.2.1 GABA <sub>A</sub> $\alpha$ 4 subunit: site of action of TAG?.....	145
5.1.2.2. Developmental switch from synaptic to extrasynaptic? .....	146
5.2. Isovaline: actions of an analgesic amino acid.....	147
5.3. Isovaline: possible mechanisms of action.....	151
5.3.1. Isovaline actions mediated by GABA <sub>B</sub> receptors.....	152
5.3.1.1. Proposed sites of isovaline action: extracellular loci.....	153
5.3.1.1.1. Isovaline may increase release of GABA from surrounding cells .	153
5.3.1.1.2. Isovaline may bind to the LIV-BP of GABA <sub>B1</sub> subunits with high affinity, preventing the ‘fly-trap’ from re-opening .....	153
5.3.1.1.3. Isovaline may cause conformational changes in GABA <sub>B</sub> receptors that confer constitutive activity .....	155
5.3.1.2. Proposed sites of isovaline action: intracellular loci .....	156
5.3.1.2.1. Isovaline may inhibit the GTPase activity of the G $\alpha$ subunit .....	156
5.3.1.2.2. Isovaline may inhibit regulators of G-protein signalling proteins..	157
5.3.1.2.3. Isovaline may interfere with normal function of intracellular tyrosine kinases.....	159
5.3.1.2.4. Isovaline may inhibit NSF proteins .....	161
5.3.2. Isovaline actions mediated by another G-protein coupled receptor .....	162
5.4. Future studies.....	163
5.4.1. Synaptic actions of isovaline .....	164
5.5. Implications of isovaline action.....	165
5.6. References.....	169

#### APPENDIX A: IMMUNOHISTOCHEMICAL IDENTIFICATION OF THE ANCHORING PROTEIN

GEPHYRIN IN VENTROBASAL THALAMUS.....	180
Brief background .....	180
Methods .....	180
Immunohistochemistry .....	180
Results .....	181
References.....	183

#### APPENDIX B: LIMITATIONS OF QUANTUM DOTS AS FLUOROPHORES FOR VISUALIZING

RECEPTORS IN TISSUE.....	184
Brief background .....	184
Methods .....	184
Tissue preparation.....	184
Immunohistochemistry .....	185
Immunohistochemistry on living slices .....	186
Physical dissociation of thalamocortical neurons.....	187
Results .....	187

Quantum dots: methodological limitations to visualization of receptor trafficking in living brain slices .....	187
Quantum dots: methodological limitations to visualization in fixed, frozen tissue	188
Quantum dots: detectable using the experimental setup.....	189
Quantum dots: only on dissociated cells .....	190
References.....	199
APPENDIX C: IMMUNOHISTOCHEMISTRY TO IDENTIFY GABA <sub>B</sub> RECEPTORS IN THE EPIDERMIS OF THE MOUSE HIND-PAW .....	200
Brief background .....	200
Methods .....	200
Tissue preparation.....	200
Immunohistochemistry .....	200
Results .....	201
Immunocytochemistry of GABA <sub>B</sub> receptors in the epidermis of the mouse hind-paw .....	201
APPENDIX D: ANIMAL CARE CERTIFICATE.....	206

## LIST OF TABLES

Table 2.1. Effects of TAG (250 $\mu\text{M}$ ) on passive properties. ....	64
Table 2.2. Effects of TAG (250 $\mu\text{M}$ ) on the fit parameters for IPSC components.....	65
Table 3.1. R-isovaline (25 $\mu\text{M}$ – 250 $\mu\text{M}$ ) did not alter properties of action potentials evoked by depolarizing current pulses. ....	99
Table 4.1: Effects of receptor antagonists on the conductance increase caused by 75 $\mu\text{M}$ R-Iva..	135

## LIST OF FIGURES

Figure 1.1. Schematic representation of the GABA <sub>B</sub> receptor. ....	19
Figure 1.2. Chemical structures of isovaline (R-isomer), glycine and GABA.....	21
Figure 2.1. Co-localization of synaptic glycine and GABA <sub>A</sub> $\alpha$ 4-containing receptors in VPL.....	55
Figure 2.2. Comparison of effects of TAG with strychnine and bicuculline on mixed IPSCs. ....	57
Figure 2.3. Effects of TAG on voltage-dependence and reversal potentials of mixed IPSCs. ....	58
Figure 2.4. TAG concentration-response curve and partially V <sub>h</sub> = -80 mV reversible antagonism of mixed IPSCs. ....	59
Figure 2.5. Effects of TAG on kinetically resolved components of mixed IPSCs.....	60
Figure 2.6. Effects of TAG at 250 $\mu$ M on pure GABAergic and glycinergic IPSCs. ..	62
Figure 3.1. Isovaline inhibited action potential and low threshold spike (LTS) firing in neurons by actions independent of glycineA receptors. ....	88
Figure 3.2. Increased conductance shunted genesis of action potential and LTS. ....	90
Figure 3.3. Increased input conductance in voltage-clamp caused persistent hyperpolarization and was concentration-dependent.....	91
Figure 3.4. Current-voltage (I/V) relationships during isovaline administration showed reversal near E <sub>K</sub> , dissimilar to glycine.....	93
Figure 3.5. Extracellular K <sup>+</sup> channel blockers prevented isovaline actions on voltage-dependent currents. ....	95
Figure 3.6. Intracellular K <sup>+</sup> channel blockade with Cs <sup>+</sup> prevented isovaline action. ....	96
Figure 3.7. Isovaline did not alter I <sub>h</sub> . ....	98
Figure 4.1. GABA <sub>B1</sub> and GABA <sub>B2</sub> receptor subunits are present in ventrobasal thalamus. ....	121
Figure 4.2. Somata show more labelling for B1 subunits than for B2 subunits. ....	123
Figure 4.3. Bath application of isovaline inhibits action potential firing by causing a persistent increase in membrane conductance.....	125
Figure 4.4. Steady-state current-voltage relationships for isovaline and baclofen are similar. ....	126
Figure 4.5. Isovaline and baclofen differ in their effects on peak and steady state outward currents. ....	128
Figure 4.6. Potential involvement of GABA <sub>B</sub> receptors in isovaline responses. ....	129
Figure 4.7. Isovaline actions require G-protein activation. ....	131
Figure 4.8. Isovaline and baclofen may activate different receptors. ....	133
Figure 5.1. Potential sites of isovaline action. ....	167
Figure A.1. Gephyrin is found throughout the ventrobasal thalamus. ....	182
Figure B.1. Quantum dots (Qdots) do not work in live brain slices.....	192
Figure B.2. Quantum dots (Qdots) do not work on fixed, frozen tissue. ....	195
Figure B.3. The experimental setup used is able to visualize Quantum Dots (Qdots)..	197
Figure B.4. Quantum dots are able to visualize glycine receptors in dissociated cells. ....	198
Figure C.1. GABA <sub>B</sub> receptors are present in the epidermis of the mouse foot pad. ....	203

## LIST OF ABBREVIATIONS

5-HT <sub>1A</sub>	5-Hydroxytryptamine, receptor 1A.
aCSF	Artificial Cerebrospinal Fluid
AIB	Aminoisobutyrate
ANOVA	Analysis of Variance
ATF4	Activating Transcription Factor 4
BAPTA	1,2-bis(o-aminophenoxy)ethane-N,N,N',N'-tetraacetic acid
BSA	Bovine Serum Albumin
cAMP	Cyclic Adenosine Monophosphate
DAPI	4',6-diamidino-2-phenylindole
DMSO	Dimethyl Sulfoxide
EGTA	ethylene glycol tetraacetic acid
GABA	$\gamma$ -Aminobutyric Acid
GDP	Guanosine Diphosphate
GIRK	G Protein-Coupled Inwardly-Rectifying Potassium Channel
GPRC6A	Family C G-Protein-Coupled Receptors
GTP	Guanosine Triphosphate
HEPES	4-(2-hydroxyethyl)-1-piperazineethanesulfonic acid
ICC	Immunocytochemistry
IPSC	Inhibitory Postsynaptic Currents
LTS	Low-Threshold Calcium Spikes
KCC2	Potassium-Chloride Co-transporter, isoform 2
KCC3	Potassium-Chloride Co-transporter, isoform 3

KCTD	Potassium Channel Tetramerization Domain
LIV-BP	Leucine-Isoleucine-Valine Binding Protein
MAP-2	Microtubule-Associated Protein 2
NKCC1	Sodium-Potassium-Chloride Co-transporter, isoform 1
nRT	Nucleus Reticularis Thalami
NSF	<i>N</i> -Methylmaleimide-Sensitive Factor
PBS	Phosphate-Buffered Saline
PKA	Protein Kinase ‘A’
QDot	Quantum Dot
RGS	Regulators of G-protein Signalling
SEM	Standard Error of the Mean
Src	Family of Non-Receptor Tyrosine Kinases (from “Sarcoma”)
TAG	6-aminomethyl-3-methyl-4H-1,2,4-benzothiadiazine-1,1-dioxide, (Taurine Antagonist)
TREK	TWIK-Related K <sup>+</sup> Channels
TTX	Tetrodotoxin
VB	Ventrobasal
VGAT	Vesicular GABA Transporter
VPL	Ventral Posterolateral
VPM	Ventral Posteromedial

## ACKNOWLEDGEMENTS

### Academic

First to Dr. Ernie Puil and Dr. David Mathers, who took a chance on an outcast student. I sincerely appreciate all of your help and guidance. I never felt that I was a subordinate, but rather a colleague, a peer. Working in this group has been challenging, exciting, and intriguing. It has been a pleasure.

Thank you to Dr. Bernard MacLeod for being on my supervisory committee, for interesting conversations, and for luring me into the world of isovaline.

Thank you to Dr. David Fedida for chairing many meetings and for helpful input.

Thank to Viktoriya Dobrovinska for all of her technical help and teaching me a few of the more important Russian words.

Thank you to Dr. Seung-Ha Oh for help with Quantum Dots, and for sharing kimchi.

Thank you to Joanne Leung for her help with Quantum Dot experiments.

Thank you to former and current graduate students in the Puil/Mathers/MacLeod group, including: AG, SM, SL, JW, CC, KA, RW, and KP, for help, guidance, meaningful conversations and even more meaningful distractions.

Thank you to Dr. Igor Putrenko for technical help and even more Russian lessons.

Thank you to other APT staff and faculty for helping me out at various times in various ways, including Dr. Stephanie Borgland, Andy Jeffries, Marnie Bymak, and Wynne Leung.

A huge thank you to Dr. Shernaz Bamji for all her help with the confocal imaging.

Thank you to Dr. Shawn Mansfield for help with NMR.

Thank you to Dr. Jane Roskams for teaching me to believe in myself and the value of a well-controlled experiment.

Thank you to former Roskams-ites, including: NJ, EC, EA, MR, JM, BM, KW, AM.

Thank you to Dr. Carol Pollock and the Zoology Department for employing me for so many years. I have gained invaluable teaching experience which will serve me well going forward. And it was fun.

Thank you to Dr. Jack B. Kelly of Carleton University, for instilling an interest in basic research, allowing to me run amok in his research lab, and support.

Thank you to Dr. Huiming Zhang of the University of Windsor for guidance and for teaching me how to perform *in vivo* electrophysiology.

Thank you to Dr. Shu Hui Wu and Dr. Tarun Ahuja of Carleton University for teaching me whole-cell patch clamp electrophysiology.

### Personal

Thank you so much to my wife, Lisa, who stands by me no matter what her better judgement would suggest. You make every day worth living.

To my boy, Colin, who is quite simply the greatest thing that has ever happened in the history of the universe.

To my family, especially my parents, Joe and Debbie, for always being supportive in every way.

To my in-laws, especially Karen, for going out of their way to help our family.

To my extended family for always being proud and supportive.

## **DEDICATION**

For my family.

“It was my understanding that there would be no math”

- Actor Chevy Chase as then-President of the United States, Gerald Ford.  
Saturday Night Live, 1976.

## **CO-AUTHORSHIP STATEMENT**

My contributions to the first manuscript were the immunohistochemistry experiments, and all design, conducting, analysis and writing associated with it. Ms. Sarah McCarthy and Dr. Ahmed Ghavanini conducted electrophysiological experiments. In collaboration with Sarah McCarthy, Drs. David Mathers and Ernie Puil co-designed the experiments, co-analysed data and co-wrote the manuscript.

My contribution to the second manuscript was in the design, conducting, and analysing all experiments and co-writing the manuscript. Drs. David Mathers and Ernie Puil co-designed experiments and co-wrote the manuscript.

With supervision from Drs. Ernie Puil and David Mathers, my contribution to the third manuscript was in the design, conducting, and analysing all experiments and co-writing the manuscript.

My contributions to chapters 3 and 4 were substantially more than my contribution to the first manuscript, and formed the major portion of my PhD work. For this reason, sections of this thesis dedicated to general introduction and discussion will focus on information relevant to the latter two manuscripts (i.e., isovaline action and GABA<sub>B</sub> receptors).

## 1. GENERAL INTRODUCTION

### **1.1 Scope of thesis**

This thesis consists of three manuscripts that examine the effects of amino acids and inhibitory neurotransmission in ventrobasal (VB) thalamus, a region of the brain responsible for processing somatosensory information, including nociception (Potes et al., 2006a). The first manuscript of this thesis examines the action of an antagonist for amino acid receptors in VB thalamus, implicating that blockade of inhibitory amino acid neurotransmitters varies with the subunit composition of the receptor. In the second manuscript, we examine the ionic mechanism of action of isovaline, an analgesic amino acid that is a structural analog of glycine and  $\gamma$ -aminobutyric acid (GABA), on neurons of VB thalamus. The third and final manuscript examines whether the action of isovaline on thalamocortical neurons is receptor-mediated. The implications of these manuscripts are discussed in the General Discussion.

In the first manuscript, we examine inhibitory synaptic input into VB thalamus using an antagonist of inhibitory amino acid receptors, TAG (taurine antagonist, 6-aminomethyl-3-methyl-4H-1,2,4-benzothiadiazine-1,1-dioxide). Earlier reports from our laboratory have shown that there are different decay kinetics of inhibitory postsynaptic currents (IPSCs) in VB thalamus (Ghavanini et al., 2006). We speculated that the heterogeneity of IPSC kinetics observed by Ghavanini et al. (2006) was due to activation of glycine receptors by glycine and  $\beta$ -amino acids (taurine and  $\beta$ -alanine). To examine this hypothesis, we use the amino acid antagonist TAG on identified glycinergic and GABA<sub>A</sub>ergic IPSCs. We were surprised to find that TAG had different effects on

glycinergic and GABA<sub>A</sub>ergic IPSCs. TAG reduced the glycinergic component in both pure and mixed IPSCs, but it only antagonized the GABA<sub>A</sub>ergic component of mixed IPSCs, not purely GABA<sub>A</sub>ergic IPSCs. We believed that this difference of GABA<sub>A</sub>ergic transmission was due to subunit composition differences of pure versus mixed IPSCs. We used immunohistochemistry to support the idea that GABA<sub>A</sub>  $\alpha$ 4 subunits were associated with glycine receptors and likely led to mixed IPSCs, while pure IPSCs were likely a result of action on GABA<sub>A</sub>  $\alpha$ 1 subunits. GABA<sub>A</sub> receptors with the  $\alpha$ 4 subunit may be responsible for TAG's antagonistic effects on the GABA<sub>A</sub>ergic component of mixed IPSCs. These results suggest that specific receptor subunits may provide targets for pharmacological tools designed to treat pain.

The second manuscript sought to identify the ionic mechanism of action of isovaline, an analgesic amino acid that is a structural analog of glycine and  $\gamma$ -aminobutyric acid (GABA), on neurons of VB thalamus. We used whole-cell patch clamp electrophysiology to identify the actions of bath-applied isovaline, measuring changes in input conductance and membrane potential, as well as current-voltage relationships, to identify which ion(s) were involved in the response. Using pharmacological blockers we confirmed a role for potassium in isovaline action.

Based on the long-lasting effects of isovaline, in the third manuscript we believed that the actions of isovaline on thalamocortical neurons were due to metabotropic receptor activation. Using whole-cell electrophysiology and pharmacological tools, we provide evidence that isovaline actions are mediated by a metabotropic receptor, possibly

GABA<sub>B</sub>. However, isovaline does not behave as an agonist at GABA<sub>B</sub> receptors; namely, it activates a persistent conductance change that increases on washout of the compound. It also does not activate all GABA<sub>B</sub> expressing neurons.

In summary, the first manuscript supports the idea that the heterogeneous antagonism by TAG of GABA<sub>A</sub>ergic IPSCs is due to the subunit composition of GABA<sub>A</sub> receptors in VB thalamus. The second manuscript shows that the novel analgesic amino acid isovaline inhibits thalamocortical neurons by activating a long-lasting potassium conductance. The third and final manuscript provides evidence that isovaline's actions are mediated by a metabotropic receptor, likely GABA<sub>B</sub>, although some of its actions are different from the GABA<sub>B</sub> agonist, baclofen.

## **1.2 Background**

### **1.2.1. Ventrobasal thalamic nuclei**

The ventrobasal (VB) thalamic complex is located in the dorsal thalamus, in the diencephalon of mammals (Jones, 1985). The VB complex is the principal thalamic centre for the processing of somatosensory information (Sherman, 2005). VB thalamus is composed of two nuclei, the ventral posterolateral (VPL) and ventral posteromedial (VPM) nuclei (Jones, 1985). This distinction is made primarily on the afferent input to each nucleus. The VPM nucleus receives input predominantly from the head and neck regions by way of the trigeminal nerve (Abe, 1978). The VPL receives input predominantly from the body via the medial lemniscus and spinothalamic tract (Applebaum *et al.*, 1979). The sizes of the nuclei vary according to the amount of

innervation density from the two regions. For example, in rodents that have whiskers on their face for sensing tactile information, the VPM tends to dominate (Jones, 1985).

There are two classes of neurons in VB thalamus, thalamocortical relay neurons and inhibitory interneurons. Thalamocortical neurons project outside the thalamus to the cortex (Yen and Jones, 1983), and have a characteristic burst firing mediated by low-threshold calcium spikes (LTSs), common to all thalamocortical neurons (Pape and McCormick, 1995). This feature endows thalamocortical neurons with the ability to have tonic and burst firing modes. Tonic firing occurs when the membrane potential is relatively depolarized which inactivates the LTS (Pape and McCormick, 1995). Upon depolarizing input, the neuron displays tonic firing of action potentials with approximately equally spaced interspike intervals. Burst firing occurs when the membrane potential of a neuron is hyperpolarized and is due to de-inactivation of LTSs. Upon depolarization, calcium channels open which causes an LTS and bursting of sodium-dependent action potentials on top of the slower calcium-mediated LTS (Weyand et al., 2001). Inhibitory interneurons lack this LTS burst firing (Turner et al., 1997), and are very few in number in VB thalamus of the rat (i.e., 0.4% of all cells; Harris and Hendrickson, 1987).

Nuclei of VB thalamus project to Brodmann's areas 1, 3, 4, 5 and 6 in the somatosensory cortex of the rat (Herkenham, 1980). VB thalamus also receives input from the cortex, from corticothalamic neurons of layer VI of primary somatosensory cortex, which likely help shape responses of VB thalamocortical neurons (Alitto and Usrey, 2003).

The nucleus reticularis thalami (nRT) is a major source of inhibition to VB thalamus. It surrounds the rostral aspect of VB thalamus and contains mostly GABAergic interneurons (Jones, 1985). The nRT receives input from both VB thalamus as well as cortex and when excited, it releases GABA onto neurons of VB thalamus as well as other nuclei of dorsal thalamus (Gentet and Ulrich, 2003).

### **1.2.2. Inhibitory neurotransmitter receptors**

Three major inhibitory receptors, GABA<sub>A</sub>, glycine and metabotropic GABA<sub>B</sub> receptors, are present in VB thalamus (Roberts et al., 1992; Ghavanini et al., 2005; Ulrich and Huguenard, 1996). Each of these receptors has a prominent role as discussed in the manuscripts of this thesis.

#### 1.2.2.1. GABA<sub>A</sub> receptors

GABA<sub>A</sub>ergic inhibition in VB thalamus has been implicated in mediating neuropathic pain, epileptogenesis and anesthesia (Roberts et al., 1992; Huguenard and Prince, 1994, Wan et al., 2003). Under physiological conditions, GABA<sub>A</sub> receptors would hyperpolarize the neuronal membrane, lowering the membrane potential away from the threshold for firing tonic action potentials. Under these circumstances, thalamocortical neurons are more likely to produce burst firing upon depolarization. This burst firing may be responsible for establishing states of consciousness like sleep and anesthesia (Wan et al., 2003).

There are three types of receptor for GABA in the central nervous system, ionotropic GABA<sub>A</sub> and GABA<sub>C</sub> receptors, and metabotropic GABA<sub>B</sub> receptors (Kandel and

Seigelbaum, 2000). GABA<sub>A</sub> receptors are heteropentamers, which form a chloride channel (Kandel and Seigelbaum, 2000). While GABA<sub>A</sub> receptors generally contain two  $\alpha$ , two  $\beta$ , and one  $\gamma$  subunit, there are nineteen GABA<sub>A</sub> subunits available which combine to form the pentamer, including  $\alpha_{1-6}$ ,  $\beta_{1-3}$ ,  $\gamma_{1-3}$ ,  $\delta$ ,  $\epsilon$ ,  $\pi$ ,  $\theta$  or  $\rho_{1-3}$  (Steiger and Russek, 2004). The  $\beta$  subunit is responsible for conferring chloride selectivity to the receptor (Jensen et al., 2002). In addition to the subunit composition of a receptor, the order of the subunits is also important, as receptor modulation is possible at interfaces between receptor subunits (Wingrove et al., 1997).

The ligand-binding domain of GABA<sub>A</sub> receptors is on the  $\alpha$ -subunit, which is also the binding site of the antagonist bicuculline (Jensen et al., 2002). Differences in the type of  $\alpha$ -subunit can alter the sensitivity of the receptor to a ligand (Mohler et al., 1992). For example, the extrasynaptic  $\alpha 4$  subunit is known to be activated with greater efficacy by taurine than the  $\alpha 1$  subunit (Jia et al., 2008). This implies that  $\beta$ -amino acids, such as taurine, might have a more prevalent role at maintaining tonic inhibition than in synaptic inhibition.

GABA<sub>A</sub>ergic and glycinergic IPSCs inhibit neurons by both hyperpolarizing the membrane potential of a neuron away from the threshold for action potential production, and by shunting excitatory input by increasing the conductance of the postsynaptic neuron. To effectively shunt incoming excitatory currents, inhibitory receptors are in high numbers at the proximal dendrites and soma (Kandel and Seigelbaum, 2000). This

allows activation of the inhibitory receptors to shunt excitatory input before the excitatory input reaches the axon hillock for action potential production.

Once activated by a ligand, GABA<sub>A</sub> receptors mediate inhibition by becoming permeable to chloride ions (Kandel and Seigelbaum, 2000). When these channels are open, negatively charged chloride ions flow across the membrane (D'Hulst et al., 2009). The functional consequence of activating a chloride current depends on the concentration gradient of chloride on either side of the membrane, as well as the chloride conductance. In adult animals, the concentration gradient of chloride is higher outside the neuronal membrane than inside (Blaesse et al., 2009), so that activation of the receptor leads to an inward movement of chloride, which hyperpolarizes the neuron. However, the chloride gradient is shifted in young animals, with lower concentrations of chloride outside the cell than there are in adults (Balakrishnan et al., 2003). This is an important distinction, as activation of GABA<sub>A</sub> receptors in younger animals leads to an efflux of chloride from the cell, and this inward current depolarizes the neuron.

The difference in chloride gradient between immature and mature animals is due to a developmental switch in the transport of chloride ions across the neuronal membrane (Blaesse et al., 2009). In young animals, transport of chloride into the neuron via NKCC1 transporters results in elevated intracellular chloride ions (Balakrishnan et al., 2003). However, in mature neurons KCC2 and KCC3 co-transporters become active in the cell membrane, which pump more chloride ions outside the cell, leading to lower chloride concentrations inside the neuronal membrane (Blaesse et al., 2006).

The magnitude and kinetics of IPSCs are determined, in part, by the number and kinetics of the single channels that give rise to the IPSCs. A greater number of activated channels leads to larger IPSCs (Sakmann, 1992). Similarly, the closing time of the single channels, in addition to diffusion of the ligand in the extracellular space, helps determine the decay rate of IPSCs, as slower single channel kinetics lead to slower rates of decay of IPSCs (Sakmann, 1992). For example, GABA<sub>A</sub> receptors containing the  $\alpha 4$  subunit are known to open for longer periods of time than those containing the  $\alpha 1$  subunit (Keramidas and Harrison, 2008).

The subunit composition of GABA<sub>A</sub> receptors varies depending on anatomical location (Pirker et al., 2000). Of relevance,  $\alpha 1$ ,  $\alpha 4$ ,  $\beta 2$ ,  $\gamma 2$  and  $\delta$  subunits are expressed abundantly in VB thalamus (Pirker et al., 2000). Fast, transient GABA<sub>A</sub>ergic responses occur due to activation of synaptic GABA<sub>A</sub> receptors containing  $\alpha 1/\beta 2/\gamma 2$  subunits (Farrar et al., 1999). GABA<sub>A</sub> receptors composed of  $\alpha 4/\beta 2/\delta$  subunits are more often located extrasynaptically, and mediate tonic inhibition (Jia et al., 2005). Upon repeated activation of inhibitory nerve terminals, spillover of GABA from the synapse would activate these extracellular receptors, hyperpolarizing the neuron. It is believed that the extrasynaptic location of  $\alpha 4/\beta 2/\delta$ -containing GABA<sub>A</sub> receptors is due to the  $\delta$  subunit (Jia et al., 2005).

The exact mechanism by which extrasynaptic GABA<sub>A</sub> receptors mediate tonic inhibition is not completely clear. Activation of these receptors most likely occurs due to spill-over

of GABA from synaptic release onto the postsynaptic neuron (Jia et al., 2005). Presumably, activation of these receptors would increase the conductance of the membrane, making it less sensitive to changes from excitatory input, effectively acting as a shunt. It was recently shown that activation of extrasynaptic GABA<sub>A</sub> receptors in CA1 hippocampal neurons results in changes to the threshold for firing an action potential and does not shunt excitatory input (Pavlov et al., 2009). This suggests that activation of extrasynaptic receptors reduces the likelihood of firing in the postsynaptic neuron by raising the threshold for action potential generation.

#### 1.2.2.2. Glycine receptors

The discovery of functional, inhibitory glycine receptors in ventrobasal thalamus expanded the early view that functional glycine receptors were only found in caudal regions of the neuraxis (Ghavanini et al., 2005). Interestingly, two types of glycinergic IPSCs, short and long, are observed in VB thalamus upon medial lemniscal stimulation (Ghavanini et al., 2006). The decay time constant of short IPSCs was 12 ms, while long IPSCs had a decay time constant of 80 ms. This matched the decay time constants from spontaneous IPSCs (Ghavanini et al., 2006). The inference of this study was that recordings were the result of two distinct receptor populations, slowly decaying  $\alpha 2$  subunit receptors and faster  $\alpha 1$  receptors.

Glycine receptors are heteropentamers that consist of  $\alpha$  and  $\beta$  subunits. The  $\alpha$  subunits are responsible for ligand-binding whereas the  $\beta$  subunits are responsible for trafficking the receptors to the synapse by interaction with the anchoring protein, gephyrin (Kirsch

and Betz, 1995). While it is possible to have functional glycine receptors that are homomeric for  $\alpha$  subunits (Kirsch and Betz, 1995), these are not strongly expressed in adult neurons and are considered to be extrasynaptic, due to the lack of the  $\beta$  subunit-gephyrin interaction (Lynch, 2009).  $\beta$  subunits are not capable of forming functional homomers (Bormann et al., 1993), likely because they are not able to bind a ligand (Lynch, 2009). The general stoichiometry of glycine receptors in mature neurons is either  $3\alpha$  and  $2\beta$  subunits (Grenningloh et al., 1987), or  $2\alpha$  and  $3\beta$  (Kuhse et al., 1993).

Four  $\alpha$  isoforms have been described,  $\alpha_{1-4}$ , in addition to a single  $\beta$  subunit (Lynch, 2009). The  $\alpha_1$  subunit is the most prevalent  $\alpha$  subunit in the adult brain, and the majority of functional, synaptic glycine receptors are believed to be composed of  $\alpha_1\beta$  heteromers (Lynch, 2009). The  $\alpha_2$  subunits are prevalent in young animals, with expression dropping substantially in adults (Becker et al., 1988). Conversely, expression of  $\alpha_1$  increases postnatally (Lynch, 2004). Expression of the  $\alpha_3$  subunit seems to be limited to nociceptive areas of the nervous system, such as in the spinal dorsal horn (Harvey et al., 2004). Indeed, mice lacking this specific subunit are immune to inflammatory pain caused by prostaglandin E2 (Harvey et al., 2004). Expression of  $\alpha_4$  appears to be restricted to the chick, as there is very little expression of the  $\alpha_4$  subunit in either rat or human (Harvey et al., 2000).

Antagonists for glycine receptors include strychnine and the chloride channel antagonist picrotoxin. Strychnine is a competitive antagonist at the ligand-binding site of the glycine receptor  $\alpha$  subunit (Lynch, 2004). Picrotoxin is an allosteric antagonist of both

GABA<sub>A</sub> and glycine receptors, although it is able to block more GABA<sub>A</sub> receptors than glycine receptors at lower doses (Lynch, 2004).

Along with GABA<sub>A</sub> receptors, glycine receptors are ionotropic receptors that are permeable to chloride ions upon activation. The developmental change in chloride ion gradient mentioned above has similar implications for glycine as for GABA<sub>A</sub> receptors. Activation of glycine receptors in juvenile animals leads to a depolarization of the neuronal membrane, whereas activation of glycine receptors in adult animals hyperpolarizes the membrane (Wang et al., 2005).

#### 1.2.2.3. GABA<sub>B</sub> receptors

GABA<sub>B</sub> receptors are heterodimers consisting of GABA<sub>B1</sub> and GABA<sub>B2</sub> subunits. Both subunits have seven transmembrane domains, and both have an extracellular region that is best modelled with a 'Venus flytrap' module in which the binding of the ligand results in closure of the two lobes of the extracellular domain (cf: Fig. 1.1; Galvez et al., 1999). The GABA<sub>B1</sub> subunit contains the agonist binding site, whereas the GABA<sub>B2</sub> subunit couples the receptor to G-proteins which inhibit adenylyl cyclase via G<sub>ai/o</sub> subunits (Hill, 1985; Kaupmann *et al.*, 1998; Galvez *et al.*, 1999). While the GABA<sub>B2</sub> subunit has a similar 'Venus flytrap' structure to GABA<sub>B1</sub>, this region of the GABA<sub>B2</sub> is not known to bind any ligand directly (Bettler and Tiao, 2006). Both subunits must heterodimerize in order to form a functional receptor (Kaupmann et al., 1998). The GABA<sub>B2</sub> subunit is required for trafficking of GABA<sub>B1</sub> to the cell membrane, as cells without GABA<sub>B2</sub> accumulate GABA<sub>B1</sub> in the endoplasmic reticulum (Kaupmann et al., 1998). While

GABA<sub>B2</sub> is able to be inserted into the cell membrane without GABA<sub>B1</sub>, it is not able to function as a receptor, likely due to its inability to bind ligands (Couve et al., 1998).

There are 2 known subtypes of GABA<sub>B1</sub> receptor, GABA<sub>B1a</sub> and GABA<sub>B1b</sub> (Bettler and Tiao, 2006). The only difference between the two subtypes is the presence of N-terminal protein interaction motifs called Sushi domains, which are involved in subcellular localization (Biermann et al., 2010). Specifically, the GABA<sub>B1a</sub> subtype is localized to axon terminals due to the presence of Sushi domains, while GABA<sub>B1b</sub> subtypes are not found in the presynaptic terminal due to the lack of Sushi domains (Biermann et al., 2010). While attempts have been made to identify pharmacologically distinct GABA<sub>B</sub> isoforms (Cunningham and Enna, 1996; Pham and Lacaille, 1996), these experiments have not been readily reproducible, are not supported by current molecular models (Bettler and Tiao, 2006). Therefore, the existence of pharmacologically distinct GABA<sub>B</sub> receptors is still a topic of debate.

Agonists of GABA<sub>B</sub> receptors include the endogenous ligand GABA, as well as baclofen (β-chlorophenyl GABA) which can be used to identify the presence of GABA<sub>B</sub> receptors (Bowery et al., 1980). These two ligands differ in their ability to activate the receptor in that GABA requires the presence of Ca<sup>2+</sup> ions to effectively stimulate the receptor, while baclofen does not (Galvez et al, 2000b). Positive allosteric modulators of GABA<sub>B</sub> include GS39738 and CGP7930, which bind to the heptathelical domain of the GABA<sub>B2</sub> subunit and potentiate the responses of agonists that bind to the GABA<sub>B1</sub> subunit

(Urwyler et al., 2005). Several compounds antagonize GABA<sub>B</sub> receptor activation, including CGP35348 and CGP52432 (Urwyler et al., 2004).

Upon activation of the GABA<sub>B</sub> receptor, the G $\alpha$  protein changes its conformation, allowing it to exchange GTP for GDP (Brown and Sihra, 2008). This conformational change allows both G-protein subunits, G $\alpha$  and G $\beta\gamma$ , to activate their respective effector proteins (see: Fig. 1.1). The G $\beta\gamma$  subunit directly couples to G-protein-coupled inwardly rectifying K<sup>+</sup> (GIRK) channels, where it activates the channels (Bettler *et al.*, 2004). G $\beta\gamma$  also directly couples to calcium channels, which it closes (Callaghan et al., 2008).

Activation of GABA<sub>B</sub> receptors can also lead to increases in other potassium channels through second messenger cascades via the G $\alpha$  subunit (see below), including outwardly rectifying and leak K<sup>+</sup> channels (Saint *et al.*, 1990; Deng *et al.*, 2009).

The G $\alpha$  subunit inhibits adenylyl cyclase activity, which leads to reduced cyclic AMP concentrations and, as a result, lower PKA levels (Hill, 1985). This change in adenylyl cyclase activity leads to alterations of a variety of transcription factors (ATF4; Steiger et al., 2004) and kinases (Src; Diverse-Pierliussi et al., 1997; PKA, Couve et al., 2002).

Activation of the G-protein subunits is terminated by the endogenous GTPase activity of the G $\alpha$  subunit. Once GTP is exchanged for GDP, the G $\alpha$  re-associates with G $\beta\gamma$  to stop the actions of the G-protein. The GTPase activity of the G $\alpha$  subunit is modified by regulator of G-protein signalling proteins (RGS), which enhances both the rate of G-protein activation and inactivation (Fig. 1.1; Fowler et al., 2007).

GABA<sub>B</sub> receptors, and the channels they activate, are vulnerable to modification from many intracellular enzymes. Protein kinase A is involved in regulating desensitization of GABA<sub>B</sub> receptors. Increasing protein kinase A, which is reduced following GABA<sub>B</sub> activation, prevents GABA<sub>B</sub> receptor desensitization (Couve et al., 2002).

Desensitization via PKA involves internalization of the receptors, and phosphorylating a specific residue on the GABA<sub>B2</sub> subunit stabilizes the location of the receptor in the cellular membrane. Conversely, inhibition of *N*-methylmaleimide-sensitive factor (NSF) proteins, which are known to be associated with GABA<sub>B</sub> receptors, prevents GABA<sub>B</sub> receptor desensitization (Pontier et al., 2006). GABA<sub>B</sub> stimulation leads to activation of Src kinase (Diverse-Pierliussi et al., 1997). Src kinase can both increase (Yue et al., 2009; Gomes et al., 2008) and decrease (Fadool et al., 1997; Clayton et al., 2009) the magnitude of potassium currents activated by GABA<sub>B</sub> receptors, including outwardly rectifying I<sub>A</sub> (Gomes et al., 2008) and inwardly rectifying K<sub>IR</sub> channels (Yue et al., 2009).

Recently, it was revealed that GABA<sub>B</sub> receptors are tightly coupled to a subfamily of KCTD (potassium channel tetramerization domain-containing) proteins through the GABA<sub>B2</sub> subunit (Schwenk et al., 2010). These KCTD proteins were found to increase potency and accelerate onset and inactivation of GABA<sub>B</sub> receptors (Schwenk et al., 2010). The presence of particular KCTD proteins was described as a potential mechanism responsible for some of the pharmacologically distinct actions of GABA<sub>B</sub> receptors (Schwenk et al., 2010).

GABA<sub>B</sub> receptors are found on both pre- and post-synaptic membranes. When pre-synaptic, they can be autoreceptors or heteroreceptors, depending on whether they exist on inhibitory or excitatory terminals (Bettler and Tiao, 2006). Presynaptic GABA<sub>B</sub> receptors are believed to inhibit neurotransmitter release predominantly via inhibition of Ca<sup>2+</sup> influx into the presynaptic terminal (Mintz and Bean, 1993). The receptors coupled to K<sup>+</sup> channels may be less common at presynaptic sites (cf. Thompson and Gahwiler, 1992). Postsynaptic GABA<sub>B</sub> receptors are generally coupled to K<sup>+</sup> channels (Ulrich and Huguenard, 1996; Luscher et al., 1997).

Postsynaptically, GABA<sub>B</sub> receptors are found around the base of dendritic spines apposed to putative glutamatergic synapses (Kulik et al., 2002). In this way, it appears as though the role of postsynaptic GABA<sub>B</sub> receptors is to shunt excitatory postsynaptic potentials (Kulik et al., 2002; Bettler and Tiao, 2006). Presumably, their activation comes about as a result of spill-over of ambient GABA from GABAergic synapses (Bettler and Tiao, 2006).

### **1.2.3. Isovaline**

Isovaline is an  $\alpha$ -amino acid that is structurally similar to glycine, as well as GABA (Fig. 1.2). Isovaline is a non-biogenic amino acid that is found as a racemate in carbonaceous meteorites (Kvenvolden et al., 1971; Zhao and Bada, 1989). Isovaline is also found as part of an antibiotic peptide constructed by filamentous fungi (Bruckner et al., 2009; Raap et al., 2005). These fungi, which include genera *Emericellopsis* and *Trichoderma*, are able to synthesize peptaibiotic antibiotics, named because they are peptides that

contain aminoisobutyrate (AIB; Bruckner et al., 2009). These compounds, which can range from 4 to 19 amino acids in length, have the remarkable ability to form voltage-dependent ion channels within lipid bilayers (Condamine et al., 1998; Raap et al., 2005). These channels increase the permeability of the bacterial cell wall which may be responsible for their antibiotic action (Condamine et al., 1998). Although they are non-biogenic, isovaline and its structural analogue, AIB, are known to be actively transported by the gut into the bloodstream (cf: Christensen, 1962).

Recently, isovaline was shown to have antinociceptive properties (MacLeod et al., 2010). Intravenous administration of isovaline in mice reduced chronic phase 2 pain in a formalin foot test. Isovaline was also effective at countering phase 2 pain when administered intrathecally in mice. Isovaline had anti-allodynic properties after treatment with strychnine. There were very few side effects of isovaline (i.e.: no sedation, scratching, agitation, or motor impairment) compared to controls. Interestingly, the S-isomer of isovaline was the only isomer effective at treating acute phase 1 pain in the formalin foot test. The antinociceptive properties, combined with few side effects, suggest that isovaline may have the potential to be an effective analgesic agent.

### **1.3. Overview and objectives**

This thesis consists of three manuscripts that examine the effects of amino acids and inhibitory neurotransmission in ventrobasal thalamus. The first manuscript examines the actions of the  $\beta$ -amino acid antagonist, TAG, on pharmacologically identified IPSCs in VB thalamus, to test whether the heterogeneity of IPSC kinetics was due to activation of

glycine receptors by glycine and  $\beta$ -amino acids. Next, we examine the ionic action of isovaline to identify how this analgesic amino acid inhibits neurons of VB thalamus. Last, we look for a receptor-based action of isovaline to determine if the persistent action observed is due to activation of a metabotropic receptor.

Following the observation that functional glycine receptors exist in ventrobasal thalamus (Ghavanini et al., 2005), two types of glycinergic IPSCs were observed in VB thalamus upon medial lemniscal stimulation (Ghavanini et al., 2006). The results of the work suggested to us that the different responses were due to heterogeneity of the receptors. We used the amino acid antagonist TAG to determine whether heterogeneity of glycinergic IPSCs was due to activation by glycine versus activation by  $\beta$ -amino acids like taurine or  $\beta$ -alanine.

In the course of the TAG work, concurrent research on novel analgesic properties provided an impetus for studying the actions of isovaline on inhibitory neurotransmitters in ventrobasal thalamus. The basis for testing isovaline was related to its chemical similarity to glycine which presumably modulated inhibitory somatosensory transmission in VB thalamus via glycine receptors. Knowing that VB thalamus receives nociceptive input from the spinothalamic tract, and that VB thalamus has functional glycine receptors, we hypothesized that isovaline activated glycine receptors in VB thalamus in the second manuscript.

On investigating an ionic mechanism of isovaline action, we were surprised to discover that the inhibitory actions of isovaline did not involve an increase in chloride conductance and was insensitive to strychnine. Isovaline increased a long-lasting potassium conductance. Both  $\mu$ -opioid and GABA<sub>B</sub> receptors are involved in an anti-nociceptive role and are prominent in VB thalamus (Potes et al., 1996b). The long-lasting action of isovaline was reminiscent of a K<sup>+</sup>-activating metabotropic receptor. The structural similarity between isovaline and GABA led us to suspect that isovaline might be activating GABA<sub>B</sub> receptors, as dealt with in the third manuscript.

## Figures

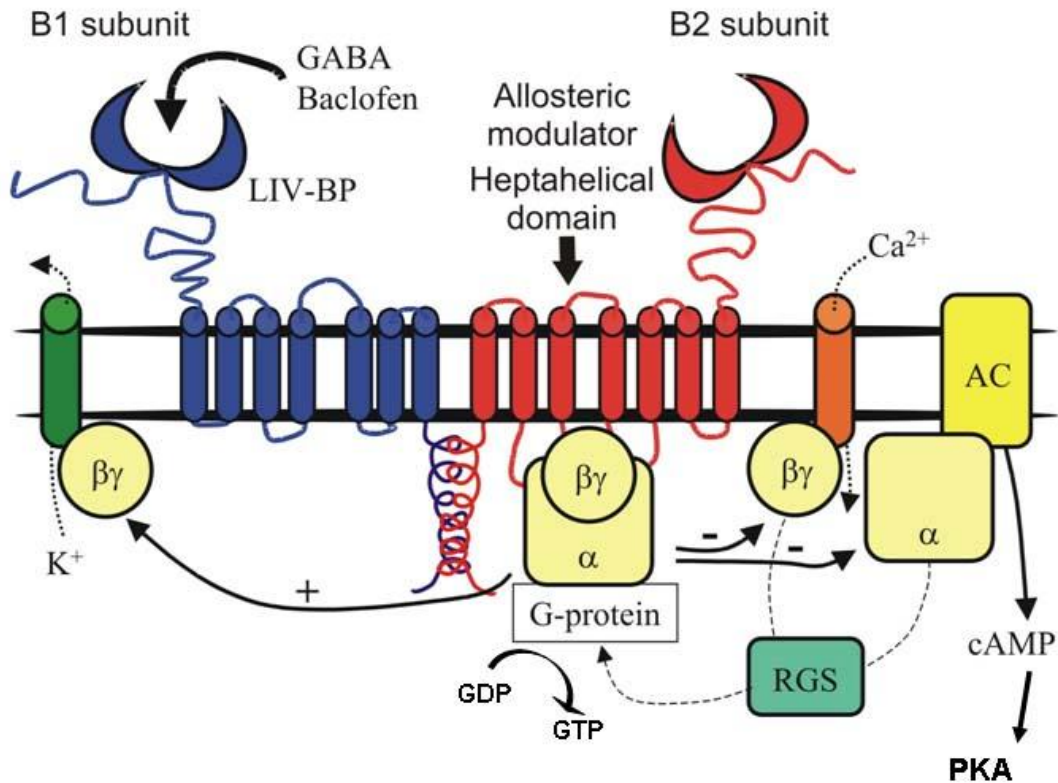


**Figure 1.1. Schematic representation of the GABA<sub>B</sub> receptor.** Binding of the ligand (GABA or Baclofen) to the 'Venus flytrap' region of the GABA<sub>B1</sub> subunit causes a conformational shift that either dissociates or alters the arrangement of Gα and Gβγ subunits by exchange of GDP for GTP at the Gα subunit. Free Gβγ subunits activate K<sup>+</sup> currents (indicated with +) as well as inhibit Ca<sup>2+</sup> channels (indicated with -). The free Gα subunit inhibits adenylyl cyclase (AC) (indicated with -), which results in lower cAMP levels, which drops PKA. The GTPase activity of Gα subunit is increased by Regulators of G-protein Signalling proteins (RGS). Once the Gα and Gβγ are re-associated, the actions of the receptor are terminated. GDP = guanosine diphosphate;

GTP = guanosine triphosphate; GABA =  $\gamma$ -aminobutyric acid; cAMP = cyclic adenosine monophosphate; PKA = protein kinase A. Figure adapted from Bowery and Smart, 2006.

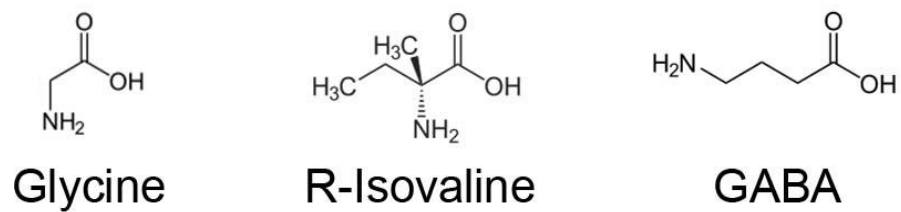


**Figure 1.2.** Chemical structures of isovaline (R-isomer), glycine and GABA (γ-amino butyric acid).

## **1.4 References**

Abe K. A study of sensory projection from jaw muscles to the cerebral cortex in the rat.

Jpn J Physiol. 28(3): 309-22. 1978.

Alitto HJ, Usrey WM. Corticothalamic feedback and sensory processing. Curr Opin

Neurobiol. 13(4):440-5. 2003.

Applebaum AE, Leonard RB, Kenshalo DR Jr, Martin RF, Willis WD. Nuclei in which functionally identified spinothalamic tract neurons terminate. J Comp Neurol.

188(4):575-85. 1979.

Balakrishnan V, Becker M, Löhrike S, Nothwang HG, Güresir E, Friauf E. Expression and function of chloride transporters during development of inhibitory neurotransmission in the auditory brainstem. J Neurosci. 23(10):4134-45. 2003.

Becker CM, Hoch W, Betz H. Glycine receptor heterogeneity in rat spinal cord during postnatal development. EMBO J. 7(12):3717-26. 1988.

Bettler B., Kaupmann K., Mossbacher J., Gassmann M. Molecular structure and physiological functions of GABA<sub>B</sub> receptors. Physiol Rev. 84: 835-867, 2004.

Bettler B., Tiao J.Y.-H. Molecular diversity, trafficking and subcellular localization of GABA<sub>B</sub> receptors. Pharmacol Ther. 110: 533-543, 2006.

Biermann B, Ivankova-Susankova K, Bradaia A, Abdel Aziz S, Besseyrias V, Kapfhammer JP, Missler M, Gassmann M, Bettler B. The Sushi domains of GABA<sub>B</sub> receptors function as axonal targeting signals. *J Neurosci.* 30(4):1385-94. 2010.

Blaesse P, Airaksinen MS, Rivera C, Kaila K. Cation-chloride cotransporters and neuronal function. *Neuron.* 61(6):820-38. 2009.

Bormann J, Rundström N, Betz H, Langosch D. Residues within transmembrane segment M2 determine chloride conductance of glycine receptor homo- and hetero-oligomers. *EMBO J.* 12(10):3729-37. 1993.

Bowery NG, Hill DR, Hudson AL, Doble A, Middlemiss DN, Shaw J, Turnbull M. (-)-Baclofen decreases neurotransmitter release in the mammalian CNS by an action at a novel GABA receptor. *Nature.* 283(5742):92-4. 1980.

Bowery N.G., Smart T.G. GABA and glycine as neurotransmitters: a brief history. *Br J Pharmacol.* 147: S109-S119, 2006.

Brown DA, Sihra TS. Presynaptic signaling by heterotrimeric G-proteins. *Handb Exp Pharmacol.* (184):207-60. 2008.

Brückner H, Becker D, Gams W, Degenkolb T. Aib and iva in the biosphere: neither rare nor necessarily extraterrestrial. *Chem Biodivers.* 6(1):38-56. 2009.

Callaghan B, Haythornthwaite A, Berecki G, Clark RJ, Craik DJ, Adams DJ. Analgesic alpha-conotoxins Vc1.1 and Rg1A inhibit N-type calcium channels in rat sensory neurons via GABA<sub>B</sub> receptor activation. *J Neurosci.* 28(43):10943-51. 2008.

Christensen H.N. Intestinal absorption with special reference to amino acids. *Gastroenterol.* 21: 37-42, 1962.

Clayton CC, Xu M, Chavkin C. Tyrosine phosphorylation of Kir3 following kappa-opioid receptor activation of p38 MAPK causes heterologous desensitization. *J Biol Chem.* 284(46):31872-81. 2009.

Condamine E, Rebuffat S, Prigent Y, Ségalas I, Bodo B, Davoust D. Three-dimensional structure of the ion-channel forming peptide trichorzianin TA VII bound to sodium dodecyl sulfate micelles. *Biopolymers.* 46(2):75-88. 1998.

Cooke J.E., Mathers D.A., Puil E. Isovaline causes inhibition by increasing potassium conductance in thalamic neurons. *Neurosci.* 164: 1235-1243, 2009.

Couve A, Filippov AK, Connolly CN, Bettler B, Brown DA, Moss SJ. Intracellular retention of recombinant GABA<sub>B</sub> receptors. *J Biol Chem.* 273(41):26361-7. 2002.

Cunningham MD, Enna SJ. Evidence for pharmacologically distinct GABA<sub>B</sub> receptors associated with cAMP production in rat brain. *Brain Res.* 720(1-2):220-4. 1996.

D'Hulst C, Atack JR, Kooy RF. The complexity of the GABA<sub>A</sub> receptor shapes unique pharmacological profiles. *Drug Discov Today.* 14(17-18):866-75. 2009.

Deng P.-Y., Xiao, Z., Yang, C., Rojanathammanee, L., Grisanti, L., Watt, J., Geiger, J.D., Liu, R., Porter, J.E., Lei, S. GABA<sub>B</sub> receptor activation inhibits neuronal excitability and spatial learning in the entorhinal cortex by activating TREK-2 K<sup>+</sup> channels. *Neuron* 63: 230-243, 2009.

Diversé-Pierluissi M, Remmers AE, Neubig RR, Dunlap K. Novel form of crosstalk between G protein and tyrosine kinase pathways. *Proc Natl Acad Sci U S A.* 94(10):5417-21. 1997.

Fadool DA, Holmes TC, Berman K, Dagan D, Levitan IB. Tyrosine phosphorylation modulates current amplitude and kinetics of a neuronal voltage-gated potassium channel. *J Neurophysiol.* 78(3):1563-73. 1997.

Farrar, S.J., Whiting, P.J., Bonnert, T.P., McKernan, R.M., 1999. Stoichiometry of a ligand-gated ion channel determined by fluorescence energy transfer. *J Biol Chem* 274(15): 10100-10104.

Fowler CE, Aryal P, Suen KF, Slesinger PA. Evidence for association of GABA(B) receptors with Kir3 channels and regulators of G protein signalling (RGS4) proteins. *J Physiol.* 580(Pt 1):51-65. 2007.

Galvez T., Parmentier M.-L., Joly C., Malitschek B., Kaupmann K., Kuhn R., Bittiger H., Froestl W., Bettler B., Pin J.-P. Mutagenesis and modeling of the GABA<sub>B</sub> receptor extracellular domain support a Venus flytrap mechanism for ligand binding. *J. Biol. Chem.* 274: 13362-13369, 1999.

Galvez T., Prezeau L., Milioti G., Franek M., Joly C., Froestl W., Bettler B., Bertrand H.-O., Blahos J., Pin J.-P. Mapping the agonist-binding site of GABA<sub>B</sub> type 1 subunit sheds light on the activation process of GABA<sub>B</sub> receptors. *J. Biol. Chem.* 275: 41166-41174, 2000a.

Galvez T., Urwyler S., Prezeau L., Mosbacher J., Joly C, Malischek B., Heid J., Brabet I., Froestl W., Bettler B., Kaupmann K., Pin J.P. Ca<sup>2+</sup> requirement for high-affinity  $\gamma$ -aminobutyric acid (GABA) binding at GABA<sub>B</sub> receptors: involvement of serine 269 of the GABA<sub>B</sub>R1 subunit. *Mol. Pharmacol.* 57: 419-426, 2000b.

Gentet LJ, Ulrich D. Strong, reliable and precise synaptic connections between thalamic relay cells and neurones of the nucleus reticularis in juvenile rats. *J Physiol.* 546(Pt 3):801-11. 2003.

Ghavanini, A.A., Mathers, D.A., Puil, E. Glycinergic inhibition in thalamus revealed by synaptic receptor blockade. *Neuropharmacology* 49, 338-349. 2005.

Ghavanini, A.A., Mathers, D.A., Kim, H.S., Puil, E. Distinctive glycinergic currents with fast and slow kinetics in thalamus. *J Neurophys.* 95, 3438-3448. 2006.

Gomes P, Saito T, Del Corso C, Alioua A, Eghbali M, Toro L, Stefani E. Identification of a functional interaction between Kv4.3 channels and c-Src tyrosine kinase. *Biochim Biophys Acta.* 1783(10):1884-92. 2008.

Grenningloh G, Rienitz A, Schmitt B, Methfessel C, Zensen M, Beyreuther K, Gundelfinger ED, Betz H. The strychnine-binding subunit of the glycine receptor shows homology with nicotinic acetylcholine receptors. *Nature.* 328(6127):215-20. 1987.

Herkenham M. Laminar organization of thalamic projections to the rat neocortex. *Science.* 207(4430):532-5. 1980.

Harris RM, Hendrickson AE. Local circuit neurons in the rat ventrobasal thalamus--a GABA immunocytochemical study. *Neuroscience.* 21(1):229-36. 1987.

Harvey RJ, Schmieden V, Von Holst A, Laube B, Rohrer H, Betz H. Glycine receptors containing the alpha4 subunit in the embryonic sympathetic nervous system, spinal cord and male genital ridge. *Eur J Neurosci.* 12(3):994-1001. 2000.

Harvey RJ, Depner UB, Wässle H, Ahmadi S, Heindl C, Reinold H, Smart TG, Harvey K, Schütz B, Abo-Salem OM, Zimmer A, Poisbeau P, Welzl H, Wolfer DP, Betz H, Zeilhofer HU, Müller U. GlyR alpha3: an essential target for spinal PGE2-mediated inflammatory pain sensitization. *Science.* 304(5672):884-7. 2004.

Hill DR. GABA<sub>B</sub> receptor modulation of adenylate cyclase activity in rat brain slices. *Br J Pharmacol.* 84(1):249-57. 1985.

Huguenard JR, Prince DA. Clonazepam suppresses GABA<sub>B</sub>-mediated inhibition in thalamic relay neurons through effects in nucleus reticularis. *J Neurophysiol.* 71(6):2576-81. 1994.

Jensen ML, Timmermann DB, Johansen TH, Schousboe A, Varming T, Ahring PK. The beta subunit determines the ion selectivity of the GABA<sub>A</sub> receptor. *J Biol Chem.* 277(44):41438-47. 2002.

Jia, F., Pignataro, L., Schofield, C.M., Yue, M., Harrison, N.L., Goldstein, P.A. An extrasynaptic GABA<sub>A</sub> receptor mediates tonic inhibition in thalamic VB neurons. *J Neurophys.* 94(6): 4491-4501. 2005.

Jia, F., Yue, M., Chandra, D., Keramidas, A., Goldstein, P.A., Homanics, G.E., Harrison, N.L. Taurine is a potent activator of extrasynaptic GABA<sub>A</sub> receptors in the thalamus. *J Neurosci.* 28(1): 106-115. 2008.

Jones EG. *The Thalamus.* Plenum Press, New York, NY. 1985.

Kandel ER, Seigelbaum SA. Synaptic Integration, *In: Principles of Neural Science.* McGraw-Hill, Toronto ON. 2000.

Kaupmann K, Malitschek B, Schuler V, Heid J, Froestl W, Beck P, Mosbacher J, Bischoff S, Kulik A, Shigemoto R, Karschin A, Bettler B. GABA(B)-receptor subtypes assemble into functional heteromeric complexes. *Nature.* 396(6712):683-7. 1998.

Keramidas, A., Harrison, N.L. (2008). Agonist-dependent single channel current and gating in  $\alpha_4\beta_2\delta$  and  $\alpha_1\beta_2\gamma_{2S}$  receptors. *J Gen Physiol.* 131(2): 163-181.

Kirsch J, Betz H. The postsynaptic localization of the glycine receptor-associated protein gephyrin is regulated by the cytoskeleton. *J Neurosci.* 15(6):4148-56. 1995.

Kuhse J, Laube B, Magalei D, Betz H. Assembly of the inhibitory glycine receptor: identification of amino acid sequence motifs governing subunit stoichiometry. *Neuron.* 11(6):1049-56. 1993.

Kulik A, Nakadate K, Nyíri G, Notomi T, Malitschek B, Bettler B, Shigemoto R.  
Distinct localization of GABA(B) receptors relative to synaptic sites in the rat cerebellum  
and ventrobasal thalamus. *Eur J Neurosci.* 15(2):291-307. 2003.

Kvenvolden K.A., Lawless J., Pering K., Peterson E., Flores J., Ponnampereuma C.,  
Kaplan I., Moore C. Evidence for extraterrestrial amino-acids and hydrocarbons in the  
Murchison meteorite. *Nature.* 228(5275): 923-926, 1970.

Luscher C., Jan L.Y., Stoffel M., Malenka R.C., Nicoll R.A. G protein-coupled inwardly  
rectifying K<sup>+</sup> channels (GIRKs) mediate postsynaptic but not presynaptic transmitter  
actions in hippocampal neurons. *Neuron* 19(3): 687-695, 1997.

Lynch JW. Molecular structure and function of the glycine receptor chloride channel.  
*Physiol Rev.* 84(4):1051-95. 2004.

Lynch JW. Native glycine receptor subtypes and their physiological roles.  
*Neuropharmacology.* 56(1):303-9. 2009.

MacLeod BA, Wang JT, Chung CC, Ries CR, Schwarz SK, Puil E. Analgesic properties  
of the novel amino acid, isovaline. *Anesth Analg.* 110(4):1206-14. 2010.

Mintz IM, Bean BP. GABA<sub>B</sub> receptor inhibition of P-type Ca<sup>2+</sup> channels in central neurons. *Neuron*. 10(5):889-98. 1993.

Mohler H, Benke D, Mertens S, Fritschy JM. GABA<sub>A</sub>-receptor subtypes differing in alpha-subunit composition display unique pharmacological properties. *Adv Biochem Psychopharmacol*. 47:41-53. 1992.

Pape HC, McCormick DA. Electrophysiological and pharmacological properties of interneurons in the cat dorsal lateral geniculate nucleus. *Neuroscience*. 68(4):1105-25. 1995.

Pavlov I, Savtchenko LP, Kullmann DM, Semyanov A, Walker MC. Outwardly rectifying tonically active GABA<sub>A</sub> receptors in pyramidal cells modulate neuronal offset, not gain. *J Neurosci*. 29(48):15341-50. 2009.

Pham TM, Lacaille JC. Multiple postsynaptic actions of GABA via GABA<sub>B</sub> receptors on CA1 pyramidal cells of rat hippocampal slices. *J Neurophysiol*. 76(1):69-80. 1996.

Pirker S, Schwarzer C, Wieselthaler A, Sieghart W, Sperk G. GABA(A) receptors: immunocytochemical distribution of 13 subunits in the adult rat brain. *Neuroscience*. 101(4):815-50. 2000.

Pontier SM, Lahaie N, Ginham R, St-Gelais F, Bonin H, Bell DJ, Flynn H, Trudeau LE, McIlhinney J, White JH, Bouvier M. Coordinated action of NSF and PKC regulates GABA<sub>B</sub> receptor signaling efficacy. *EMBO J.* 25(12):2698-709. 2006.

Potes C.S., Neto F.L., Castro-Lopes J.M. Inhibition of pain behavior by GABA<sub>B</sub> receptors in the thalamic ventrobasal complex: Effect on normal rats subjected to the formalin test of nociception. *Brain Res.* 1115(1): 37-47, 2006a.

Potes, C.S., Neto F.L., Castro-Lopes J.M. Administration of baclofen, a  $\gamma$ -aminobutyric acid type B agonist in the thalamic ventrobasal complex, attenuates allodynia in monoarthritic rats subjected to the ankle-bend test. *J Neurosci Res.* 83(3): 515-523, 2006b.

Raap J, Erkelens K, Ogrel A, Skladnev DA, Brückner H. Fungal biosynthesis of non-ribosomal peptide antibiotics and alpha, alpha-dialkylated amino acid constituents. *J Pept Sci.* 11(6):331-8. 2005.

Roberts WA, Eaton SA, Salt TE. Widely distributed GABA-mediated afferent inhibition processes within the ventrobasal thalamus of rat and their possible relevance to pathological pain states and somatotopic plasticity. *Exp Brain Res.* 89(2):363-72. 1992.

Saint, D., Thomas, T., Gage, P.W. GABA<sub>B</sub> agonists modulate a transient potassium current in cultured mammalian hippocampal neurons. *Neurosci Lett.* 118: 9-13, 1990.

Sakmann B. Elementary steps in synaptic transmission revealed by currents through single ion channels. *Science*. 256(5056):503-12. 1992.

Schwenk J, Metz M, Zolles G, Turecek R, Fritzius T, Bildl W, Tarusawa E, Kulik A, Unger A, Ivankova K, Seddik R, Tiao JY, Rajalu M, Trojanova J, Rohde V, Gassmann M, Schulte U, Fakler B, Bettler B. Native GABA(B) receptors are heteromultimers with a family of auxiliary subunits. *Nature*. 465(7295):231-5. 2010.

Sherman SM. Thalamic relays and cortical functioning. *Prog Brain Res*. 149:107-26. 2005.

Steiger JL, Russek SJ. GABAA receptors: building the bridge between subunit mRNAs, their promoters, and cognate transcription factors. *Pharmacol Ther*. 101(3):259-81. 2004.

Steiger JL, Bandyopadhyay S, Farb DH, Russek SJ. cAMP response element-binding protein, activating transcription factor-4, and upstream stimulatory factor differentially control hippocampal GABA<sub>B</sub>R1a and GABA<sub>B</sub>R1b subunit gene expression through alternative promoters. *J Neurosci*. 24(27):6115-26. 2004.

Thompson SM, Gähwiler BH. Comparison of the actions of baclofen at pre- and postsynaptic receptors in the rat hippocampus in vitro. *J Physiol*. 451:329-45. 1992.

Turner JP, Anderson CM, Williams SR, Crunelli V. Morphology and membrane properties of neurones in the cat ventrobasal thalamus in vitro. *J Physiol.* 505 (3):707-26. 1997.

Ulrich D., Huguenard J.R. GABA<sub>B</sub> receptor-mediated responses in GABAergic projection neurones of rat reticularis thalami in vitro. *J. Physiol.* 493: 845-854, 1996.

Urwyler S., Gjoni T., Kaupmann K., Pozza M.F., Mosbacher J. Selected amino acids, dipeptides and arylalkylamine derivatives do not act as allosteric modulators at GABA<sub>B</sub> receptors. *Eur J Pharmacol.* 483: 147-153, 2004.

Urwyler S, Gjoni T, Koljatić J, Dupuis DS. Mechanisms of allosteric modulation at GABA<sub>B</sub> receptors by CGP7930 and GS39783: effects on affinities and efficacies of orthosteric ligands with distinct intrinsic properties. *Neuropharmacology.* 48(3):343-53. 2005.

Wan X, Mathers DA, Puil E. Pentobarbital modulates intrinsic and GABA-receptor conductances in thalamocortical inhibition. *Neuroscience.* 121(4):947-58. 2003.

Wang F, Xiao C, Ye JH. Taurine activates excitatory non-synaptic glycine receptors on dopamine neurones in ventral tegmental area of young rats. *J Physiol.* 565(Pt 2):503-16. 2005.

Weyand TG, Boudreaux M, Guido W. Burst and tonic response modes in thalamic neurons during sleep and wakefulness. *J Neurophysiol.* 85(3):1107-18. 2001.

Wingrove PB, Thompson SA, Wafford KA, Whiting PJ. Key amino acids in the gamma subunit of the gamma-aminobutyric acidA receptor that determine ligand binding and modulation at the benzodiazepine site. *Mol Pharmacol.* 52(5):874-81. 1997.

Yen CT, Jones EG. Intracellular staining of physiologically identified neurons and axons in the somatosensory thalamus of the cat. *Brain Res.* 280(1):148-54. 1983.

Yue P, Lin DH, Pan CY, Leng Q, Giebisch G, Lifton RP, Wang WH. Src family protein tyrosine kinase (PTK) modulates the effect of SGK1 and WNK4 on ROMK channels. *Proc Natl Acad Sci U S A.* 106(35):15061-6. 2009.

Zhao M., Bada J.L. Extraterrestrial amino acids in Cretaceous/Tertiary boundary sediments at Stevns Klint, Denmark. *Nature* 339(6224): 463-465, 1989.

## 2. <sup>1</sup>FIRST MANUSCRIPT: EFFECTS OF THE $\beta$ -AMINO ACID ANTAGONIST TAG ON THALAMOCORTICAL INHIBITION

### 2.1. Introduction

In the central nervous system, receptor antagonism is instrumental for elucidating the nature of the neurotransmitter that mediates synaptic inhibition. For issues of co-mediation by  $\gamma$ -aminobutyric acid (GABA) and glycine, the selectivities of antagonists are critical for identifying inhibitory postsynaptic currents (IPSCs). In mixed IPSCs, bicuculline or gabazine antagonizes the GABA<sub>A</sub>ergic component and not glycine receptors, whereas the reverse is true for strychnine which only blocks the glycinergic component (Jonas et al., 1998; Dumoulin et al., 2001). Combined GABA<sub>A</sub> and glycine receptor antagonism eliminates the mixed IPSCs, frequently observed in thalamic neurons, which less commonly display pure GABA<sub>A</sub>ergic and pure glycinergic IPSCs (Ghavanini et al., 2005; cf. cerebellum, Dumoulin et al., 2001).

The observed biophysical characteristics of mixed and pure IPSCs may result from precise receptor subtypes that play a crucial role in transmitter agonist recognition and kinetic properties (cf. Takahashi et al., 1992; Keramidas and Harrison, 2008). Thus, the  $\alpha_1\beta_2\gamma_2$  GABA<sub>A</sub> receptor subtype which is abundant at forebrain synapses (cf. Farrar et al., 1999) likely mediates the pure GABA<sub>A</sub>ergic IPSCs that decay with a time constant of ~22 ms) (Ghavanini et al., 2006). Although the presence of the  $\delta$  subunit often results in receptor expression in the extrasynaptic membrane, atypical GABA<sub>A</sub> receptors of

---

<sup>1</sup> A version of this chapter has been published. Mathers DA, McCarthy, SM, Cooke JE, Ghavanini, AA. and Puil, E. (2009) Effects of the  $\beta$ -amino acid antagonist TAG on thalamocortical inhibition. *Neuropharmacology*. 56: 1097-1105.

composition  $\alpha_4\beta_2\delta$  (Korpi et al., 2002) likely occur in synapses on ventrobasal neurons (Jia et al., 2008).

The extent to which  $\alpha_4$  GABA<sub>A</sub> receptors determine the pharmacological and biophysical properties of mixed and pure IPSCs is presently unclear. Previous studies have shown that  $\alpha_1\beta_2\gamma_2$  and  $\alpha_4\beta_2\delta$  GABA<sub>A</sub> receptors differ in their pharmacological properties (Jia et al., 2005). Taurine and  $\beta$ -alanine are full agonists at  $\alpha_4\beta_2\delta$  receptors (Jia et al., 2008), but are partial agonists at  $\alpha_1\beta_2\gamma_2$  receptors (cf. Wu et al., 1993; Hussy et al., 1997). The observations suggest that these  $\beta$ -amino acids may activate  $\alpha_4$  GABA<sub>A</sub> receptors in producing mixed IPSCs.

In view of previous studies, we also considered the possibility that the endogenous  $\beta$ -amino acids, in addition to glycine itself, may activate glycine receptors in the mixed IPSCs. Endogenous  $\beta$ -amino acids activate glycine receptors on neurons of the hippocampus (Mori et al., 2002), nucleus accumbens (Jiang et al., 2004), and amygdala, (McCool and Botting, 2000). The glycinergic component decays rapidly or slowly (Ghavanini et al., 2006). In this component, the kinetically distinct currents likely reflect two receptor populations that contain  $\alpha_1$  glycine subunits (faster decay) or co-assembled  $\alpha_1$  and  $\alpha_2$  subunits (slower decay, cf. Takahashi et al., 1992; Singer and Berger, 1999). The faster decay correlates to short-duration channel bursts induced by glycine, taurine and  $\beta$ -alanine. The slower decay correlates to long-duration bursts induced mainly by the  $\beta$ -amino acids. On these grounds, therefore,  $\beta$ -amino acids may contribute to the glycinergic component of mixed IPSCs and to pure glycinergic IPSCs.

If available, a selective  $\beta$ -amino acid antagonist would facilitate analysis of inhibition in the thalamus. Early studies on the role of taurine as a transmitter resulted in discovery of the putative antagonist, TAG (6-aminomethyl-3-methyl-4H-1,2,4-benzothiadiazine-1,1-dioxide (Yarbrough et al., 1981; Girard et al., 1982). In central neurons, TAG antagonized the firing depression induced by  $\beta$ -amino acids, and not by glycine or GABA (Okamoto et al., 1983; Padjen et al., 1989; Billard and Batini, 1991). This selectivity of TAG for receptors activated by taurine and  $\beta$ -alanine was compatible with its antagonism of  $\beta$ -amino acid binding in tissue homogenates (Martin et al., 1981; Frosini et al., 2003). While these actions likely involved extrasynaptic receptors, there is little information about TAG actions on synaptic currents.

In the first part of the present studies, we sought to visualize  $\alpha_4$  GABA<sub>A</sub> receptors in the ventrobasal nuclei. We used confocal microscopy to visualize  $\alpha_{1/2}$  glycine and  $\alpha_4$  GABA<sub>A</sub> receptor subunits and inhibitory nerve terminals. In the second part, we determined TAG's actions on pharmacologically and kinetically defined IPSCs, evoked by electrical stimulation of the medial lemniscus. We sought to clarify the selectivity of TAG, relative to strychnine and bicuculline on IPSCs that involved populations of GABA<sub>A</sub>, glycine, or both receptor systems. One expectation was that TAG's effects would reveal heterogeneities in GABA<sub>A</sub>ergic and glycinergic transmission.

## **2.2. Methods**

### **2.2.1. Animals and slice preparation**

All experiments on Sprague-Dawley rats (12-14 days old) were approved by University of British Columbia Committee on Animal Care. The brain was removed from the anesthetized animal and submerged in ice-cold artificial cerebrospinal fluid (aCSF) bubbled with 95% O<sub>2</sub> and 5% CO<sub>2</sub>. The aCSF contained (in mM): 124 NaCl, 26 NaHCO<sub>3</sub>, 1.25 NaH<sub>2</sub>PO<sub>4</sub>, 2.5 KCl, 2 MgCl<sub>2</sub>, 2 CaCl<sub>2</sub>, and 10 dextrose. Parasagittal slices (200-250 µm) were cut using a vibroslicer (Campden Instruments Ltd., London, England) and submerged for 1.5 h in aCSF (pH 7.3-7.4) at room temperature (23-25°C).

### **2.2.2. Tissue preparation and immunocytochemistry**

Sprague-Dawley rats (P12) were anesthetized with pentobarbital (40 mg/kg) and transcardially perfused with cold 0.1% PBS, followed by 4% formaldehyde. The brain was dissected and post-fixed in 4% formaldehyde for 2 h at 4°C, followed by submersion in 30% sucrose for 24-48 h at 4°C. The tissue was embedded with Tissue-Tek embedding medium (Sakura Finetek, Torrance, CA) and frozen in liquid nitrogen. Sagittal sections were made at 14 µm thickness and stored at -20°C.

Immunocytochemistry (ICC) was performed on sections, post-fixed in 4% formaldehyde for 10 min. The sections were permeabilized with 0.1% Triton X-100, blocked with 0.5% BSA in PBS, and incubated in primary antibody overnight at 4°C in PBS solution containing 0.1% BSA. The primary antibodies were mouse anti-microtubule associated protein-2 (MAP-2; 1:200, Thermo Scientific, Waltham MA, ms249), goat anti-GABA<sub>A</sub>

$\alpha_4$  subunit (1:500; Santa Cruz Biotechnology Inc; sc-7355), rabbit anti-glycine receptor  $\alpha_{1/2}$  subunit (1: 200; Abcam, Cambridge, MA; ab23809), and guinea pig anti-vesicular GABA transporter (VGAT; 1:1000; Chemicon; ab5855). The VGAT antibody visualized inhibitory presynaptic terminals by binding to the vesicular transporter shared by GABA and glycine (Dumoulin et al., 1999).

Secondary antibodies purchased from Invitrogen (Burlington, ON), were incubated for 1 h at room temperature. Secondary antibodies were goat anti-mouse Alexa 594 (MAP-2), chicken anti-goat Alexa 488 (GABA<sub>A</sub>  $\alpha_4$ ), chicken anti-rabbit Alexa 647 (glycine  $\alpha_{1/2}$ ), and goat anti-guinea pig Alexa 594 (VGAT). To prevent secondary cross-reaction, the antibodies used to label  $\alpha_4$  and  $\alpha_{1/2}$  subunits were applied at room temperature for 1 h, the sections were fixed again with 4% formaldehyde, and received the secondary antibody for labelling VGAT. Sections were coverslipped with Prolong Gold (Invitrogen, Burlington, ON) and allowed to cure overnight before imaging.

### **2.2.3. Imaging and quantification**

Low magnification images were captured using an Axioskop 2 MOT microscope, (Zeiss, Jena, Germany) fitted with a SPOT camera (Diagnostic Instruments, Sterling Heights, MI) and Northern Eclipse software (Empix Imaging, Mississauga, Ontario, Canada). High magnification images were captured using an Olympus Fluoview 1000 confocal microscope (60x/1.4 Oil Plan-Apochromat objective). Images were modified slightly using Adobe Photoshop software to enhance visualization. Briefly, presynaptic terminals and postsynaptic receptor subunits were analyzed at a threshold of 65, to eliminate

background and ensure only puncta were quantified. The incidence of co-localization of puncta for two or three antibodies was quantified using Image J (National Institutes of Health, Bethesda, MD). A minimum pixel number of 10 was used to define a punctum (cf. Bamji et al., 2006). The amount of random co-localization was assessed by rotating a staining channel by 90 degrees prior to calculation. The incidence of chance co-localization of all three antibodies was only 3%.

#### **2.2.4. Electrophysiological recording**

Recording electrodes pulled from borosilicate tubing (WP-Instruments, Sarasota, USA), had resistances of 5-10 M $\Omega$  after filling with solution that contained (in mM): 140 K-gluconate, 5 KCl, 4 NaCl, 3 MgCl<sub>2</sub>, 1 CaCl<sub>2</sub>, 10 EGTA, 1 HEPES, 3 Mg-adenosine triphosphate, 0.3 Na<sub>2</sub>-guanosine triphosphate. The pH was adjusted to 7.3-7.4 using 50% gluconic acid or KOH.

The slices were immobilized in the recording chamber and superfused with oxygenated aCSF at a rate of 2 ml/minute at room temperature. The ionotropic glutamate receptor blocker, kynureate (1 mM), was used to isolate IPSCs (Ghavanini et al., 2005). The ventrobasal nuclei were identified using DIC microscopy at 400x magnification (Axioscope, Carl Zeiss, Germany).

Whole-cell IPSCs were recorded with a List EPC-7 (HEKA, Lambrecht, Germany), filtered at 3 kHz and analyzed using pClamp software (Axon Instruments). Recorded neurons were located predominantly at the margin of the ventrobasal complex, near the

reticular nucleus (cf. Fig. 1A,B). A bipolar electrode (5 M $\Omega$ ) was placed in medial lemniscus, ~3 mm from the recording electrode. Stimuli were adjusted to produce just-maximal IPSCs (rate, <0.5 Hz). The stimulus artifacts often were removed by subtraction, for clarity. The Nernst potentials for Cl<sup>-</sup> and K<sup>+</sup> were -53 mV and -84 mV. Neurons were held at  $V_h = -80$  mV.

### **2.2.5. Current clamp data analysis**

Membrane potential was corrected for junction potential of -11 mV. Membrane input resistance and time constant were calculated from <5 mV voltage responses to hyperpolarizing current pulses. Action potentials were elicited from -60 mV by current pulse injection and recorded at an apparent bandwidth of DC – 2 kHz. In view of the distortions resulting from patch-clamp amplifiers operating in current-clamp mode (cf. Magistretti et al., 1998), we did not quantify the effects of TAG on action potentials.

### **2.2.6. IPSC classification and analysis**

We defined purely glycinergic or GABA<sub>A</sub>ergic IPSCs as >95% inhibition of the IPSC amplitude by strychnine (2  $\mu$ M) or bicuculline (20  $\mu$ M), respectively (Ghavanini et al., 2005). Mixed IPSCs required both antagonists for >95% abolition, always decayed biexponentially and were separable into two categories on pharmacological and kinetic grounds (cf. Ghavanini et al., 2006). We defined Type 1 IPSCs as having a rapidly decaying component (time constant,  $\tau = \sim 9$  ms) eliminated by strychnine, and a bicuculline-sensitive component with  $\tau = \sim 40$  ms). We defined Type 2 IPSCs as also

showing this GABA<sub>A</sub>ergic component, accompanied with a strychnine-sensitive component which decayed very slowly ( $\tau = \sim 230$  ms).

For kinetic analysis, 10 successive IPSCs were aligned at their peaks, averaged and their decay phase was fitted with single ( $y = A \cdot \exp(-t/\tau)$ ) or double exponential ( $y = A_1 \cdot \exp(-t/\tau_1) + A_2 \cdot \exp(-t/\tau_2)$ ) functions using the Levenberg-Marquadt method with a sum of squared errors minimization. Here,  $A$ ,  $A_1$  and  $A_2$  were fit amplitude components with time constants  $\tau$ ,  $\tau_1$  and  $\tau_2$ .

### **2.2.7. Drugs**

Bicuculline methiodide, strychnine, and kynurebate (Sigma Chemical Company, St. Louis, USA) were applied by superfusion. TAG was a gift of Merck Frosst Company (Montreal, Quebec, Canada) or was synthesized by BioFine International (Vancouver, BC, Canada). TAG was dissolved in dimethyl sulphoxide (DMSO) and diluted in aCSF to a final DMSO concentration of 0.01%. Control applications of DMSO did not affect IPSCs. Fluid exchange with the bath media required 4-6 min (Mathers et al., 2007).

A concentration-response relationship for TAG antagonism was established using cumulative applications. The fitting equation for sigmoid relationships was  $y = \text{maximal response} / (1 + \text{IC}_{50} - [\text{TAG}]^n)$ , where  $\text{IC}_{50}$  was the concentration causing half-maximal block and  $n$ , the slope of the sigmoid curve. The percentage inhibition of IPSC amplitude was calculated from the relationship  $[(\text{control amplitude} - \text{amplitude during antagonist}) / \text{control amplitude}] \times 100$ .

application)/control amplitude] x 100%. Recovery of IPSCs from the effects of antagonists was defined as restitution to >75% of the control amplitude.

### **2.2.8. Statistical analysis**

All data were expressed as mean  $\pm$  SEM. Application of the Kolmogorov-Smirnov test showed that electrophysiological data occasionally deviated from a normal distribution. In these cases we employed the non-parametric Wilcoxon test, with significance defined as  $P < 0.05$ . Because reversal of TAG effects proceeded slowly, it was not always possible to obtain washout values for IPSC parameters, precluding the use of ANOVA tests or their non-parametric equivalents.

## **2.3. Results**

### **2.3.1. Co-localization of GABA<sub>A</sub> $\alpha_4$ subunits and glycine receptors with inhibitory nerve terminals**

Assuming an involvement in mixed IPSCs, we predicted that synaptic GABA<sub>A</sub>  $\alpha_4$  receptors should occur predominantly on neurons that express synaptic glycine receptors. We confirmed this possibility using ICC methods, including an antibody against VGAT which identified synaptic receptor clusters in ventrobasal thalamus of P12 rats.

Figure 2.1A shows a low-power epifluorescence micrograph of a sagittal section through the thalamus, delineating the ventral posterolateral (VPL), ventral posteromedial (VPM) and reticular nuclei (nRT). Neuronal somata and major processes were visualized by staining with an antibody against microtubule-associated protein-2 (MAP-2, red). Cell

nuclei were stained with DAPI (blue). The large V in Fig. 2.1A points to the VPL region where recording electrodes were typically placed and detailed immunocytochemical studies were performed. Fig. 2.1B is a confocal image of this anatomical region in another slice, stained for GABA<sub>A</sub>  $\alpha_4$  subunits (green) and glycine  $\alpha_{1/2}$  subunits (red), with nuclei stained using DAPI (blue). Punctate and diffuse staining on somata was evident for both the GABA<sub>A</sub> and glycine receptor subunits. Yellow staining in Fig. 2.1B indicates numerous puncta in which GABA<sub>A</sub>  $\alpha_4$  and glycine  $\alpha_{1/2}$  subunits were co-localized.

Figure 2.1C shows high power confocal views of the neurons contained in the box in Fig. 2.1B, stained for glycine  $\alpha_{1/2}$  subunits (red, left panel) and GABA<sub>A</sub>  $\alpha_4$  subunits (green, right panel). Punctate (large arrow heads) and diffuse (small arrows) staining was evident in somatic regions for both receptors. High power confocal images in Fig. 2.1D-F were obtained from the VPL nucleus of another slice. These images represent the same optical section stained for VGAT (Fig. 2.1D), GABA<sub>A</sub>  $\alpha_4$  subunits (Fig. 2.1E) and glycine  $\alpha_{1/2}$  subunits (Fig. 2.1F). White arrows indicate puncta of co-localized staining for the 3 antigens, whereas arrowheads indicate puncta of positive staining only for VGAT (D),  $\alpha_4$  GABA<sub>A</sub> (E), or glycine  $\alpha_{1/2}$  (F). In each case, a lack of staining for the remaining antigens implied spatially distinct locations for the antigens.

Glycine receptor  $\alpha_{1/2}$  subunits were co-localized with VGAT, and inferred to be synaptic in 436/817 puncta (53%). GABA<sub>A</sub>  $\alpha_4$  subunits were co-localized with VGAT, and inferred to be synaptic in 497/919 puncta (54%). Of synaptic glycine  $\alpha_{1/2}$  subunits, 379/436 puncta were co-localized with GABA<sub>A</sub>  $\alpha_4$  subunits (87%). Of synaptic GABA<sub>A</sub>

$\alpha_4$  subunits, 379/497 puncta were co-localized with glycine receptor  $\alpha_{1/2}$  subunits (76%). Hence, VPL neurons exhibited a high degree of co-localization of GABA<sub>A</sub>  $\alpha_4$  and glycine  $\alpha_{1/2}$  receptor subunits, closely apposed to release sites for inhibitory amino acids.

### **2.3.2. TAG effects on membrane properties**

Applications were performed on 57 neurons, displaying stable potentials at rest near -55 mV. TAG application at 250  $\mu$ M (cf. Mathers 1993) did not significantly alter membrane potential, input resistance or membrane time constant (Table 1). TAG had no effect on action potential firing evoked by current injection (cf. Methods). TAG had negligible effects on the voltage-current relationship in most neurons at potentials depolarized from rest to threshold for action potentials. The absence of significant effects on membrane properties were consistent with anticipated receptor antagonism.

### **2.3.3. Effects on mixed IPSCs**

We studied the effects of TAG on the mixed IPSCs of neurons receiving GABA<sub>A</sub>ergic and glycinergic inputs. In 19 such neurons, we applied TAG (250  $\mu$ M) prior to application of other antagonists and observed incomplete IPSC blockade, as shown for the sample neuron of Figure 2.2A. Initial application of TAG reduced this IPSC by 24%. On TAG washout, maximal antagonism by strychnine (2  $\mu$ M) caused a similar reduction (28%). Co-application with bicuculline (20  $\mu$ M) eliminated the portion that remained after strychnine.

The effects of TAG were attributable to blockade of both GABA<sub>A</sub> and glycine receptors. In a second group of 19 neurons we first applied bicuculline to block GABA<sub>A</sub> receptors. Co-application of TAG with bicuculline reduced the remaining IPSC component, as shown for the sample neuron of Figure 2.2B. In this neuron, bicuculline reduced IPSC amplitude by 14%. Co-application with TAG produced a further 24% reduction in IPSC amplitude, attributable to blockade of glycine receptors.

In a third group of 19 neurons, we first applied strychnine to block glycine receptors. Co-application of TAG with strychnine reduced the remaining IPSC component, as shown for the sample neuron of Figure 2.2C. In this neuron, strychnine application produced a 30% reduction in the IPSC. Co-application with TAG eliminated the IPSC, attributable to blockade of the GABA<sub>A</sub> receptor mediated component.

In the 19 neurons administered TAG (250 μM) before the other antagonists, the reduction in peak amplitude of mixed IPSCs averaged  $62 \pm 6\%$ . The amplitude reduction by TAG did not differ from the suppression caused by first application of bicuculline in the second group of 19 neurons ( $59 \pm 4\%$ ,  $P > 0.05$ ). Surprisingly, TAG suppression of the mixed IPSC exceeded that due to first application of strychnine in the third group of 19 neurons ( $41 \pm 4\%$ ,  $P < 0.05$ ).

We determined the effects of TAG (250 μM) on the mixed IPSC amplitude which outwardly rectified in control media (Fig. 2.3). Without TAG, the IPSCs were largest in amplitude at -80 mV and diminished to zero at or near the chloride Nernst potential,  $E_{Cl}$

(-53 mV). While suppressing IPSC amplitude, TAG application did not greatly change rectification. TAG did not alter the reversal potential of the IPSC near -54 mV (Fig. 2.3E). In summary, TAG actions were voltage-independent and did not alter rectification of the mixed IPSC amplitude, consistent with being a receptor antagonist.

#### **2.3.4. Concentration-response relationship**

We determined the relationship of concentration to effect on mixed IPSCs by application of TAG in a stepwise, cumulative manner to 7 of the 19 previously untreated neurons. As shown in Figure 2.4A, TAG produced a concentration-dependent reduction in the peak amplitude. The concentration-response curve was well-described by a single Hill function with an  $IC_{50}$  of 67  $\mu$ M and a Hill coefficient of  $0.8 \pm 0.8$ . Even at 1 mM, TAG did not eliminate the IPSCs, producing a ~70% reduction in peak amplitude (Fig. 2.4A). Since blockade was not significantly enhanced by stepping TAG concentration from 250  $\mu$ M to 1 mM, we employed the lower concentration for the remaining experiments.

The reduction in the amplitude of mixed IPSCs commenced within 2-4 minutes of TAG application. The effects reached a steady-state value within 5-10 min and were slowly reversible. We observed recovery to ~50 % of control amplitude in many neurons after a 50 min washout period (Fig. 2.4B). Recovery was incomplete in the majority of neurons despite washout periods of  $\geq 90$  min. Although we sometimes observed full recovery from the effects of TAG, the effects of bicuculline usually reversed within 30 min.

### 2.3.5. Effects on mixed IPSC components with isolated decay kinetics

To further analyze the actions of TAG, we isolated the glycinergic and GABA<sub>A</sub>ergic components from their mixed condition. Figure 2.5A shows the effects of TAG on a typical Type 1 IPSC. Evoked in control conditions, this IPSC was well-described by the sum of 2 exponential terms. After application of bicuculline, the slower decay component ( $\tau = 26$  ms) was eliminated, indicating mediation by GABA<sub>A</sub> receptors. Bicuculline did not alter the amplitude or decay time constant of the faster IPSC component ( $\tau = 6.4$  ms). Co-application with TAG reduced the amplitude of the faster component by 18%, with negligible effects on the decay time constant. These observations indicated that TAG antagonized receptor mediation of the faster component. TAG reversibly reduced this component by an average of  $46 \pm 5\%$  in 9 neurons, with negligible effects on decay kinetics (see Table 2).

Figure 2.5B shows the effects of TAG on a typical Type 2 IPSC. In control conditions, this current was well-described by the sum of 2 exponential components with decay time constants  $\tau = 10.8$  ms and  $\tau = 111$  ms. TAG application reduced both component amplitudes, with negligible effects on the decay time constants. After TAG washout, strychnine application eliminated the slower component, without affecting the faster component. Co-application with bicuculline abolished the IPSC, demonstrating that the faster component was mediated by GABA<sub>A</sub> receptors. Table 2 summarizes the effects of TAG on the bicuculline-sensitive component of mixed IPSCs in 9 neurons. In 2 of these neurons, TAG completely abolished the component (cf. Fig. 2.2C). TAG reversibly

reduced the amplitude of the component by an average of  $56 \pm 10\%$  with no significant change in decay kinetics.

### **2.3.6. Effects on pure GABA<sub>A</sub>ergic and glycinergic IPSCs**

To assess selectivity, we determined the effects of TAG on 6 IPSCs mediated solely by GABA, and 4 IPSCs mediated only by glycine-like amino acids. The pure GABA<sub>A</sub>ergic IPSCs identified by abolition by bicuculline and resistance to strychnine antagonism, decayed with a mean time constant of  $21 \pm 6$  ms. TAG had negligible effects on the amplitude and decay kinetics of pure GABA<sub>A</sub>ergic IPSCs (Fig. 2.6A; Table 2). The absence of changes in these IPSCs during and after TAG application confirmed that negligible rundown of IPSC amplitude occurred in the timeframe of our experiments.

Pure glycinergic IPSCs identified by abolition by strychnine and resistance to bicuculline antagonism, decayed with a mean time constant of  $6.1 \pm 0.6$  ms. TAG reduced the amplitude of pure glycinergic IPSCs in all neurons by an average of  $61 \pm 6\%$  (see Fig. 2.6B). TAG application did not significantly affect the decay time constant of these currents ( $8.1 \pm 2.4$  ms,  $n = 4$ ,  $P > 0.05$ ). In 3 out of the 4 glycinergic IPSCs, this component was accompanied by a slower component, forming an IPSC that we designated as a Type 3 (Fig. 2.6B). Similar slowly decaying components were observed in the 3 Type 2 IPSCs (cf. Fig. 2.5B). As shown in Table 2, TAG reduced the amplitude of the slower components in 6 pooled neurons by an average of  $49 \pm 7\%$ , with negligible effects on the decay kinetics.

## **2.4. Discussion**

This study on the effects of TAG demonstrated an unusual spectrum of antagonist actions on medial lemniscal inhibition, consistent with blockade of  $\beta$ -amino acid activation of glycine and GABA<sub>A</sub> receptors. TAG did not affect pure GABA<sub>A</sub>ergic IPSCs. Our ICC studies showed that  $\alpha_{1/2}$  glycine- and atypical  $\alpha_4$  GABA<sub>A</sub>- receptors were co-localized at inhibitory synapses. Given the ICC results, mixed IPSCs likely involved  $\alpha_4$  GABA<sub>A</sub> receptors. On mixed IPSCs, TAG was equi-effective in reducing the amplitudes of the GABA<sub>A</sub>ergic, and the faster or slower glycinergic component, as well as the pure glycinergic IPSC. These results implicate heterogeneity between pure and mixed inhibitory currents in ventrobasal neurons.

The chief finding was TAG's ability to diminish all contributions to mixed IPSCs, identified pharmacologically and by their kinetic components. To a similar extent, TAG decreased the amplitudes of the faster or slower glycinergic component and pure glycinergic IPSCs, as well as the GABA<sub>A</sub>ergic component. These effects are in line with previous studies on other central neurons (cf. *Introduction*) showing that TAG attenuates responses to  $\beta$ -amino acids without greatly affecting responses to glycine or GABA (cf. Curtis et al., 1982; Mathers, 1993). As deduced from the effects of TAG, synaptic inhibition may involve  $\beta$ -amino acids.

The simplest explanation for our observations of incomplete antagonism is that TAG antagonized the  $\beta$ -amino acid contributions to the mixed IPSCs and pure glycinergic IPSCs. Electrical stimulation of the medial lemniscus may have released glycine and  $\beta$ -

amino acids, as well as GABA. Glycine and the  $\beta$ -amino acids bind to different sites on the glycine receptor (Vafa et al., 1999; Han et al., 2001), consistent with a differential blockade of their actions by TAG (cf. *Introduction*). Taurine activates bicuculline-sensitive currents by partial agonism at classical GABA<sub>A</sub> receptors (cf. Hussy et al., 1997), or by full agonism at  $\alpha_4$  GABA receptors (Jia et al., 2008). Taurine and GABA are co-localized in nerve terminals at some synapses (Ottersen et al., 1988) and high affinity taurine transporters are present in thalamic nuclei (Pow et al., 2002). Due to the three-dimensional nature of our slice preparations, the spatial resolution of our confocal images is less than can be attained in monolayer cell cultures. Nevertheless, our observations indicate that GABA<sub>A</sub>  $\alpha_4$  and glycine receptor subunits co-localize at the same nerve endings, signifying co-release, or perhaps occur under very closely apposed nerve terminals, compatible with co-transmitting pathways.

Synaptic GABA<sub>A</sub> receptors that mediate the mixed IPSC in neurons of young rats appear to differ in some aspects from the classical receptors. TAG did not affect the pure GABA<sub>A</sub>ergic IPSCs which we assume resulted from GABA activation of the prevalent  $\alpha_1$  form of the GABA<sub>A</sub> receptor (Farrar et al., 1999). Compared to the  $\alpha_1$  form,  $\alpha_4$  GABA<sub>A</sub> receptors have higher affinity for taurine (Jia et al., 2008). Hence, taurine may co-activate the GABA<sub>A</sub>ergic component of mixed IPSCs, susceptible to TAG blockade. Receptors containing  $\alpha_4$  subunits open in longer duration bursts than receptors containing  $\alpha_1$  subunits (Keramidas and Harrison, 2008). However, the tendency for the GABA<sub>A</sub>ergic component of mixed IPSCs to decay more slowly than pure GABA<sub>A</sub>ergic IPSCs was not significant (cf. Table 2).

The effects of TAG were attributable to antagonism at postsynaptic receptors. TAG lacked effects on membrane properties. We observed a trend towards lower input resistance upon TAG application that did not reach significance. This trend and the relatively high standard errors in these measurements may have reflected the ability of TAG to block the neuronal transport of endogenous taurine (cf. Lewin et al., 1994). When applied to neurons exhibiting mixed IPSCs, TAG behaved like a submaximal dose-combination of strychnine and bicuculline.

Conceivably, TAG may have acted presynaptically to suppress the release of GABA or glycine. However, TAG does not inhibit GABA release from rat cortical synaptosomes (Girard et al., 1982), and pure IPSCs eliminated by bicuculline were not suppressed by the antagonist. In spinal cord (Jonas et al., 1998) and trapezoid body neurons (Turecek and Trussel, 2001), glycine enhances GABA release by actions on strychnine-sensitive presynaptic receptors. Hence TAG may have suppressed GABA release indirectly, by blocking the facilitatory effect of glycine on GABA release. This mechanism also seems unlikely since strychnine did not occlude TAG actions on the bicuculline-sensitive components of mixed IPSCs.

The functional significance of the heterogeneous inhibition revealed in this study remains unclear. In contrast to higher species, there is little evidence for distinct subtypes of neurons within the ventrobasal complex of rats (Harris, 1986). However, small changes in the decay time course of IPSCs greatly affect rebound burst firing and oscillogenesis in

thalamocortical neurons (Sohal et al., 2006). As recently shown, co-agonism by glycine and GABA at glycine receptors alters the decay rate of glycinergic IPSCs (Lu et al., 2008). Co-release of glycine or GABA with  $\beta$ -amino acids may fine-tune synaptic current kinetics, affecting the duration of inhibition and firing pattern of thalamocortical neurons.

Our studies focused on synaptic inhibition rather than extrasynaptic inhibitory responses, as previously. We showed that TAG had little or no effect on pure GABA<sub>A</sub>ergic IPSCs but suppressed the GABA<sub>A</sub>ergic component of mixed IPSCs, possibly by interacting with an atypical form of GABA receptor. TAG antagonized the glycinergic components which occur separately as pure IPSCs or in combination with the GABA<sub>A</sub>ergic component of mixed IPSCs. Thus, TAG has a unique spectrum of synaptic effects, distinct from classical glycine- and GABA<sub>A</sub>-receptor antagonism.

## Figures

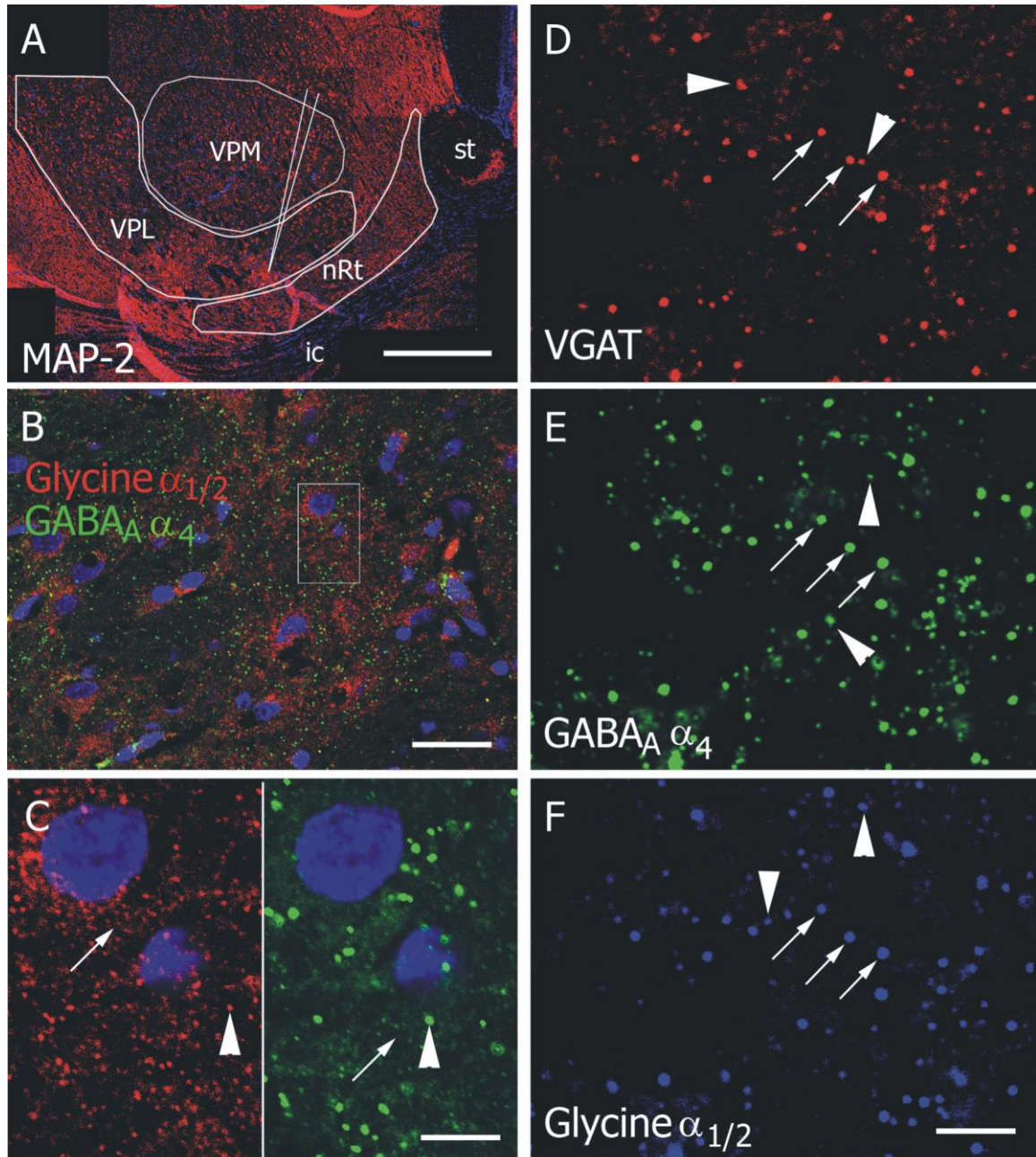


**Figure 2.1. Co-localization of synaptic glycine and GABA<sub>A</sub>  $\alpha_4$ -containing receptors in VPL.** (A) Low power epifluorescence photomicrograph montage showing sagittal section of rat thalamus (P12) stained with antibody to MAP-2 (red), with nuclei counter-

staining using DAPI (blue). Ventroposterolateral (VPL), ventroposteromedial (VPM), and reticular (nRT) nuclei of the thalamus are outlined. Note that MAP-2 staining was absent in the white matter of the stria terminalis (st) or the internal capsule (ic). The large V points to the VPL region used for recording and detailed immunocytochemical studies. (B) Confocal image of this region in another slice, stained for GABA<sub>A</sub> receptor  $\alpha_4$  subunits (green) and glycine receptor  $\alpha_{1/2}$  subunits (red) with DAPI nuclear staining (blue). Co-localized staining for the two receptor subunits is indicated by yellow puncta. (C) High power confocal images of the neurons in the box in (B), stained for glycine receptor  $\alpha_{1/2}$  subunits (red, left) and GABA<sub>A</sub>  $\alpha_4$  subunits (green, right). Punctate (large arrow heads) and diffuse (small arrows) staining was evident for both receptor subunits in somatic regions. (D-F) In a further slice, a field similar to that in (C) is shown at high magnification, stained using antibodies for (D) VGAT (red), (E) GABA<sub>A</sub>  $\alpha_4$  subunits (green) and (F) glycine receptor  $\alpha_{1/2}$  subunits (blue), captured with a confocal microscope. White arrows in D-F indicate where staining for all three antigens overlapped, showing co-localization. Arrowheads indicate where staining was positive for the specified antigen but negative for the remaining two, showing no co-localization. Scale bars are (A) 500  $\mu\text{m}$ , (B) 15  $\mu\text{m}$  and (C) 5  $\mu\text{m}$ . Scale bar in F is 5  $\mu\text{m}$  and applies to D-F.

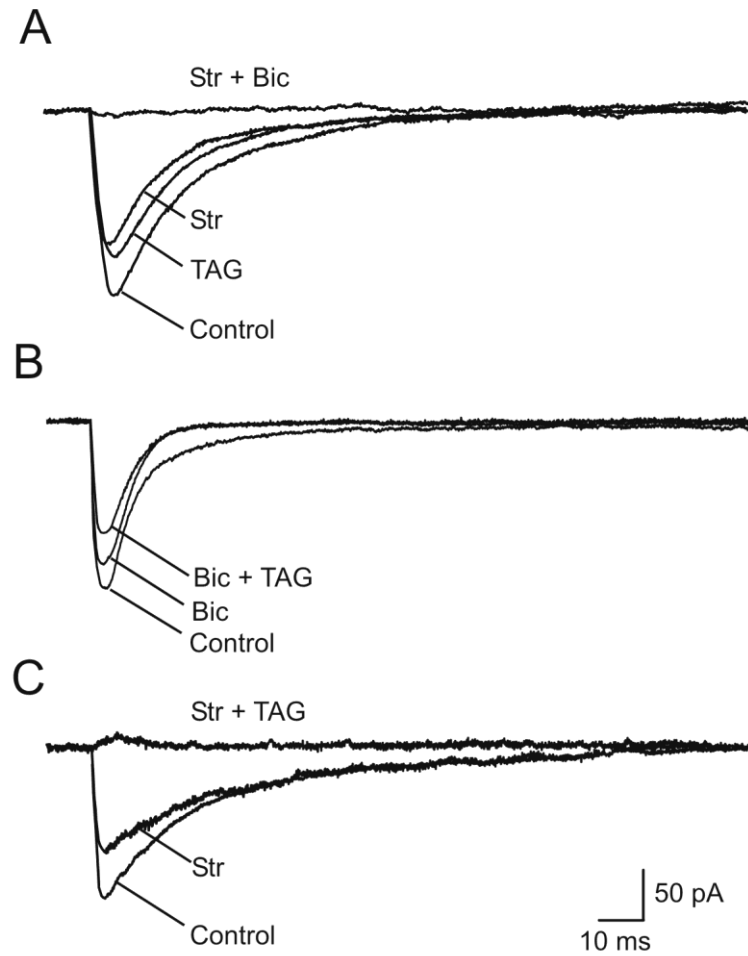


**Figure 2.2. Comparison of effects of TAG with strychnine and bicuculline on mixed IPSCs.** TAG (250  $\mu$ M) reduced the amplitude of IPSCs and pharmacologically isolated components in 3 sample neurons (A-C). The order of drug application is read upwards from each control. Neurons were voltage-clamped at  $V_h = -80$  mV.

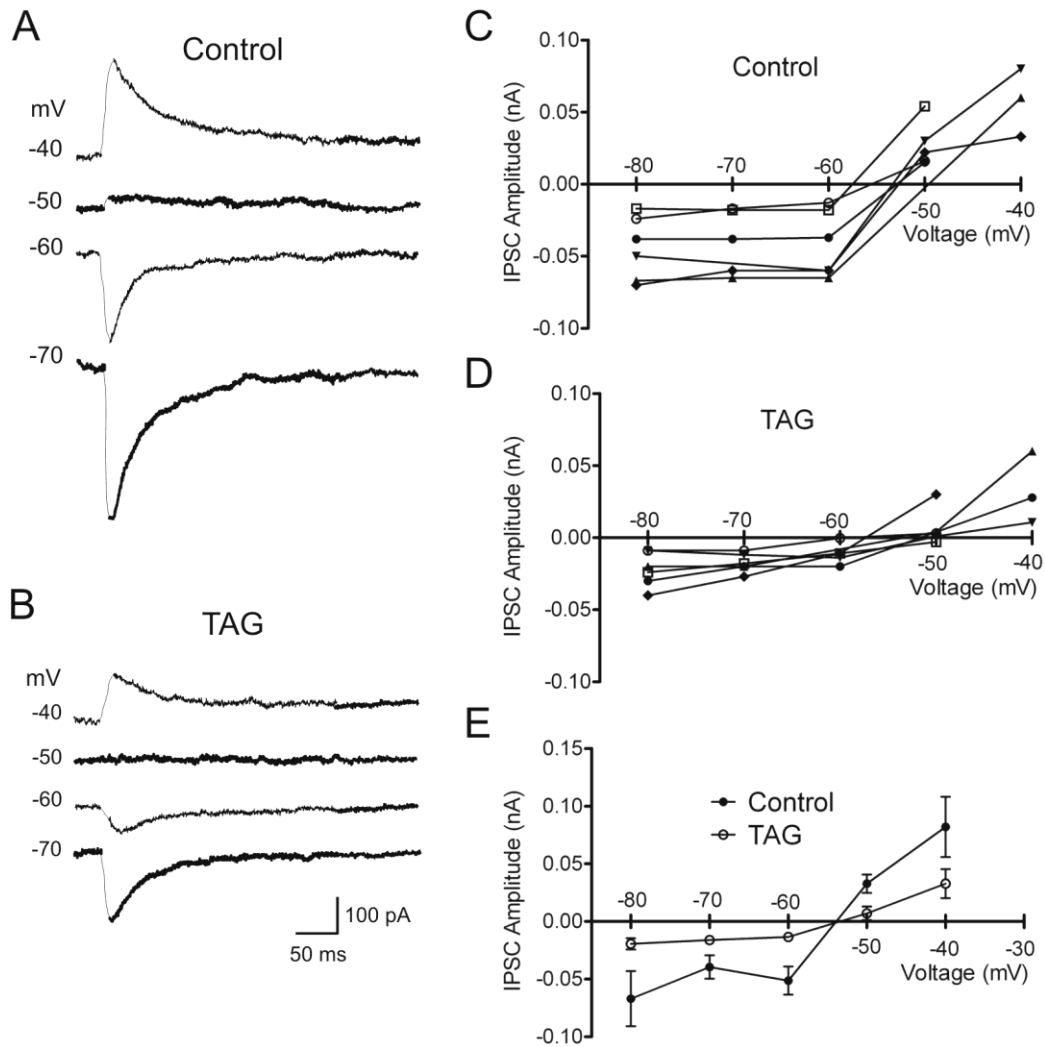


**Figure 2.3. Effects of TAG on voltage-dependence and reversal potentials of mixed IPSCs.** (A-B) Amplitude of control IPSC was reduced by TAG application (250 μM) which also did not greatly change the IPSC reversal potential near -50 mV. Panels (C-D) show IPSC current-voltage relationships for 6 neurons in control (C) and during 250 μM TAG application (D). (E) Mean IPSC current-voltage relationships for these neurons showed that TAG did not alter the IPSC reversal potential which was -54 mV, near  $E_{Cl}$ .

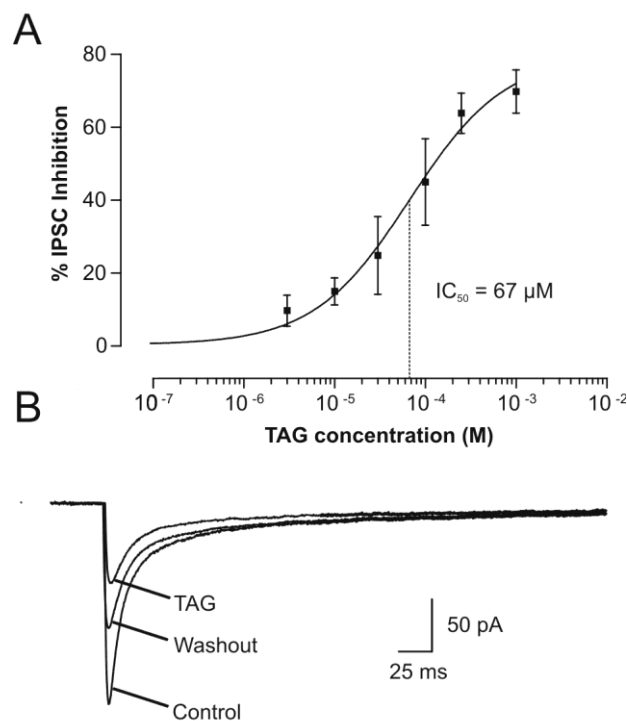


**Figure 2.4. TAG concentration-response curve and partially  $V_h = -80$  mV reversible antagonism of mixed IPSCs.** (A) TAG was applied cumulatively in a stepwise manner to 7 neurons at  $V_h = -80$  mV. The data points, fitted with a sigmoidal function, yielded an  $IC_{50}$  (dashed line) and Hill slope of 0.8. (B) In this representative neuron voltage-clamped at  $V_h = -80$  mV, TAG ( $250 \mu\text{M}$ ) reduced IPSC amplitude by 63% within 8 min of starting the application. Washout of TAG for ~45 min partially restored the IPSC, which remained depressed by 37% relative to control.

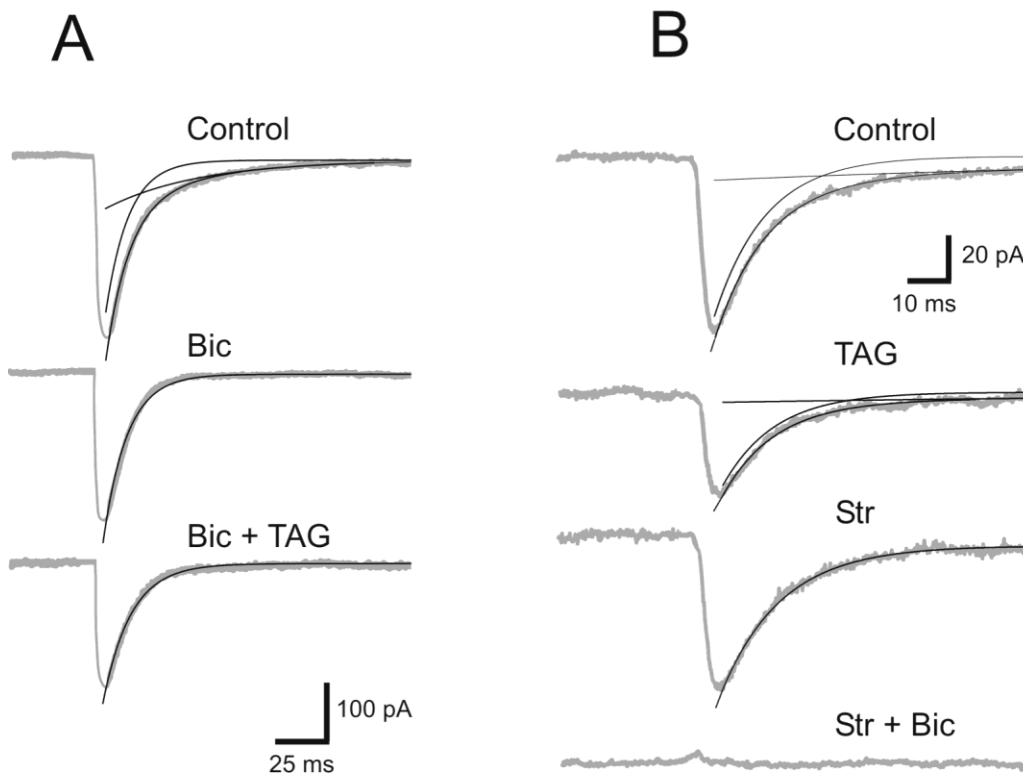


**Figure 2.5. Effects of TAG on kinetically resolved components of mixed IPSCs. (A)**

Type 1 IPSC was well described by a biexponential function (smooth curve superimposed on IPSC). The parameters of the faster component were  $A_1 = -143$  pA,  $\tau = 6.4$  ms and of the slower component were  $A_2 = -46$  pA,  $\tau = 26$  ms. Bicuculline (Bic, 20  $\mu$ M) reduced control amplitude by 15% and resulted in a monoexponential decay with parameters of  $A = -151$  pA and  $\tau = 6.6$  ms. Co-application of Bic and TAG (250  $\mu$ M) reduced the amplitude of the remaining monoexponential component, yielding parameters of  $A = -124$  pA and  $\tau = 7.7$  ms. IPSC parameters returned to near control values after a 60 minute washout of both antagonists (not shown). (B) Type 2 IPSC was well described by a biexponential function with parameters of  $A_1 = -69$  pA and  $\tau_1 = 10.8$  ms (faster), and  $A_2 = -10$  pA and  $\tau_2 = 111$  ms (slower component). TAG (250  $\mu$ M)

reduced IPSC amplitude by 43%, while the decay remained biexponential with parameters of  $A_1 = -41$  pA and  $\tau_1 = 11$  ms (faster component), and  $A_2 = -4.4$  pA and  $\tau_2 = 123$  ms (slower component). Following washout of TAG in 60 minutes, strychnine (Str, 2  $\mu$ M) reduced amplitude by 11% relative to control and changed decay to an exponential function with parameters of  $A = -71$  pA and  $\tau = 13$  ms. Co-application of Str with Bic abolished the IPSC.  $V_h = -80$  mV.

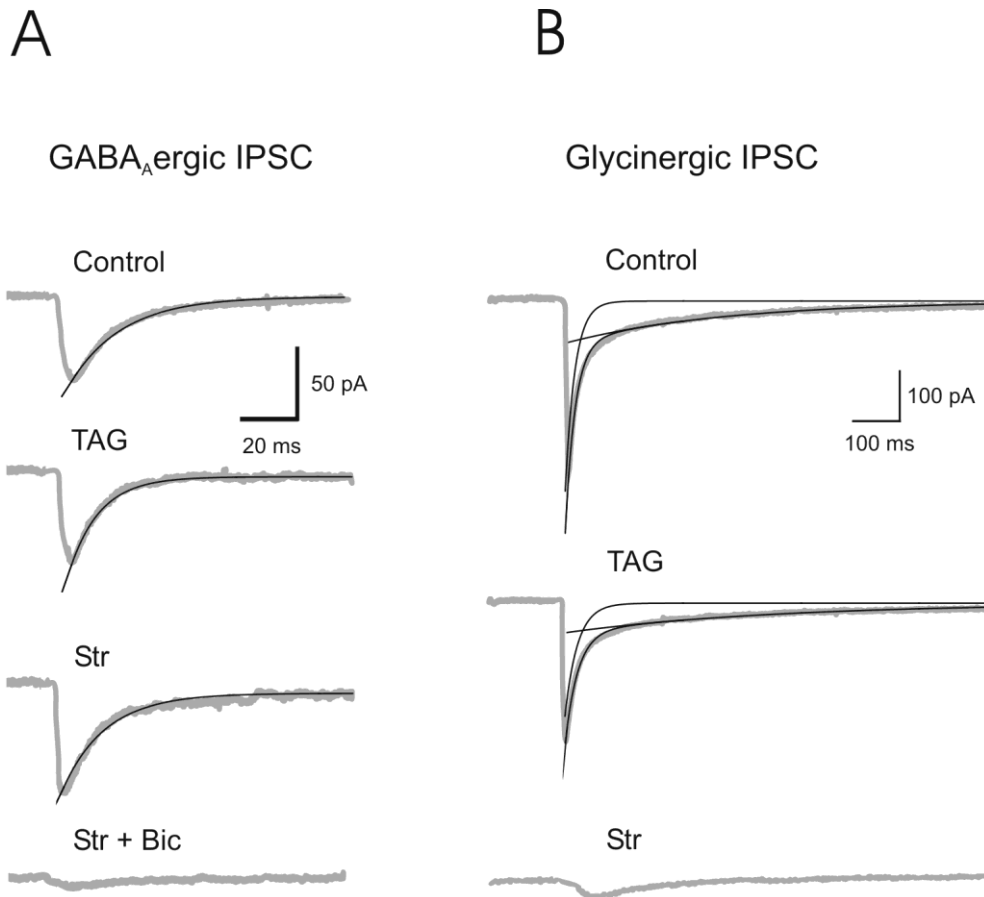


**Figure 2.6. Effects of TAG at 250  $\mu$ M on pure GABAergic and glycinergic IPSCs.**

(A) TAG had no effects on an IPSC, subsequently eliminated by bicuculline (Bic). The control decayed monoexponentially with parameters of  $A = -55$  pA and  $\tau = 20$  ms. TAG application resulted in decay well described by monoexponential function with parameters of  $A = -62$  pA and  $\tau = 14$  ms. After TAG washout, strychnine (Str, 2  $\mu$ M) did not significantly change the amplitude or decay parameters ( $A = -66$  pA,  $\tau = 20$  ms). Co-application of Str with Bic (20  $\mu$ M) abolished the IPSC. (B) Effects of TAG on a Type 3 IPSC, subsequently eliminated by Str. The IPSC had biphasic decay kinetics, well fit with parameters of  $A_1 = -174$  pA and  $\tau_1 = 9.2$  ms (faster component), and  $A_2 = -39$  pA and  $\tau_2 = 151$  ms (slower component). TAG reduced IPSC by 38%, still with

biexponential decay ( $A_1 = -104$  pA and  $\tau_1 = 12$  ms, faster component;  $A_2 = -27$  pA and  $\tau_2 = 201$  ms, slower component). After TAG washout, Str ( $2 \mu\text{M}$ ) reduced IPSC to a negligible level.  $V_h = -80$  mV.

**Table 2.1. Effects of TAG (250  $\mu$ M) on passive properties.**

Property (n =19 neurons)	Control	TAG
–		
Membrane potential (mV)	$-53 \pm 1$	$-49 \pm 2$
Input resistance (M $\Omega$ )	$323 \pm 44$	$222 \pm 38$
Membrane time constant (ms)	$41 \pm 6$	$26 \pm 7$
Capacitance (pF)	$130 \pm 10$	$120 \pm 30$

For all parameters,  $P > 0.05$ , paired  $t$ -test.

**Table 2.2. Effects of TAG (250  $\mu$ M) on the fit parameters for IPSC components.**

Component	Parameter	Control	TAG	Wash
Faster glycinergic				
(n=9)	Amplitude (pA)	-76 $\pm$ 20	-41 $\pm$ 11*	-63 $\pm$ 46
	Time constant (ms)	8.7 $\pm$ 1.2	8.7 $\pm$ 1.0	12 $\pm$ 5
Slower glycinergic				
(n=6)	Amplitude (pA)	-25 $\pm$ 7	-14 $\pm$ 5*	-18 $\pm$ 8
	Time constant (ms)	-228 $\pm$ 87	235 $\pm$ 42	-159 $\pm$ 36
Mixed GABA <sub>A</sub> ergic				
(n=9)	Amplitude (pA)	-134 $\pm$ 72	-59 $\pm$ 26*	-162 $\pm$ 88
	Time constant (ms)	43 $\pm$ 11	30 $\pm$ 8	44 $\pm$ 15
Pure GABA <sub>A</sub> ergic				
(n=6)	Amplitude (pA)	-87 $\pm$ 47	-74 $\pm$ 33	-93 $\pm$ 51
	Time constant (ms)	21 $\pm$ 6	17 $\pm$ 6	16 $\pm$ 6

\* Significantly different from control ( $P < 0.05$ , Wilcoxon test).

Data are mean  $\pm$  S.E.M.

## **2.5. References**

Bamji, S.X., Rico, B., Kimes, N., Reichart, L.F., 2006. BDNF mobilizes synaptic vesicles and enhances synapse formation by disrupting cadherin- $\beta$ -catenin interactions. *Journal of Cell Biology* 174; 289-299.

Billard, J.M., Batini, C., 1991. Decreased sensitivity of cerebellar nuclei neurons to GABA and taurine: effects of long-term inferior olive destruction in the rat. *Neuroscience Research* 9, 246-256.

Curtis, D.R., Leah, J.D., Peet, M.J., 1982. Lack of specificity of a 'taurine-antagonist'. *Brain Research* 244, 198-199.

Dumoulin, A., Rostaing, P., Bedet, C., Levi, S., Isambert, M.F., Henry, J.P., Triller, A., Gasnier, B., 1999. Presence of the vesicular inhibitory amino acid transporter in GABAergic and glycinergic terminal boutons. *Journal of Cell Science* 112, 811-823.

Dumoulin, A., Triller, A., Dieudonne, S., 2001. IPSC kinetics at identified GABAergic and mixed GABAergic and glycinergic synapses onto cerebellar Golgi cells. *Journal of Neuroscience* 21, 6045-6057.

Farrar, S.J., Whiting, P.J., Bonnert, T.P., McKernan, R.M., 1999. Stoichiometry of a ligand-gated ion channel determined by fluorescence energy transfer. *Journal of Biological Chemistry* 274, 10100-10104.

Frosini, M., Sesti, C., Dragoni, S., Valoti, M., Palmi, M., Dixon, H.B.F., Machetti, F., Sgaragli, G., 2003. Interactions of taurine and structurally related analogues with the GABAergic system and taurine binding sites of rabbit brain. *British Journal of Pharmacology* 138, 1163-1171.

Ghavanini, A.A., Mathers, D.A., Puil, E., 2005. Glycinergic inhibition in thalamus revealed by synaptic receptor blockade. *Neuropharmacology* 49, 338-349.

Ghavanini, A.A., Mathers, D.A., Kim, H.S., Puil, E., 2006. Distinctive glycinergic currents with fast and slow kinetics in thalamus. *Journal of Neurophysiology* 95, 3438-3448.

Girard, Y., Atkinson, J.G., Haubrich, D.R., Williams, M., Yarbrough, G.G., 1982. Aminomethyl-1,2,4-benzothiadiazines as potential analogues of  $\gamma$ -aminobutyric acid. Unexpected discovery of a taurine antagonist. *Journal of Medicinal Chemistry* 25, 113-116.

Han, N.L., Haddrill, J.L., Lynch, J.W., 2001. Characterization of a glycine receptor domain that controls the binding and gating mechanisms of the  $\beta$ -amino acid agonist, taurine. *Journal of Neurochemistry* 79, 636-647.

Harris, R.M., 1986. Morphology of physiologically identified thalamocortical relay neurons in the rat ventrobasal thalamus. *Journal of Comparative Neurology* 251, 491-505.

Hussy, N., Deleuze, C., Pantaloni, A., Desarmenien, M.G., Moos, F., 1997. Agonist action of taurine on glycine receptors in rat supraoptic magnocellular neurons: possible role in osmoregulation. *Journal of Physiology* 502, 609-621.

Jia, F., Pignataro, L., Schofield, C.M., Yue, M., Harrison, N.L., Goldstein, P.A. (2005). An extrasynaptic GABA<sub>A</sub> receptor mediates tonic inhibition in thalamic VB neurons. *Journal of Neurophysiology* 94, 4491-4501.

Jia, F., Yue, M., Chandra, D., Keramidas, A., Goldstein, P.A., Homanics, G.E., Harrison, N.L., 2008. Taurine is a potent activator of extrasynaptic GABA<sub>A</sub> receptors in the thalamus. *Journal of Neuroscience* 28, 106-115.

Jiang, Z., Krnjević, K., Wang, F., Yeh, J.H., 2004. Taurine activates strychnine-sensitive glycine receptors in neurons freshly isolated from nucleus accumbens of young rats. *Journal of Neurophysiology* 91, 248-257.

Jonas, P., Bischofberger, J., Sandkuhler, J., 1998. Corelease of two fast neurotransmitters at a central synapse. *Science* 281, 360-361.

Keramidas, A., Harrison, N.L. (2008). Agonist-dependent single channel current and gating in  $\alpha_4\beta_2\delta$  and  $\alpha_1\beta_2\gamma_2S$  receptors. *Journal of General Physiology* 131, 163-181.

Korpi, E.R., Mihalek, R.M., Sinkkonen, S.T., Hauer, B., Hevers, W., Homanics, G.E., Sieghart, W., Luddens, H., 2002. Altered receptor subtypes in the forebrain of GABA<sub>A</sub> receptor  $\delta$  subunit-deficient mice: recruitment of  $\gamma_2$  subunits. *Neuroscience* 109, 733-743.

Lewin, L., Rassin, D.K., Sellstrom, A., 1994. Net taurine transport and its inhibition by a taurine antagonist. *Neurochemical Research* 19, 347-352.

Lu, T., Rubio, M.E., Trussell, L.O., 2008. Glycinergic transmission shaped by the corelease of GABA in a mammalian auditory synapse. *Neuron* 57, 524-535.

Magistretti, J., Mantegazza, M., de Curtis, M., Wanke, E., 1998. Modalities of distortion of physiological voltage signals by patch-clamp amplifiers: a modeling study.

*Biophysical Journal* 74, 831-842.

- Martin, G.E., Bendesky, R.J., Williams, W., 1981. Further evidence for selective antagonism of taurine by 6-aminomethyl-3-methyl-4H-1,2,4-benzothiadiazine-1,1-dioxide. *Brain Research* 299, 530-535.
- Mathers, D.A., 1993. Effects of the benzothiadiazine TAG on channel activation at mammalian glycine receptors. *Neuroscience Letters* 149, 23-26.
- Mathers, D.A., Wan, X., Puil, E., 2007. Barbiturate activation and modulation of GABA<sub>A</sub> receptors in neocortex. *Neuropharmacology* 52, 1160-1168.
- McCool, B.A., Botting, S.K., 2000. Characterization of strychnine-sensitive glycine receptors in acutely isolated adult rat basolateral amygdala neurons. *Brain Research* 859, 341-351.
- Mori, M., Gahwiler, B.H., Gerber, U., 2002.  $\beta$ -Alanine and taurine as endogenous agonists at glycine receptors in rat hippocampus in vitro. *Journal of Physiology* 539, 191-200.
- Okamoto, K., Kimura, H., Sakai, Y., 1983. Evidence for taurine as an inhibitory neurotransmitter in cerebellar stellate interneurons: selective antagonism by TAG (6-aminomethyl-3-methyl-4H,1,2,4-benzothiadiazine-1,1-dioxide). *Brain Research* 265, 163-168.

Ottersen, O.P., Madsen, S., Storm-Mathisen, J., Somogyi, P., Scopsi, L., Larsson, L.I., 1988. Immunocytochemical evidence suggests that taurine is colocalized with GABA in the Purkinje cell terminals, but that the stellate cell terminals predominantly contain GABA: a light- and electronmicroscopic study of the rat cerebellum. *Experimental Brain Research* 72, 407-416.

Padjen, A.L., Mitsoglou, G.M., Hassessian, H., 1989. Further evidence in support of taurine as a mediator of synaptic transmission in the frog spinal cord. *Brain Research* 488, 288-296.

Pow, D.V., Sullivan, R., Reye, P., Hermanussen, S., 2002. Localization of taurine transporters, taurine, and  $^3\text{H}$  taurine accumulation in the rat retina, pituitary, and brain. *Glia* 37, 153-168.

Singer, J.H., Berger, A.J., 1999. Contribution of single-channel properties to the time course and amplitude variance of quantal glycine currents recorded in rat motoneurons. *Journal of Neurophysiology* 81, 1608-1616.

Sohal, V.S., Pangratz-Fuehrer, S., Rudolph, U., Huguenard, J.R., 2006. Intrinsic and synaptic dynamics interact to generate emergent patterns of rhythmic bursting in thalamocortical neurons. *Journal of Neuroscience* 26, 4247-4255.

Takahashi, T., Momiyama, A., Hirai, K., Hishinuma, F., Akagi, H., 1992. Functional correlation of fetal and adult forms of glycine receptors with developmental changes in inhibitory synaptic receptor channels. *Neuron* 9, 1155-1161.

Turecek, R., Trussell, L.O., 2001. Presynaptic glycine receptors enhance transmitter release at a mammalian central synapse. *Nature* 411, 587-590.

Vafa, B., Lewis, T.M., Cunningham, A.M., Jacques, P., Lynch, J.W., Schofield, P.R., 1999. Identification of a new ligand binding domain in the  $\alpha_1$  subunit of the inhibitory glycine receptor. *Journal of Neurochemistry* 73, 2158-2166.

Wu, F.S., Gibbs, T.T., Farb, D.H., 1993. Dual activation of GABA<sub>A</sub> and glycine receptors by  $\beta$ -alanine: inverse modulation by progesterone and 5 $\alpha$ -pregnan-3 $\alpha$ -ol-20-one. *European Journal of Pharmacology* 246, 239-246.

Yarbrough, G.G., Singh, D.K., Taylor, D.A., 1981. Neuropharmacological characterization of a taurine antagonist. *Journal of Pharmacology and Experimental Therapeutics* 219, 604-613.

### **3. <sup>2</sup>SECOND MANUSCRIPT: ISOVALINE CAUSES INHIBITION BY INCREASING POTASSIUM CONDUCTANCE IN THALAMIC NEURONS**

#### **3.1 Introduction**

Isovaline is an amino acid that resembles glycine-like amino acids, especially endogenous  $\alpha$ -alanine and glycine. Although originally found in carbonaceous meteorites (Kvenvolden et al., 1970; Zhao and Bada, 1989), some filamentous fungi synthesize isovaline (Brückner et al., 2009). Fungi grown in media supplemented with RS-isovaline produce a membrane-modifying antibiotic that contains the R-enantiomer (Raap et al., 2005). Both enantiomers of synthetic isovaline can serve as a substrate for amino acid transporters in the gastrointestinal tract (Christensen, 1962). Recently, we demonstrated that the R- and S- enantiomers have analgesic properties when administered intravenously or intrathecally to mice (B.A. MacLeod et al., submitted for publication). However, the pharmacology of isovaline has received little attention.

Inhibition mediated by glycine receptors plays an important role in the central processing of pain information (Zeilhofer, 2005). On administration, glycine-like amino acids suppress hyperalgesia induced by strychnine (Beyer et al., 1988; Yaksh, 1989). Glycine<sub>A</sub> receptors identified by antagonism with strychnine mediate ionotropic inhibition in nociceptive regions of the neuraxis (brainstem, Miraucourt et al., 2007; thalamus, Ghavanini et al., 2005; spinal cord, Racz et al., 2005). Glycine agonists that activate

---

<sup>2</sup> A version of this chapter has been published. Cooke JE, Mathers DA and Puil, E. (2009) Isovaline causes inhibition by increasing potassium conductance in thalamic neurons. *Neuroscience*. 164: 125-1243.

these receptors shunt excitatory currents and reduce firing of such neurons (cf. Ghavanini et al., 2005). At least in theory, prospective analgesics would mimic glycinergic inhibition (cf. Khandwala and Loomis, 1998).

On a basis of the chemical similarity, we anticipated that R-isovaline could suppress the firing of neurons by mimicking the inhibitory actions of glycine in the thalamus. We investigated this possibility using patch clamp recording in the whole-cell configuration in slices of rodent brain.

## **3.2 Experimental procedures**

### **3.2.1. Tissue preparation for immunohistochemistry**

Experiments were approved by the Animal Care Committee at the University of British Columbia. Sprague-Dawley rats (P12) were anesthetized with pentobarbital (40 mg/kg) and transcardially perfused with cold 0.1% PBS, followed by 4% formaldehyde. The brain was dissected and post-fixed in 4% formaldehyde for 2 h at 4°C, followed by submersion in 30% sucrose for 24-48 h at 4°C. The tissue was embedded with Tissue-Tek embedding medium (Sakura Finetek, Torrence, CA) and frozen in liquid nitrogen. Sagittal sections were made at 14 µm thickness and stored at -20°C.

Immunohistochemistry was performed on sections post-fixed in 4% formaldehyde for 10 min. The sections were permeabilized with 0.1% Triton X-100, blocked with 0.5% bovine serum albumin (BSA) in phosphate buffered saline (PBS), and incubated in primary antibody overnight at 4°C in PBS solution containing 0.1% BSA. The primary

antibody was rabbit anti-glycine receptor  $\alpha_{1/2}$  subunit (1: 200; Abcam, Cambridge, MA; ab23809). Sections were incubated in chicken anti-rabbit Alexa 488 secondary antibody for 1 hour at room temperature (Invitrogen, Burlington, ON), followed by 4',6-diamidino-2-phenylindole (DAPI) nuclear counterstain. Sections were coverslipped with Prolong Gold (Invitrogen, Burlington, ON) and allowed to cure overnight before imaging.

Images were captured using an Axioskop 2 MOT epifluorescence microscope (Zeiss, Jena, Germany), fitted with a SPOT camera (Diagnostic Instruments, Sterling Heights, MI) and Northern Eclipse software (Empix Imaging, Mississauga, Ontario, Canada). Image brightness was modified slightly using Adobe Photoshop software to enhance visualization.

### **3.2.2. Slice preparation for electrophysiology**

Tissue preparation for recording is described in detail by Ghavanini et al. (2006). Briefly, the brains of anesthetized rats (P10-15) were placed in oxygenated artificial cerebrospinal fluid (aCSF) at 4°C. Hemispheres were sectioned sagittally into 250  $\mu\text{m}$  thick slices using a vibroslicer (Campden Instruments, London, UK) and incubated for >1 h at 23-25°C in aCSF containing (in mM): 124 NaCl, 26 NaHCO<sub>3</sub>, 1.25 NaH<sub>2</sub>PO<sub>4</sub>, 2.5 KCl, 2 MgCl<sub>2</sub>, 2 CaCl<sub>2</sub>, and 25 dextrose, saturated with 95:5% mixture of O<sub>2</sub> and CO<sub>2</sub>. In some experiments the extracellular K<sup>+</sup> concentration was increased from 2.5 to 5.25 or 9.25 mM, corresponding to K<sup>+</sup> Nernst potentials of -103, -84 and -70 mV. The Nernst potential for Cl<sup>-</sup> was constant at -53 mV.

### 3.2.3. Electrophysiology

Recording procedures were similar to those described previously (Ghavanini et al., 2005). Slices were immobilized in a Perspex recording chamber (volume ~2 ml) and perfused at room temperature (22-24°C) with oxygenated aCSF at a rate of ~2 ml/min. Thalamocortical neurons were visualized at 400x magnification with a differential interference contrast microscope (Axioscope II, Zeiss, Germany).

Recording pipettes were filled with a solution containing (in mM): 133 K-gluconate, 12 KCl, 4 NaCl, 0.5 CaCl<sub>2</sub>, 10 EGTA, 1 HEPES, 3 Mg-adenosine triphosphate, and 0.3 disodium guanosine triphosphate. The pH was adjusted to 7.3-7.4 using 50% gluconic acid or KOH. For K<sup>+</sup> channel blockade in some experiments, cesium salts replaced the potassium salts of gluconate and chloride. In some experiments, the high affinity calcium chelator 1,2-bis(o-aminophenoxy)ethane-N,N,N',N'-tetraacetic acid (BAPTA) replaced EGTA.

Whole-cell, patch clamp recordings were performed using a List EPC 7 amplifier (HEKA, Germany) in current- and voltage-clamp modes. Electrode resistances ranged from 4 to 7 MΩ. Series resistance ranged from 10 to 30 MΩ, and data were discarded if series resistance increased by more than 25%. Signals were filtered (DC-3 kHz), digitized at 10 kHz, and analyzed using pClamp software (Axon Instruments, Sunnyvale CA). Neurons had stable resting potentials and showed burst firing when depolarized from -80 mV. Membrane potentials were corrected for a junction potential of -11 mV.

Input conductance was averaged from steady-state currents in response to -5 mV steps from -70 mV.

#### **3.2.4. Drugs**

Drugs for bath application were either freshly prepared or diluted from stock solutions just prior to use. ZD7288 was purchased from Tocris Cookson (St. Louis, MO), cesium chloride (CsCl) was purchased from Sigma Aldrich (St. Louis, MO) and tetrodotoxin (TTX) was purchased from Alomone Labs (Jerusalem, Israel). R-isovaline was synthesized by BioFine International (Vancouver, BC). The dose-response relationship for R-isovaline was established using single-concentration bath applications to individual neurons. Each neuron tested was subjected to only one experimental condition.

#### **3.2.5. Data analysis**

Data were analyzed and graphed using GraphPad Prism (San Diego, CA), and CorelDraw software (Ottawa, ON). Differences between control and isovaline treatment groups were analyzed using one-way ANOVA, with Bonferroni's post-hoc test for comparison at specific time points. The Pearson correlation coefficient was used to study the relationship between input conductance and current amplitude required to elicit action potentials. Differences were considered significant when  $p < 0.05$ . All data were expressed as means  $\pm$  SEM, where n was number of neurons.

### **3.3. Results**

#### **3.3.1. Effects of R-isovaline on evoked firing in ventroposterolateral neurons**

In this paper we examined a total of 94 neurons with mean resting membrane potential of  $-72 \pm 0.8$  mV and input resistance of  $330 \pm 16$  M $\Omega$ . The neurons were located mostly in the ventroposterolateral (VPL) nucleus. As shown in the sagittal brain section in Fig. 3.1A, this area of the thalamus stained intensively with an antibody to  $\alpha_1$  and  $\alpha_2$  subunits of the glycine receptor. Other thalamic regions, such as the ventroposteromedial (VPM) nucleus, showed markedly less staining with the glycine  $\alpha_{1/2}$  antibody. The high-power insert in Fig. 3.1A shows a group of glycine  $\alpha_{1/2}$ -positive VPL neurons, with nuclei counterstained using DAPI. These observations confirmed the presence of glycine receptor subunits in the ventrobasal thalamus.

We compared effects of isovaline and glycine on firing of action potentials and low threshold spikes (LTSs) evoked by current-pulse injection. Application of isovaline (25  $\mu$ M) inhibited action potentials, either eliminating or reducing their number per pulse (Fig. 3.1B,  $n = 8$ ; 2C,  $n = 8$ ). Isovaline also eliminated the LTSs that gave rise to action potential firing in bursts (Fig. 3.1D,E). Unexpectedly, the inhibitory effects induced by isovaline were resistant to blockade with even high concentrations of strychnine (Fig. 3.1C;  $n = 6$ ). We confirmed that functional glycine<sub>A</sub> receptors were present in the preparations (cf. Ghavanini et al., 2005). The inhibition of firing due to application of 150  $\mu$ M glycine (Fig. 3.1F) was susceptible to antagonism by 2  $\mu$ M strychnine (Fig. 3.1G;  $n = 5$ ). Importantly, the neuron shown in Fig. 3.1F was insensitive to isovaline

application. Hence the inhibitory effects of isovaline were not consistent with an involvement of glycine<sub>A</sub> receptors.

### **3.3.2. Mechanism of inhibitory action on evoked firing**

The inhibitory action of isovaline was surmountable by increasing the depolarizing stimulus. As shown in Figure 3.2A, application of isovaline eliminated action potentials elicited by a 120 pA current-pulse whereas an increase to 180 pA restored the action potentials. The increase in current required to restore the first action potential in the response was significantly correlated to the conductance increase caused by isovaline (Fig. 3.2B;  $r = 0.838$ ;  $n = 8$ ). Similar restoration of the LTS and accompanying burst was observed on increasing the amplitude of the hyperpolarizing current pulse (Fig. 3.2D). Isovaline had no effects on the threshold, amplitude, half width, or rates of rise and fall of action potentials (Table 1) (Insert Table 1 about here). These observations suggested that isovaline acted by shunting action potential and LTS generation.

### **3.3.3. Effects on membrane properties**

Under voltage-clamp conditions, isovaline (25  $\mu\text{M}$ ) produced membrane effects on 11 out of 17 neurons. The input conductance determined from the current response to a step from -70 to -75 mV, increased on isovaline application (Fig. 3.3A). The remaining 6 neurons failed to respond to 25  $\mu\text{M}$  with a  $\geq 10\%$  change in conductance, despite observation for 25-30 min. The responsive neurons showed a 15-20% increase in conductance that further increased to  $\sim 60\%$  during isovaline washout. Under current-clamp conditions, these neurons hyperpolarized by 1-5 mV (Fig. 3.3A, lower) which

mirrored the conductance changes over the same time course. In a majority of neurons, the effects of isovaline did not reverse after washout for up to 2 h. However, several neurons either completely or partly recovered during a 20 min washout period. Figure 3.3B shows the reversibility of effects on conductance and potential in 3 neurons. In summary of most neurons, isovaline application at 25  $\mu\text{M}$  triggered persistent changes in conductance and hyperpolarization.

#### **3.3.4. Dose-response relationship**

Given the persistent effects, we examined the dose-dependence of the conductance change by applying each concentration only once to a neuron and slice. As shown in Figure 3.3C, a non-sigmoidal relationship was evident between the conductance increase and isovaline concentration. An apparently maximal response occurred at  $\sim 100 \mu\text{M}$  whereas higher concentrations resulted in smaller conductance changes. This unusual relationship suggested that isovaline did not act like conventional amino acid ligands (cf. Discussion). The lack of a response to isovaline concentrations of 10  $\mu\text{M}$  to 25 mM did not apparently correlate to the anatomical location of the tested neuron. For example, we observed that there were both responsive and non-responsive neurons in VPL and VPM nuclei (Fig. 3.3D).

#### **3.3.5. Current-voltage (I-V) relationship for isovaline action**

Our observations of a conductance increase combined with a hyperpolarization implicated  $\text{K}^+$  currents in isovaline action. To study this possibility, we examined isovaline effects on steady-state I-V relationships of neurons clamped to -70 mV (Fig.

3.4A,B). The individual currents evoked by steps between -120 and -20 mV showed that isovaline increased net outward current. In the I-V relationships, this increase was evident at potentials positive to  $E_K$  (-103 mV). The difference current showed that isovaline application caused a large increase in outward rectification between -100 and -50 mV and a small net inward current at potentials negative to  $E_K$ , with a reversal at  $-91 \pm 4$  mV ( $E_{R-Iva}$ ). These results suggested that  $K^+$  was the main contributor to the isovaline-induced current.

Because  $E_{R-Iva}$  was depolarized by 12 mV from  $E_K$ , a  $Cl^-$  current may have contributed to  $E_{R-Iva}$ . For reference, we determined the I-V relationships during glycine application in 5 neurons (Figs. 3.4C,D). As expected, glycine actions were eliminated by strychnine, reversed close to  $E_{Cl}$  and hence, were mostly attributable to  $Cl^-$  current. Co-application of strychnine and isovaline to 6 neurons did not result in a significantly different  $E_{R-Iva}$  ( $-90 \pm 6$  mV;  $p > 0.05$ , ANOVA). Thus, there was little or no glycine<sub>A</sub> receptor involvement in isovaline's action.

### 3.3.6. Identifying the ionic basis for isovaline inhibition

Potassium channel blockers prevented the effects of isovaline. We studied isovaline effects on neurons treated with the  $K^+$  channel blockers,  $Ba^{2+}$  (100  $\mu$ M) and  $Cs^+$  (3 mM). Pre-treatment of  $Ba^{2+}$  in 6 neurons reduced the magnitude of inward rectification on stepping from -70 to -120 mV (Fig. 3.5A). On co-application with isovaline (75  $\mu$ M), no additional change in current was observed in this voltage range or at voltages up to -30 mV (Fig. 3.5B;  $p > 0.05$ ). Pre-treatment of  $Cs^+$  in 6 neurons greatly reduced the

magnitude of inward rectification (Fig. 3.5C). On co-application with isovaline (75  $\mu\text{M}$ ), no additional change in current was observed in this voltage range or at voltages up to -30 mV (Fig. 3.5D;  $n = 4$ ,  $p > 0.05$ ). These results demonstrated that  $\text{K}^+$  currents were largely responsible for the effects of isovaline.

Replacement of intracellular  $[\text{K}^+]$  with the blocker  $\text{Cs}^+$  in 5 neurons reduced the average inward current elicited by hyperpolarizing steps from -70 to -110 mV, compared to 6 neurons with normal intracellular  $[\text{K}^+]$  (Fig. 3.6A). Co-application of isovaline to the 5 neurons with intracellular  $\text{Cs}^+$  produced negligible effects on conductance over the voltage range -90 to -60 mV (Fig. 3.6B;  $p > 0.05$ ). The small difference current observed at voltages negative to -90 mV may have reflected unblocking of  $\text{K}^+$  channels by inward  $\text{K}^+$  currents (cf. Armstrong, 1966). The blockade with intracellular  $\text{Cs}^+$  confirmed that  $\text{K}^+$  currents were the major contributors to isovaline actions.

### **3.3.7. Effects of altering extracellular $\text{K}^+$ concentration on $E_{\text{R-Iva}}$**

As a further test for  $\text{K}^+$  involvement, we altered the extracellular  $\text{K}^+$  concentration,  $[\text{K}^+]_e$ , and determined the subsequent effects on  $E_{\text{R-Iva}}$ . An increase in  $[\text{K}^+]_e$  from 2.5 mM shifted  $E_{\text{R-Iva}}$  to more positive potentials, remaining slightly depolarized from the calculated values of  $E_{\text{K}}$  (Fig. 3.6C). While a major contribution of  $\text{K}^+$  conductances to isovaline actions seemed assured, we investigated possible contributions from other cationic conductances.

Co-application with TTX (300 nM) had little or no effect on the isovaline-induced conductance change (data not shown). An isovaline action on a persistent  $\text{Na}^+$  conductance was unlikely because TTX did not shift  $E_{\text{R-Iva}}$  towards  $E_{\text{K}}$  (data not shown; cf. Fig. 3.4B). An involvement of  $\text{Ca}^{2+}$  currents also was unlikely because replacement of EGTA by the fast chelator BAPTA (10 mM) in the recording pipette did not reduce isovaline-induced currents or produce a hyperpolarizing shift in  $E_{\text{R-Iva}}$ , as expected for  $\text{Ca}^{2+}$ -dependent  $\text{K}^+$  currents (data not shown). In short, indirect effects due to mediator release or actions on voltage-dependent  $\text{Na}^+$  and  $\text{Ca}^{2+}$  channels did not likely contribute to isovaline actions.

We examined the possibility that action on a hyperpolarization-activated  $\text{Na}^+/\text{K}^+$  current ( $I_{\text{h}}$ ) contributed to the isovaline-induced current. On blockade of inwardly rectifying  $\text{K}^+$  currents with  $\text{Ba}^{2+}$  (100  $\mu\text{M}$ ) and stepping from -70 mV to -120 mV for 4 s,  $I_{\text{h}}$  was apparent as a slowly activating inward current (cf. Fig. 3.7A). In 6 neurons, isovaline did not alter the amplitude of  $I_{\text{h}}$  (Fig. 3.7B;  $p > 0.05$ , ANOVA). Without  $\text{Ba}^{2+}$ , co-application of isovaline with the  $I_{\text{h}}$  blocker, ZD7288 did not prevent the appearance of an outward current at potentials positive to, and inward current negative to  $E_{\text{K}}$  (Fig. 3.7C). Using  $t$ -test comparisons ( $p > 0.05$ ), the amplitude of the isovaline-induced current was not altered by ZD7288 in 3 neurons (-120 mV,  $-37 \pm 41$  pA; -40 mV,  $65 \pm 23$  pA) from 6 control neurons (-120 mV,  $-32 \pm 15$  pA; -40 mV,  $70 \pm 14$  pA). After pre-treatment with ZD7288,  $E_{\text{R-Iva}}$  was  $-99 \pm 4$  mV, not different from control ( $n = 3$ ,  $p > 0.05$ ,  $t$ -test). These results indicated that the deviation of  $E_{\text{R-Iva}}$  from  $E_{\text{K}}$  was not due to activation of  $I_{\text{h}}$  by isovaline.

### **3.4. Discussion**

Our research has shown that R-isovaline inhibited thalamic neurons through an unexpected mechanism, distinct from agonist action at the glycine<sub>A</sub>-receptor. On isovaline application, ventrobasal neurons developed rectifying K<sup>+</sup> currents in a dose-dependent, long-lasting manner. The increased conductance shunted action potential or LTS generation and hyperpolarized neurons. The decreased excitability of these neurons may partly account for the anti-nociceptive effects of isovaline when administered systemically in pain models (cf. Introduction).

The chief reason for the depression of excitability produced by isovaline was the increased input conductance, which shunted action potential generation and caused a hyperpolarization. Isovaline did not affect threshold, half width, amplitude, rate of rise and fall of action potentials or LTSs (Table 1). The depression extended to a shunt of LTS firing observed during TTX-blockade of Na<sup>+</sup> channels. Shunting was apparent from the restoration of evoked firing on increasing the magnitude of injected current. Hence isovaline did not alter voltage-dependent Na<sup>+</sup> and K<sup>+</sup> conductances in the action potential and T-type Ca<sup>2+</sup> conductance in the LTS. Since  $E_{Cl}$  was positive to the resting potential, the major current in isovaline action was not mediated by Cl<sup>-</sup>. The combination of a conductance increase and hyperpolarization implicated K<sup>+</sup>.

An examination of the current-voltage relationships revealed that isovaline acted by increasing K<sup>+</sup> conductance. The reversal potential ( $E_{R-Iva}$ ) for this action was near  $E_K$ .

On increasing extracellular  $[K^+]$ ,  $E_{R-Iva}$  shifted to more depolarized voltages with a slope similar to prediction by the Nernst equation. In contrast, glycine elicited currents that reversed in polarity near  $E_{Cl}$  (cf. Ghavanini et al., 2005). Whereas strychnine antagonized the glycine currents, isovaline-induced currents were insensitive to strychnine. Hence isovaline was not an agonist at glycine<sub>A</sub> receptors, but acted predominantly through  $K^+$  currents.

Observations on blockers of  $K^+$  currents demonstrated a major role for rectifiers. Intracellular  $Cs^+$  which blocks rectifying and leak  $K^+$  currents (cf. Golshani et al., 1998) suppressed the responses to isovaline. Extracellular  $Ba^{2+}$  or  $Cs^+$  which blocked the inward rectifier,  $I_{Kir}$ , and leak current (McCormick and Pape, 1990; Wan et al. 2003), also prevented the responses. At holding potentials near rest, a constitutive  $I_h$  confounded measurements of the voltage-independent current. During ZD7288 blockade of  $I_h$ , however, isovaline increased the leak current at  $V_h = -70$  mV (cf. Figure 3.7C). Isovaline induced appreciable currents at potentials positive to  $-60$  mV indicating involvement of additional  $K^+$  currents, such as outward rectifiers. These results were consistent with isovaline actions on several types of  $K^+$  channels.

We observed that  $E_{R-Iva}$  was several millivolts depolarized to  $E_K$ . Chelation by internal BAPTA or application of TTX or ZD7288 had little effect on isovaline-induced currents. Hence, the offset was not due to  $Ca^{2+}$  involvement, voltage-dependent  $Na^+$  channels, or  $I_h$  activation. The large conductance shunt introduced by isovaline may have impaired voltage control at remote dendritic sites. However, errors of this type should cause

overestimation rather than underestimation of  $E_{R-Iva}$  negativity (cf. Ries and Puil, 1999). Although a strychnine-insensitive  $Cl^-$  current or a mixed cationic conductance may have contributed, the source of the offset in  $E_{R-Iva}$  remains unknown.

In this study, many neurons did not respond to isovaline application in a range of 10  $\mu$ M to 25 mM. At 25  $\mu$ M which was the most commonly tested dose, isovaline did not produce a conductance change of >10% in 6 out of 17 neurons. It is conceivable that a first application at a higher dose may have elicited a response in these neurons. The reasons for failure of neurons to respond remain unknown but may relate to an absence of a presumed receptor for isovaline.

This study has identified isovaline's ability to inhibit neurons and the main aspects of its mechanism of action. Other substances with analgesic properties cause inhibition by increasing  $K^+$  conductance (reviewed by Ocana et al., 2004), with selective coupling to G-protein-coupled inwardly rectifying  $K^+$  channels (GIRK channels). Metabotropic receptors are frequently coupled to GIRK channels, as with acetylcholine muscarinic, GABA<sub>B</sub>, 5-hydroxytryptamine 5-HT<sub>1A</sub>, nociceptin, and opioid receptors (e.g., Pham and Lacaille, 1996; Brunton and Charpak 1998). In view of these possibilities, the exact signalling pathways that couple isovaline application to development of  $K^+$  currents require detailed study.

In summary, our results showed that R-isovaline was not an agonist at glycine<sub>A</sub> receptors. R-isovaline inhibited firing in nociceptive thalamus by a shunt mechanism, mainly

reflecting an increased  $K^+$  conductance. Isovaline enhanced  $K^+$  currents including rectifying and possibly leak currents that were sensitive to block by  $Cs^+$  and  $Ba^{2+}$ . Isovaline responses were notably long-lasting and displayed a non-sigmoidal relationship with dose. Shunting of action potentials would impair faithful transmission of pain information to cortex. An ability to shunt action potentials and spike bursts in cortico-thalamocortical circuits suggests that isovaline may produce analgesia without sedative side-effects.

**Figures**

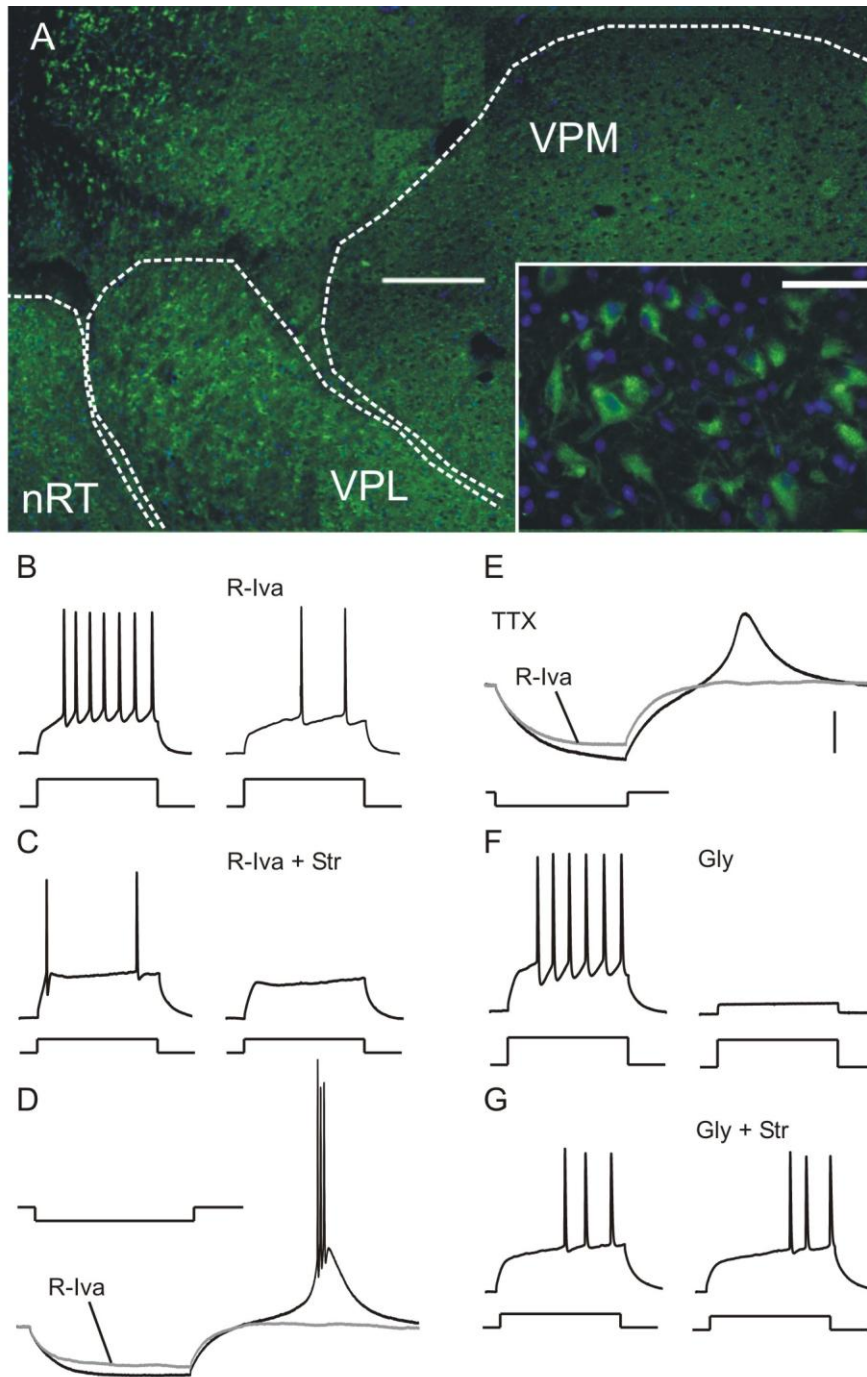


**Figure 3.1. Isovaline inhibited action potential and low threshold spike (LTS) firing in neurons by actions independent of glycineA receptors. (A) Low-power**

epifluorescence micrograph montage shows sagittal section of rat thalamus (P12) stained with glycine  $\alpha_{1/2}$  antibody (green), with nuclei counter-staining using DAPI (blue). Ventroposterolateral (VPL), ventroposteromedial (VPM), and reticular (nRT) nuclei are outlined. The insert shows a high-power image taken from the VPL nucleus, showing numerous glycine  $\alpha_{1/2}$  antibody-positive cells. Scale bar is 250  $\mu\text{m}$  in A, 50  $\mu\text{m}$  in insert. (B, D) Application (4-5 min) of isovaline (R-Iva, 25  $\mu\text{M}$ ) decreased frequency of action potentials evoked by pulse injection (90 pA, 400 ms) and eliminated LTS evoked at offset of hyperpolarizing pulse injection. (E) During TTX blockade of action potentials, R-Iva (75  $\mu\text{M}$ ) eliminated LTS in association with increased conductance (reduced pulse amplitude). Co-application with strychnine (Str, 20  $\mu\text{M}$ ) did not prevent inhibition (C). (F, G) In 2 neurons, glycine application (150  $\mu\text{M}$ ) caused inhibition of action potentials that was prevented by co-application with Str (2  $\mu\text{M}$ ). Neuron in F was previously found to be unresponsive to isovaline. Vertical bar represents 25 mV for B, C, F, G and 15 mV in D, 10 mV in E. Current pulse calibration, 90 pA in B.  $V_h = -70$  mV as in subsequent figures.

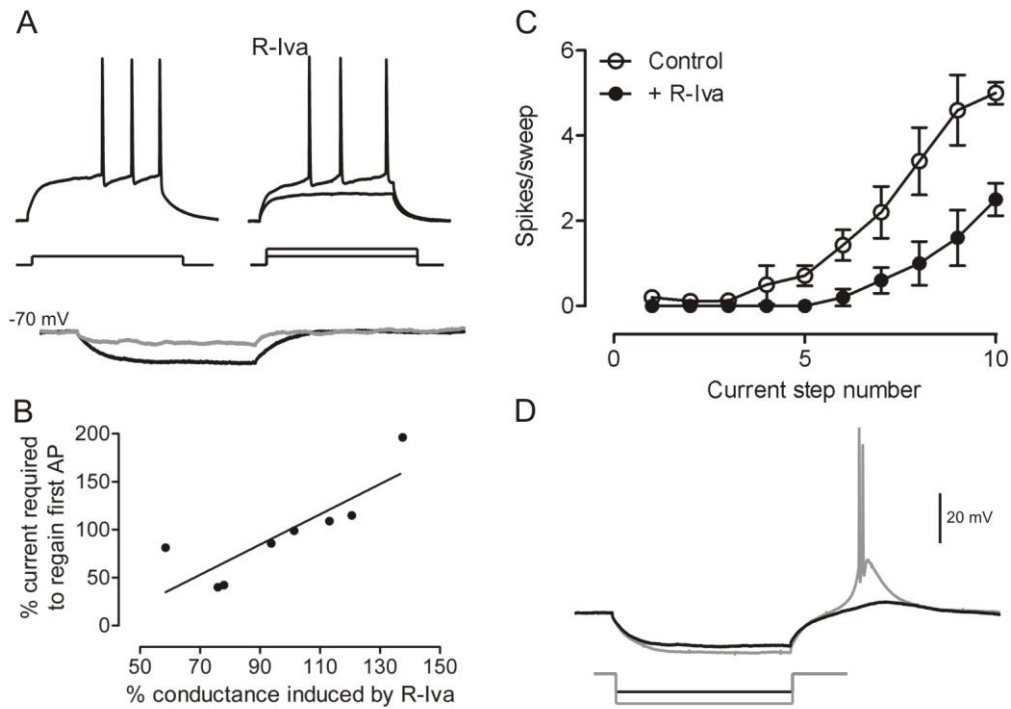


**Figure 3.2. Increased conductance shunted genesis of action potential and LTS. (A)**

Blockade of firing (120 pA pulse) by isovaline was surmountable by increasing pulse amplitude to 180 pA. Lower record in (A) shows that 22 mV hyperpolarization (black) due to a 25 pA pulse was reduced to 13 mV by isovaline (grey), demonstrating a 41% increase in conductance in the same neuron. (B,C) Increase in current required to restore the first action potential in response correlated to the conductance increase induced by isovaline ( $r = 0.838$ ,  $n = 8$  neurons). Isovaline decreased total number of spikes/400 ms pulse in all 8 neurons. (D) Total blockade of LTS (45 pA pulse) by isovaline was surmountable by increasing pulse amplitude to 75 pA (grey).

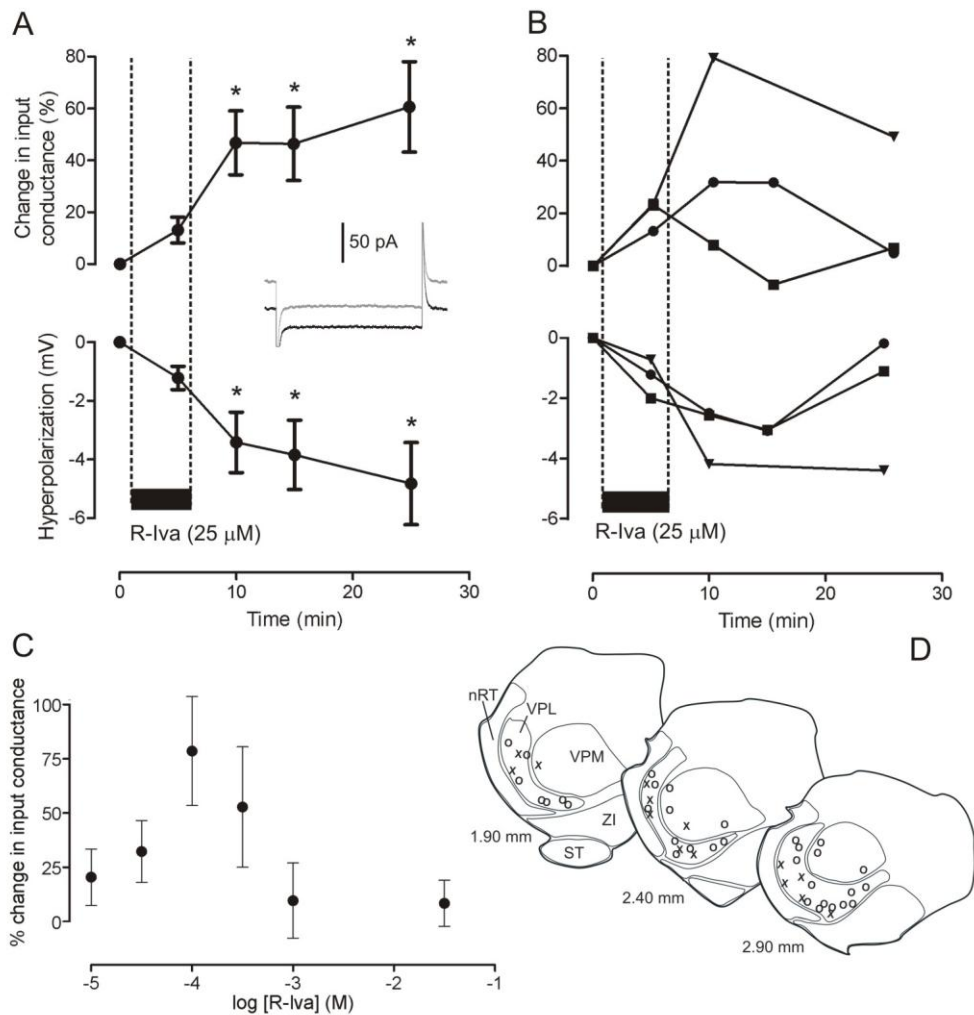


**Figure 3.3. Increased input conductance in voltage-clamp caused persistent hyperpolarization and was concentration-dependent.** (A) Conductance and potential changes greatly outlasted period of application (black bars in A and B). Insert shows determination of input conductance using 400 ms voltage steps from  $-70$  to  $-75$  mV (control current, black trace; current after isovaline, grey trace).  $*p < 0.05$ , ANOVA compared with control,  $n = 11$ . (B) Three neurons showed substantial reversibility of

changes induced by isovaline. (C) Dose-response relationship for isovaline was non-sigmoidal, showing a maximal response near 100  $\mu\text{M}$  ( $n = 37$ ).

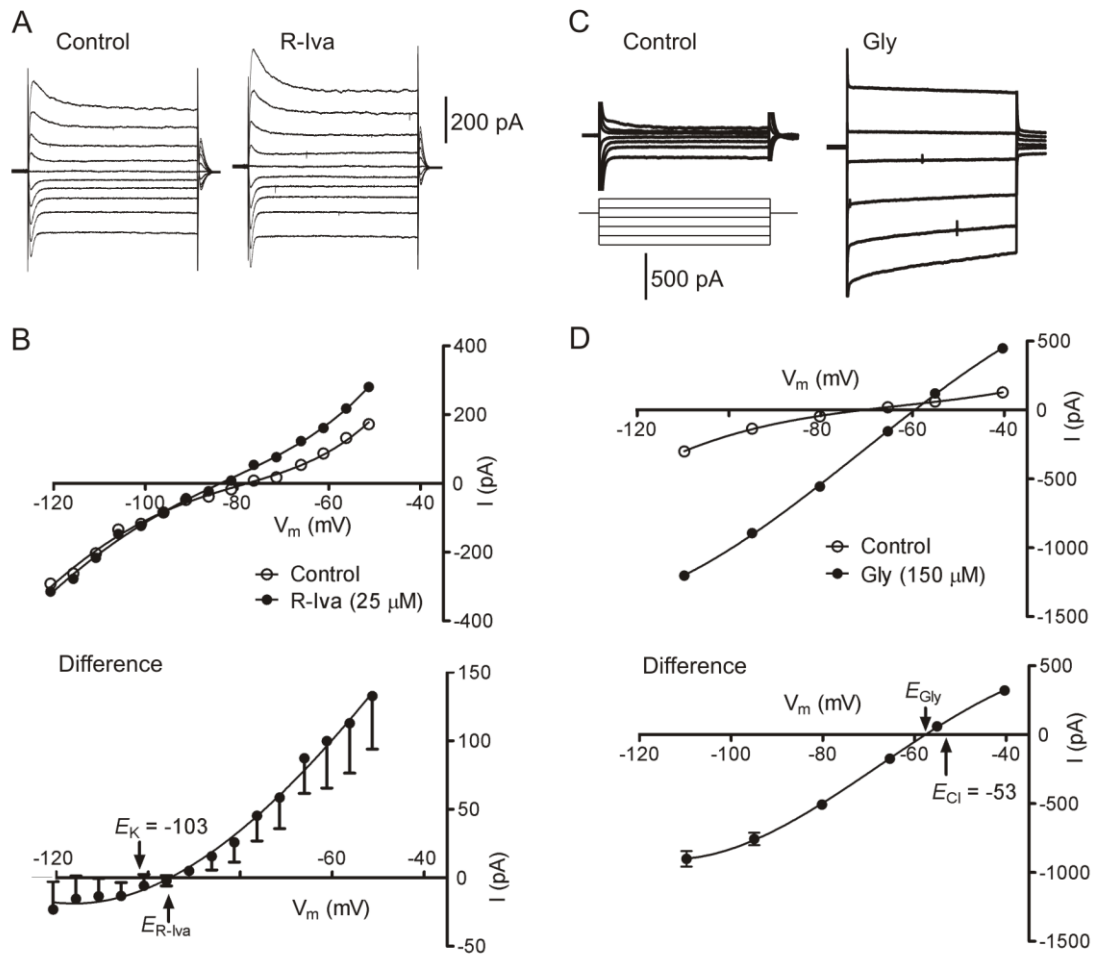


**Figure 3.4. Current-voltage (I/V) relationships during isovaline administration**

**showed reversal near  $E_K$ , dissimilar to glycine.** (A) Isovaline (R-Iva, 75  $\mu\text{M}$ ) increased the magnitude of currents in a neuron stepped in 10 mV increments between -120 and -30 mV ( $V_h = -70$  mV, 400 ms pulses). (B) I/V relationships averaged for 6 neurons (error bars omitted for clarity) showed that 25  $\mu\text{M}$  isovaline induced outward current at potentials positive to, and a small inward current negative to  $E_K$  (-103 mV). Difference current shows reversal potential ( $E_{\text{R-Iva}}$ ) near -91 mV. (C) Glycine (150  $\mu\text{M}$ ) increased rectifying currents in neuron stepped from  $V_h = -70$  mV to between -110 and -40 mV. Note decrease in holding current. (D) Glycine applied to 5 neurons (error bars omitted

for clarity) induced outward current at potentials positive to, and inward current at potentials negative to the reversal potential for glycine action ( $E_{\text{Gly}}$ ) which was near  $E_{\text{Cl}}$ .

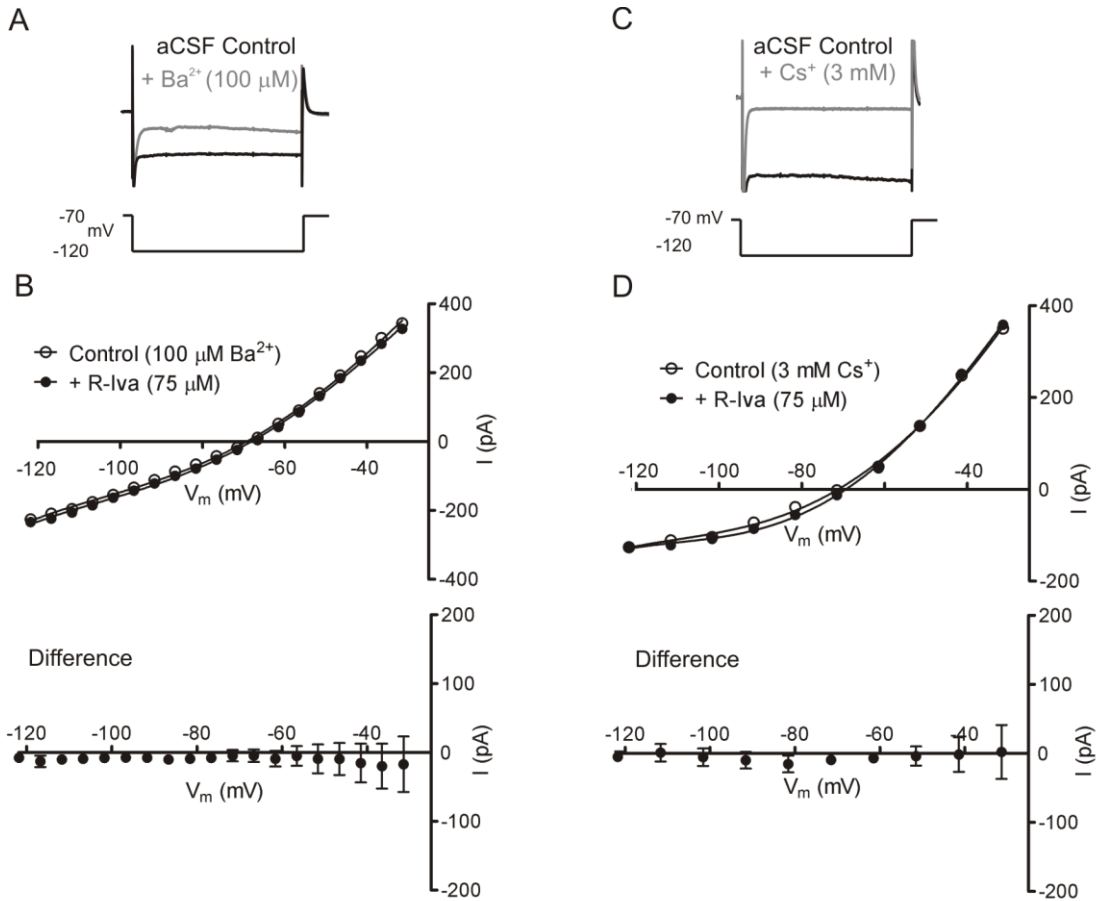


**Figure 3.5. Extracellular K<sup>+</sup> channel blockers prevented isovaline actions on voltage-dependent currents.** (A) An exemplary neuron in which Ba<sup>2+</sup> (100 μM; grey trace) reduced inward current due to a voltage step from -70 to -120 mV. (B) Co-application of isovaline (75 μM) with Ba<sup>2+</sup> to 6 neurons did not increase conductance in the voltage range of -120 to -30 mV (cf. difference curve). (C) An exemplary neuron in which Cs<sup>+</sup> (3 mM; grey trace) reduced the current due to voltage step from -70 to -120 mV. (D) Co-application of isovaline (75 μM) to 4 neurons did not increase conductance in the voltage range of -120 to -30 mV (cf. difference curve).

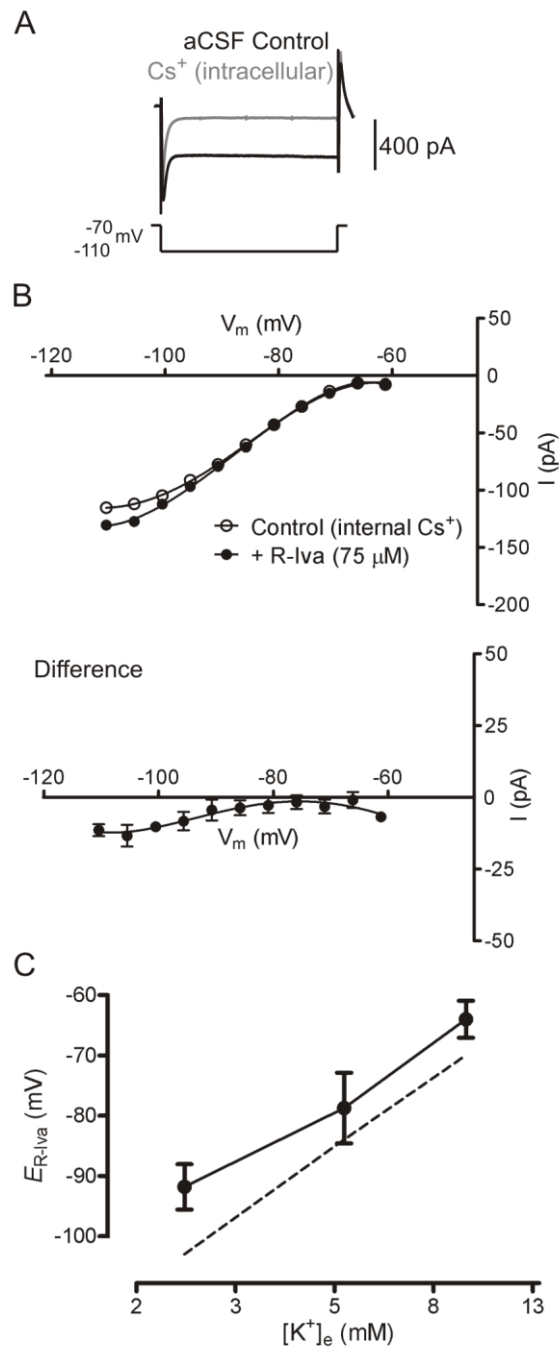


**Figure 3.6. Intracellular K<sup>+</sup> channel blockade with Cs<sup>+</sup> prevented isovaline action.**

(A) In 5 neurons where intracellular Cs<sup>+</sup> replaced K<sup>+</sup> (grey trace), there was a marked decrease in the inward current, compared to 6 neurons with normal K<sup>+</sup> (black trace). (B) Isovaline (75 μM) applied to 6 neurons recorded with intracellular Cs<sup>+</sup> did not cause a

conductance increase in the voltage range of -90 to -60 mV (cf. difference curve). (C)

On varying the external  $[K^+]$ , the reversal potential for isovaline was close to, but slightly more depolarized than  $E_K$ .

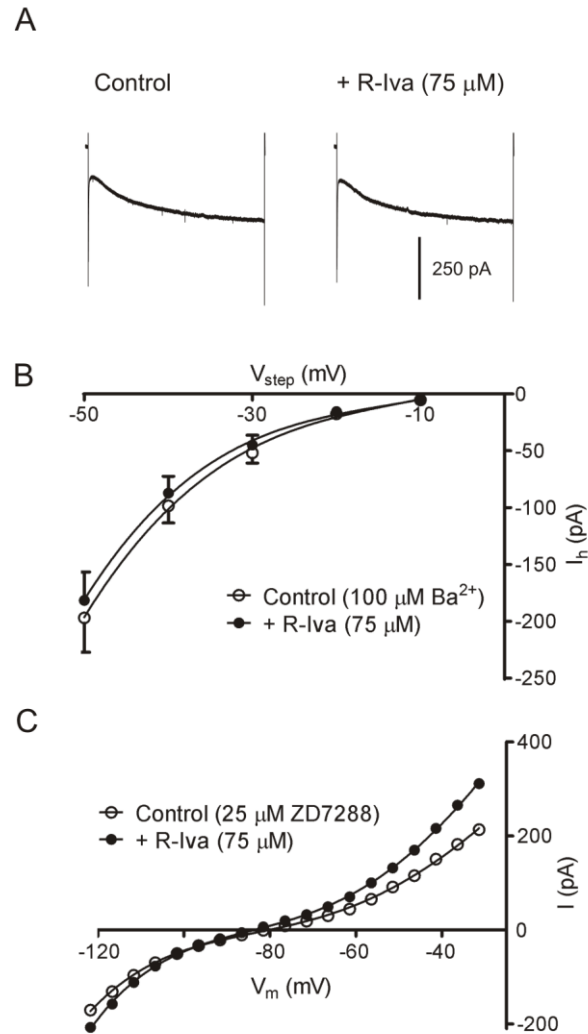


**Figure 3.7. Isovaline did not alter  $I_h$ .** (A)  $I_h$  evoked by 4s steps from -70 mV to -120 mV was unchanged in a neuron on application of 75  $\mu$ M isovaline.  $I_h$  was obtained by subtracting the current amplitude at 40 ms after beginning of the pulse from the amplitude near the end of the pulse. (B) In 6  $Ba^{2+}$ -treated neurons, the mean amplitude of  $I_h$  evoked by the indicated voltage steps ( $V_{step}$ ) from  $V_h = -70$  mV was unchanged after application of isovaline. (C) Mean I-V relationships for 3 neurons determined during ZD7288 application and co-application with isovaline.

**Table 3.1. R-isovaline (25  $\mu$ M – 250  $\mu$ M) did not alter properties of action potentials evoked by depolarizing current pulses.**

	Control	Isovaline	5' wash	10' wash	20' wash
Threshold (mV)	-44 $\pm$ 2	-44 $\pm$ 2	-43 $\pm$ 2	-43 $\pm$ 3	-44 $\pm$ 2
Amplitude (mV)	60 $\pm$ 2	58 $\pm$ 2	59 $\pm$ 2	59 $\pm$ 2	62 $\pm$ 1
Rate of rise (mV/ms)	84 $\pm$ 10	75 $\pm$ 8	78 $\pm$ 10	82 $\pm$ 7	89 $\pm$ 5
Rate of fall (mV/ms)	-20 $\pm$ 2	-19 $\pm$ 2	-20 $\pm$ 2	-20 $\pm$ 2	-23 $\pm$ 1
Half width (ms)	1.5 $\pm$ 0.2	1.6 $\pm$ 0.2	1.5 $\pm$ 0.2	1.4 $\pm$ 0.1	1.2 $\pm$ 0.1

Data are mean  $\pm$  S.E.M, n = 8. ANOVA showed no significant differences in any parameter. Action potentials were elicited from a holding potential of -70 mV.

### **3.5. References**

Armstrong C (1966), Time course of TEA<sup>+</sup>-induced anomalous rectification in squid giant axons. *J. Gen. Physiol.* **50(2)**: 491-503.

Beyer C, Banas C, Gomora P, Komisaruk BR (1988), Prevention of the convulsant and hyperalgesic action of strychnine by intrathecal glycine and related amino acids. *Pharmacol. Biochem. Behav.* **29**: 73-78.

Brückner, H, Becker, D, Gams, W, Degenkolb, T (2009), Aib and iva in the biosphere: neither rare nor necessarily extraterrestrial. *Chem. Biodivers.* **6**: 38-56.

Brunton J, Charpak S (1998),  $\mu$ -Opioid peptides inhibit thalamic neurons. *J. Neurosci.* **18**: 1671-1678.

Christensen HN (1962), Intestinal absorption with special reference to amino acids. *Gastroenterol.* **21**: 37-42.

Ghavanini AA, Mathers DA, Puil E (2005), Glycinergic inhibition in thalamus revealed by synaptic receptor blockade. *Neuropharmacol.* **49**: 338-349.

Ghavanini AA, Mathers DA, Kim HS, Puil E (2006), Distinctive glycinergic currents with fast and slow kinetics in thalamus. *J. Neurophysiol.* **95**: 3438-3448.

Golshani P, Warren RA, Jones EG (1998), Progression of change in NMDA, non-NMDA, and metabotropic glutamate receptor function at the developing corticothalamic synapse. *J. Neurophysiol.* **80**: 143-154.

Khandwala H, Loomis CW (1998), Milacemide, a glycine pro-drug, inhibits strychnine-allodynia without affecting normal nociception in the rat. *Pain* **77**: 87-95.

Kvenvolden KA, Lawless J, Pering K, Peterson E, Flores J, Ponnampereuma C, Kaplan I, Moore C (1970), Evidence for extraterrestrial amino-acids and hydrocarbons in the Murchison meteorite. *Nature* **228**: 923-926.

McCormick DA, Pape H-C (1990), Properties of a hyperpolarization-activated cation current and its role in rhythmic oscillation in thalamic relay neurones. *J. Physiol.* **431**: 291-318.

Miracourt LS, Dalle R, Voisin DL (2007), Glycine inhibitory dysfunction turns touch into pain through PKC $\gamma$  interneurons. *PLoS ONE* [Epub] [www.plosone.org](http://www.plosone.org) **11**: e1116.

Ocana M, Cendán CM, Cobos EJ, Entrena JM, Baeyens JM (2004), Potassium channels and pain: present realities and future opportunities. *Eur. J. Pharmacol.* **500**: 203-219.

Pham TM, Lecaille J-C (1996), Multiple postsynaptic actions of GABA via GABA $_B$  receptors on CA1 pyramidal cells of rat hippocampal slices. *J. Neurophysiol.* **76**: 69-80.

Raap, J, Erkelens, K, Ogrel, A, Skladnev, DA, Brückner, H (2005), Fungal biosynthesis of non-ribosomal peptide antibiotics and alpha, alpha-dialkylated amino acid constituents. *J. Peptide Sci.* **11**: 331-338.

Racz I, Schutz B, Abo-Salem OM, Zimmer A (2005), Visceral, inflammatory and neuropathic pain in glycine receptor  $\alpha$  3-deficient mice. *Neuroreport* 16: 2025-2028.

Ries CR, Puil E (1999), Ionic mechanism of isoflurane's actions on thalamocortical neurons. *J. Neurophysiol.* **81**: 1802-1809.

Wan X, Mathers DA, Puil E (2003), Pentobarbital modulates intrinsic and GABA-receptor conductances in thalamocortical inhibition. *Neurosci.* **121**: 947-958.

Yaksh TL (1989), Behavioral and autonomic correlates of the tactile evoked allodynia produced by spinal glycine inhibition: effects of modulatory receptor systems and excitatory amino acid antagonists. *Pain* 37:111-123.

Zeilhofer, HU (2005), The glycinergic control of spinal pain processing. *Cell. Mol. Life Sci.* **62**: 2027-2035.

Zhao M, Bada JL (1989), Extraterrestrial amino acids in Cretaceous/Tertiary boundary sediments at Stevns Klint, Denmark. *Nature* **339**: 463-465.

## 4. <sup>3</sup>THIRD MANUSCRIPT: METABOTROPIC RECEPTORS FOR THE NOVEL AMINO ACID ISOVALINE

### 4.1. Introduction

The rare amino acid isovaline (2-amino-2-methylbutanoic acid) is structurally similar to glycine and to another neurotransmitter, 4-aminobutanoic acid ( $\gamma$ -aminobutyric acid or GABA). In earlier experiments, we found that antagonists of ionotropic receptors for glycine-like amino acids and GABA did not prevent the shunting inhibition and conductance increase induced by isovaline in thalamic neurons (Cooke *et al.*, 2009).

These actions were mostly attributable to a long-lasting activation of outwardly rectifying currents (Cooke *et al.*, 2009). The sensitivity of isovaline currents to  $K^+$  channel blockers, their reversal near  $E_K$  and Nernstian behavior on changing the extracellular  $[K^+]$  confirmed  $K^+$  current involvement in isovaline inhibition in the ventrobasal nuclei.

While in theory, isovaline could directly activate  $K^+$  channels, the persistent nature of the response suggested a linkage of the  $K^+$  currents to metabotropic receptors.

Potential receptors for isovaline are especially interesting in view of recent demonstrations of the anti-nociceptive properties of systemically administered isovaline in rodent pain models (MacLeod *et al.*, 2010). Indeed isovaline may activate inhibitory systems involved in nociceptive processing at different levels of the neuraxis. In the thalamus, GABA<sub>B</sub> and opioid receptors mediate metabotropic inhibition (Brunton and Charpak, 1998; Potes *et al.*, 2006a; 2006b; Andreou *et al.*, 2010). While opioid receptors

---

<sup>3</sup> A version of this chapter will be submitted for publication. Cooke JE, Mathers DA and Puil, E. (2010) Metabotropic receptors for the novel amino acid isovaline.

(e.g., for small peptides) that activate G-protein-coupled  $K^+$  currents are widespread in the brain, isovaline has greater chemical similarity to GABA agonists. Hence our working hypothesis was that isovaline activated GABA<sub>B</sub> receptors on ventrobasal neurons.

GABA<sub>B</sub> receptors are heterodimers consisting of GABA<sub>B1</sub> and GABA<sub>B2</sub> subunits. The GABA<sub>B1</sub> subunit contains the agonist binding site, whereas the GABA<sub>B2</sub> subunit couples the receptor to G-proteins which inhibit adenylyl cyclase via G<sub>ai/o</sub> subunits (Kaupmann *et al.*, 1998; Galvez *et al.*, 1999; Bettler and Tiao, 2006). Agonists of GABA<sub>B</sub> receptors activate G-protein-coupled inwardly rectifying  $K^+$  (GIRK) channels (Bettler *et al.*, 2004), as well as outwardly rectifying and leak  $K^+$  channels (Saint *et al.*, 1990; Deng *et al.*, 2009). The receptors coupled to  $K^+$  channels are less commonly present at presynaptic sites (cf. Thompson and Gahwiler, 1992). In ventrobasal neurons that modulate nociceptive and other sensory inputs (Guilbaud *et al.*, 1980; Price, 1995), the postsynaptic GABA<sub>B</sub> receptors are coupled to  $K^+$  channels (Ulrich and Huguenard, 1996).

In the thalamus, GABA<sub>B</sub> agonists are known to have anti-nociceptive properties (Potes *et al.*, 2006b). Hence, we used immunohistochemical methods to verify the presence of GABA<sub>B1</sub> and GABA<sub>B2</sub> receptor subunits in ventrobasal nuclei, as well as pharmacological methods and slice preparations to elucidate isovaline actions on the receptor mechanisms. We also compared actions of baclofen (4-amino-3-(4-

chlorophenyl)butanoic acid), a canonical GABA<sub>B</sub> agonist with actions similar to GABA (Bowery, 2006).

## **4.2. Methods**

All experiments were approved by the Animal Care Committee at the University of British Columbia.

### **4.2.1. Slice preparation**

Sprague-Dawley rats (P10-15) were decapitated under deep isoflurane anesthesia and their brains placed in oxygenated artificial cerebrospinal fluid (aCSF) at 4°C which contained (in mM): 124 NaCl, 26 NaHCO<sub>3</sub>, 1.25 NaH<sub>2</sub>PO<sub>4</sub>, 2.5 KCl, 2 MgCl<sub>2</sub>, 2 CaCl<sub>2</sub>, and 25 dextrose. Hemispheres were sectioned sagittally into 250 µm thick slices using a vibroslicer (Campden Instruments, London, UK) and incubated for >1 h at 23-25°C in aCSF saturated with a 95:5% mixture of O<sub>2</sub> and CO<sub>2</sub>.

### **4.2.2. Electrophysiology**

Slices were immobilized with polypropylene mesh in a Perspex recording chamber (volume, ~2 ml) and perfused at room temperature (22-24°C) with oxygenated aCSF at a rate of ~2 ml/min. Thalamocortical neurons were visualized at 400x magnification with a differential interference contrast microscope (Axioscope II, Zeiss, Germany).

Recording pipettes were made from borosilicate glass tubing (World Precision Instruments, Sarasota FL) filled with a solution containing (in mM): 133 K-gluconate, 12

KCl, 4 NaCl, 0.5 CaCl<sub>2</sub>, 10 EGTA, 1 HEPES, 3 Mg-adenosine triphosphate, and 0.3 disodium guanosine triphosphate (GTP). In some experiments, GTP was omitted and replaced with trilithium guanosine 5'-[β-thio]diphosphate (GDP-β-S; 1 mM; Sigma Aldrich, St. Louis, MO) or tetralithium guanosine 5'-[γ-thio]triphosphate (GTP-γ-S; 0.3 mM; Sigma Aldrich, St. Louis, MO). The pH was adjusted to 7.3-7.4 using 50% gluconic acid or KOH.

Whole-cell, patch clamp recordings were performed using a List EPC 7 amplifier (HEKA, Germany) in current- and voltage-clamp modes. Electrode resistances ranged from 4 to 7 MΩ. Series resistance ranged from 5 to 30 MΩ, and data were discarded if series resistance increased by more than 25%. Signals were filtered (DC to 3 kHz), digitized at 10 kHz, and analyzed using pClamp software (Axon Instruments, Sunnyvale CA). Neurons had stable resting potentials and showed burst firing when depolarized from -80 mV. Membrane potentials were corrected for a junction potential of -11 mV. Input conductance was averaged from 10 steady-state currents in response to -5 mV steps of 400 ms duration delivered from a holding potential,  $V_h = -70$  mV. Current-voltage relationships were obtained using voltage commands of -120 mV to -30 mV (10 mV increments), delivered from  $V_h = -70$  mV. In the standard extracellular K<sup>+</sup> concentration of 2.5 mM, the K<sup>+</sup> Nernst potential was calculated as -103 mV.

#### **4.2.3. Drugs**

Drugs for bath application were either freshly prepared or diluted from stock solutions just prior to use. Strychnine, picrotoxin, R(+)-baclofen, 4-aminopyridine and CGP35348

were purchased from Sigma Aldrich (St. Louis, MO). CGP7930 was obtained from Tocris Bioscience (Ellisville, MO). Naloxone was obtained from Endo Pharmaceuticals (Newark, DE). Curare and tetrodotoxin (TTX) were purchased from City Chemical Corp (West Haven, CT) and Alomone Labs (Jerusalem, Israel). R-isovaline was synthesized by BioFine International (Vancouver, BC).

In some experiments, R-isovaline was applied locally from a pipette placed ~25  $\mu\text{m}$  from the cell soma. The amino acid was ejected using 0.5 psi pressure pulses of 1 s duration delivered by a  $\text{N}_2$  powered applicator. (Picospritzer II, General Valve Corp., Fairfield, NJ). In view of the lack of reversibility in membrane responses to isovaline (cf. Cooke *et al.*, 2009), the dose-response relationship for local application was established by applying a single isovaline concentration to each neuron. The distance of the puffing electrode was estimated at 25  $\mu\text{m}$  using the fine focus objective of the microscope and a piece of agar sectioned at 100  $\mu\text{m}$  and dipped in Trypan blue. A complete rotation of the fine objective knob went the distance of approximately 100  $\mu\text{m}$  in the agar cube. The soma of recorded neurons was roughly a quarter of a rotation of the fine focus knob away from the tip of the puffing electrode.

#### **4.2.4 Data analysis**

Data were analyzed and graphed using GraphPad Prism (San Diego, CA), and CorelDraw software (Ottawa, ON). Where appropriate, differences between treatment groups were analyzed using student's t-test, paired t-test, one-way ANOVA, or two-way ANOVA, with Bonferroni's post-hoc tests for comparison at specific data points. Fisher's exact

test was used to evaluate whether the ratio of responders to non-responders was significantly different between isovaline and baclofen groups. Differences were considered significant when  $p < 0.05$ . All data were expressed as means  $\pm$  SEMs, with  $n$  being the number of neurons.

#### **4.2.5. Tissue preparation for immunohistochemistry**

Sprague-Dawley rats (P12) were anesthetized with pentobarbital (40 mg/kg) and transcardially perfused with cold 0.1% PBS, followed by 4% formaldehyde. Brains were dissected and post-fixed in 4% formaldehyde for 2 h at 4°C, followed by submersion in 30% sucrose for 24-48 h at 4°C. The tissue was embedded with Tissue-Tek embedding medium (Sakura Finetek, Torrance, CA) and frozen in liquid nitrogen. Sagittal sections were made at 14  $\mu$ m thickness and stored at -20°C.

Immunohistochemistry was performed on sections post-fixed in 4% formaldehyde for 10 min. The sections were permeabilized with 0.1% Triton X-100, blocked with 0.5% bovine serum albumin (BSA) in phosphate buffered saline (PBS) and incubated in primary antibody overnight at 4°C in PBS solution containing 0.1% BSA. The primary antibodies were mouse anti-GABA<sub>B</sub>R1 subunit (1:100; ab55051; Abcam, Cambridge, MA) and rabbit anti-GABA<sub>B</sub>R2 subunit (1:100; ab75838; Abcam, Cambridge, MA). Sections were incubated in goat anti-mouse Alexa 546 and goat anti-rabbit Alexa 488 secondary antibodies for 1 h at room temperature (Invitrogen, Burlington, ON) followed by 4',6-diamidino-2-phenylindole (DAPI) nuclear counterstain. Sections were

coverslipped with Prolong Gold (Invitrogen, Burlington, ON) and allowed to cure overnight before imaging.

High magnification images were captured using an Olympus Fluoview 1000 confocal microscope (10x and 60x/1.4 oil Plan-Apochromat objectives). For co-localization, a minimum pixel number (5) was used to define a punctum. Co-localized puncta were quantified using Image J software (NIH, Bethesda, MD). Random co-localization was assessed by rotating a staining channel by 90°. The number of subunits within the soma was quantified by outlining the soma using the magnetic lasso tool in Photoshop and cropping all other pixels out of the image. The subunit labelling was measured for each fluorescence mark of 2 pixels<sup>2</sup> or greater, and was counted for GABA<sub>B1</sub> and GABA<sub>B2</sub> subunits individually. Differences were analyzed using a student's t-test.

### **4.3. Results**

#### **4.3.1. Immunocytochemistry in ventrobasal thalamus**

Using antibodies against GABA<sub>B1</sub> and GABA<sub>B2</sub> subunits, we sought to identify GABA<sub>B</sub> receptors in the thalamic area of electrical recording. Similar to the adult rat (Kulik et al., 2002), staining for GABA<sub>B</sub> subunits was ubiquitous in the VB nuclei (Fig. 4.1A,C). The immunoreactivity in nucleus reticularis thalami (nRT) appeared less dense (Fig. 4.1A, top inset). VB regions presumably occupied by fine dendrites showed extensive staining for GABA<sub>B1</sub> and GABA<sub>B2</sub> subunits. Proximal dendrites showed mostly GABA<sub>B1</sub>, not GABA<sub>B2</sub> labelling (arrows in Fig. 4.1B). On high magnification, GABA<sub>B1</sub> and GABA<sub>B2</sub> subunits (arrows in Fig. 4.1D) showed co-labelling in 675/2440 puncta (28%; arrowheads

in Fig. 4.1D). Labelling of GABA<sub>B2</sub> subunits were co-localized with GABA<sub>B1</sub> occurred in 675/2766 (24%). Co-localization was reduced to ~12% when one staining channels was rotated by 90° (see Methods).

Somata indicated by DAPI-stained nuclei showed prominent labelling for GABA<sub>B1</sub> subunits, but little staining for GABA<sub>B2</sub> subunits (arrowheads in Fig. 4.1B). Figure 4.2 shows the quantification of B1 and B2 subunits on somata. After isolating the somata from the background image (Fig. 4.2A), we quantified (see Methods) the numbers of GABA<sub>B1</sub> and GABA<sub>B2</sub> subunits per soma (Fig. 4.2B-D). There were significantly fewer pixels representing GABA<sub>B2</sub> subunits than GABA<sub>B1</sub> subunits per soma.

### **4.3.2. Isovaline effects on bath and local applications**

Previous experiments showed that the responsiveness of thalamocortical neurons to bath applied isovaline was variable and largely irreversible during extended periods of recording (Cooke *et al.*, 2009). We confirmed these observations (cf. Fig. 4.3A), showing that bath application of isovaline (~ED<sub>50</sub> = 75 μM) shunted action potentials and low-threshold Ca<sup>2+</sup> spikes in 9 out of 13 neurons. The 4 remaining neurons did not respond to isovaline. As evident in voltage-clamp (Fig. 4.3B), the isovaline response (Fig. 4.3B,C) at 10 min after terminating the application was an increase in membrane conductance of 48 ± 8 % (n = 20). The time course of the conductance increase was long-lasting (Fig. 4.3C), usually for the duration of an experiment (1-2 h). These data from a different population sample are consistent with our earlier findings.

In an effort to obtain a more refined dose-response relationship and reversibility, we applied isovaline locally from a micropipette (Fig. 4.3D,E). We tested responsiveness to concentrations that ranged from  $10^{-8}$  to  $10^{-4}$  M. For locally applied isovaline, 27 out of 37 neurons (73 %) showed an increase of  $\geq 10$  % in conductance. At 10 min after ceasing an application, isovaline (1  $\mu$ M) increased conductance by  $136 \pm 53$  % (range 77-242 %,  $n = 3$ ). The conductance increase persisted for the duration of recording which was up to 2h (Fig. 4.3D). The concentration-response curve reached a maximum near 1  $\mu$ M (Fig. 4.3E). While the percentage of neurons responsive to isovaline was independent of concentration, many neurons displayed substantial effects to locally applied isovaline that were largely irreversible.

#### **4.3.3. Isomer-specific actions of isovaline**

Application of the S-isomer of isovaline (S-Iva) did not produce the large, long-lasting effects of the R-isomer. We applied S-Iva to 3 neurons at 10  $\mu$ M, 25  $\mu$ M, and 250  $\mu$ M, and found that there was no significant increase in conductance at any point in our recording ( $p > 0.05$ , ANOVA; Fig. 4.3E, 25  $\mu$ M S-Iva).

#### **4.3.4 Comparison to baclofen, GABA<sub>B</sub> agonist**

We examined the ability of isovaline to mimic the effects of baclofen on the same, and different neurons. As shown in Figure 4.4, both substances increased outward currents in neurons stepped from a holding potential of -70 to -30 mV and slightly increased when stepped from -70 to -120 mV (cf. Fig. 4.4A and 4.4B). The averaged current-voltage (I/V) relationships (Fig. 4.4C,D) indicated a greater enhancement of outward compared

to inward currents for both substances. The difference currents obtained from subtraction of drug and control conditions verified this observation, and showed the similarities of isovaline and baclofen currents (Fig. 4.4E;  $p > 0.05$ , ANOVA). The intersections of isovaline and baclofen with their control curves yielded reversal potentials that were not different from  $E_K$  ( $= -103$  mV,  $p > 0.05$ , ANOVA) or from each other. The reversal potential for isovaline ( $E_{R-Iva}$ , 18 neurons) was  $-92 \pm 3$  mV and that for baclofen ( $E_{Bac}$ , 9 neurons) was  $-95 \pm 2$  mV (not significant;  $p > 0.05$ , ANOVA). Hence isovaline had actions on steady state currents that were similar to baclofen.

#### **4.3.5. Outward currents are activated by isovaline, not baclofen**

Isovaline and baclofen differed in their effects on the outward current activated by depolarizing steps. Figure 4.5 shows that isovaline increased the outward current evoked in 4 neurons by stepping the membrane from  $-70$  mV to  $-30$  mV. In contrast, baclofen had little effect on the peak outward current but increased the steady state current in 6 neurons. Application of 4-aminopyridine (4-AP, 1 mM), an A-current blocker, substantially reduced the magnitude of both peak and steady-state currents in 3 neurons (data not shown). In these neurons, isovaline still increased the peak current ( $p > 0.05$ , t-test) but had no effect on the steady state current ( $p < 0.05$ , t-test).

Hence some of the isovaline-induced outward current was an A-like current, and was not activated by baclofen.

#### **4.3.6. Absence of extracellular $\text{Ca}^{2+}$ does not alter isovaline action**

The literature suggests that baclofen reversibly activates  $\text{GABA}_B$  receptors even in the absence of extracellular  $[\text{Ca}^{2+}]$  and differs from GABA in this respect (cf. Galvez *et al.*, 2000b). In a subset of experiments, we found that the I/V relationship induced by isovaline was not significantly different than control in 4 neurons tested with a nominally  $\text{Ca}^{2+}$ -free aCSF (data not shown;  $p < 0.05$ ; ANOVA). Similarly, isovaline induced a significant increase in fast outward, A-like current under conditions of low  $\text{Ca}^{2+}$  (data not shown;  $p > 0.05$ ; ANOVA).

#### **4.3.7. Potential involvement of $\text{GABA}_B$ receptors**

We studied the effects of a positive modulator and an antagonist of  $\text{GABA}_B$  receptors, applied by bath, to address whether isovaline activated  $\text{GABA}_B$  receptors. CGP7930 is a positive allosteric modulator at recombinant  $\text{GABA}_B$  receptors (Urwyler *et al.*, 2001). By itself, CGP7930 (30  $\mu\text{M}$ ) did not appreciably change conductance (Fig. 4.6A). Co-application of CGP7930 with isovaline enhanced the responses to cumulatively applied increasing doses of isovaline, compared to a cumulatively applied doses of isovaline applied alone (Fig. 4.6A, left). The CGP7930-induced potentiation of a single dose of 10  $\mu\text{M}$  isovaline was greater than control at all time points tested (Fig. 4.6A, right). Figure 4.6C shows that the responses to isovaline in 3 neurons were significantly greater during co-application with CGP7930 ( $p < 0.05$ ).

In other experiments, we observed that pre-treatment with 100  $\mu\text{M}$  CGP35348, an orthosteric  $\text{GABA}_B$  antagonist (Gjoni and Urwyler, 2009) prevented responses to

isovaline. Subsequent co-application with isovaline (25  $\mu$ M) did not evoke a conductance increase in 9 neurons at voltages in the range of -110 to -30 mV (Fig. 4.6B). Attempts to counteract the long-lasting actions of isovaline by applying CGP35348 (100  $\mu$ M) were unsuccessful after establishing a response to isovaline. In 3 neurons, CGP35348 did not reverse a conductance increase of  $\geq 10$  % caused by 25  $\mu$ M isovaline (data not shown). Figure 4.6C shows that the responses to isovaline in 9 neurons were significantly abrogated during co-application with CGP35348 ( $p < 0.05$ ).

We studied the effects of non-hydrolysable analogues of GTP, applied internally in the recording pipettes to block G-proteins (cf. Labouebe *et al.*, 2007). Internal perfusion with 1 mM GDP- $\beta$ -S (Pin *et al.*, 2004) in place of GTP had no effect on input conductance (Fig. 4.7E). However, perfusion with 300  $\mu$ M GTP- $\gamma$ -S (David *et al.*, 2006) increased input conductance by about 2-fold compared with GTP perfusion (Fig. 4.7E). GTP- $\gamma$ -S also enhanced inward rectification at potential negative to  $E_K$ , without altering currents at other membrane potentials (Fig. 4.7F).

When GTP was replaced by GDP- $\beta$ -S in 8 neurons, isovaline did not significantly increase conductance, measured >15-20 min after whole-cell breakthrough (Fig. 4.7A). In 5 neurons where GTP- $\gamma$ -S replaced GTP, isovaline again did not significantly increase conductance (Fig. 4.7A). The results summarized in Figure 4.7C showed that isovaline responses were dependent on G-protein activation. Similarly, the ability of baclofen to increase input conductance was evident in 7 neurons perfused with GTP, but was abrogated in neurons perfused with the non-hydrolysable GTP analogs (Fig. 4.7B, D).

#### **4.3.8. Dissimilarities to baclofen**

We examined the possibility that isovaline and baclofen increased conductance by acting on the same receptor population. A chi-square test ( $p < 0.05$ ) revealed that the fraction of neurons responding to isovaline (54 out of 77, 70%) was less than the fraction activated by baclofen (16 out of 17, 94%; Figure 4.8A). Moreover, 3 neurons that did not respond to 100  $\mu\text{M}$  isovaline, did respond to a subsequent application of baclofen (5  $\mu\text{M}$ ) with substantial conductance increase (Fig. 4.8B). A high concentration of isovaline (1 mM) did not greatly alter the effect of baclofen (5  $\mu\text{M}$ ) on 4 neurons (Fig. 4.8C). However, when an optimal dose of isovaline (100  $\mu\text{M}$ ) is co-applied with baclofen (5  $\mu\text{M}$ ) to 3 neurons, the baclofen-induced conductance increase is much less than in an initial application of baclofen alone (Fig. 4.8D). Control experiments showed that a second application of baclofen is able to induce a conductance increase that is not significantly different from the initial conductance increase (Fig. 4.8E;  $p < 0.05$ , t-test). In summary, isovaline and baclofen differ in their ability to activate GABA<sub>B</sub> receptors, but they appear to require the same machinery to exert their effects.

#### **4.4. Discussion**

The chief finding was that isovaline activated metabotropic receptors, mediating a long-lasting inhibition of thalamic neuron excitability. A GABA<sub>B</sub>-like receptor mediated the responses which in several respects resembled GABA<sub>B</sub>-agonist actions. The shared effects of R-isovaline and R-baclofen included the ionic nature of response, G-protein dependency, and insensitivity to extracellular, nominally zero  $[\text{Ca}^{2+}]$ . Significantly,

isovaline had actions which were atypical of GABA<sub>B</sub> receptor activation. These actions included slow response kinetics, voltage-dependent K<sup>+</sup> current involvement, and in some neurons, an insensitivity of baclofen-receptors to isovaline.

#### **4.4.1. GABA<sub>B</sub> agonist-like actions**

The effects of isovaline on the membrane properties decreased neuron excitability, similar to a GABA<sub>B</sub> agonist. As previously (Cooke et al., 2009), isovaline inhibited firing by increasing conductance. This increase produced a net inward current at potentials negative to  $E_K$  and net outward current at potentials positive to  $E_K$ . The inhibitory effects were similar to those resulting from GABA<sub>B</sub> receptor activation in ventrobasal neurons (cf. Ulrich and Huguenard, 1996). The steady-state current-voltage relationships for isovaline and baclofen did not differ, both reversing near  $E_K$ . These effects of isovaline were consistent with activated GABA<sub>B</sub> receptors.

#### **4.4.2. Pharmacological properties consistent with GABA<sub>B</sub> agonism**

Manipulation of GABA<sub>B</sub> receptors by application of antagonist or modulator had marked effects on isovaline actions. The GABA<sub>B</sub> antagonist, CGP35348, prevented isovaline from inducing a conductance increase, whereas antagonists of GABA<sub>A</sub>, GABA<sub>C</sub>, glycine, opioid, and nicotinic receptors, were ineffective in altering the responses. Co-application of isovaline with CGP7930, an allosteric modulator of the GABA<sub>B</sub> receptor (Urwyler *et al.*, 2005), potentiated the conductance increase. CGP35348 antagonizes effects of baclofen in thalamic neurons (Potes et al., 2006) and CGP7930 potentiates baclofen-induced inhibition in other central neurons (Chen et al., 2005). Hence the sensitivity of

isovaline responses to antagonism and modulation was similar to that of baclofen, implicating the involvement of the GABA<sub>B</sub> receptor system.

The specificity of these effects argues in support of the proposal that isovaline activated GABA<sub>B</sub> receptors. We cannot exclude the possibility that isovaline may act partly through another G-protein coupled receptor system, such as the “GABA<sub>B</sub>-like receptor” (Calver et al., 2003) or the Family C G-protein-coupled receptor (Christiansen et al., 2007). This sort of mechanism may account for the potentiation of baclofen responses by other amino acids, including isoleucine (Urwyler et al., 2004). However, our immunocytochemical studies demonstrated co-localization of GABA<sub>B1</sub> and GABA<sub>B2</sub> subunits in ventrobasal thalamus. It seems likely therefore that a functional relationship between these subunits is prerequisite for the responses to isovaline.

#### **4.4.3. G-protein dependency and role of GIRK channels**

As observed for baclofen, when we compromised G-protein activation and deactivation by applying non-hydrolyzable analogues of GTP and GDP to the neuron's interior, we observed no response to isovaline application. Internal application of the GTP- $\gamma$ -S analogue alone resulted in increased membrane conductance and the appearance of an inwardly rectifying current that reversed near  $E_K$ . This observation was consistent with activation of GIRK current, likely due to liberation of G $\beta\gamma$  subunits from G-protein coupled receptors. Hydrolysis of GTP by G $\alpha$  subunits is necessary for inactivation of G $\beta\gamma$  dimers and closure of GIRK channels (Fowler et al., 2007). As expected therefore, GTP- $\gamma$ -S application produced the sustained current. The analogue GDP- $\beta$ -S which

prevents liberation of G $\beta\gamma$  subunits, failed to activate a significant current. Both nucleotides prevented a conductance increase to isovaline application. Hence, the responses to isovaline application were likely G-protein dependent.

We found that membrane currents activated by isovaline displayed outward rectification, rather than strong inward rectification typical of GIRK currents. Previous studies over a more narrow range of membrane voltage have ascribed baclofen's effects on thalamic neurons to activation of leak K<sup>+</sup> channels (Ulrich and Huguenard, 1996). In cortical neurons, GABA<sub>B</sub> receptor activation by baclofen causes a G $\alpha$ -mediated inhibition of adenylate cyclase activity. The fall in cAMP levels results in reduced PKA phosphorylation of TREK-2 leak channels, and an increased leak K<sup>+</sup> current (Deng et al., 2009). This mechanism may account for a large portion of K<sup>+</sup> current activated by isovaline. We also observed that isovaline increased the 4-aminopyridine-sensitive current in depolarized neurons, as reported for baclofen in hippocampal neurons (Saint et al., 1990). A fall in intracellular PKA activity would enhance such transient K<sup>+</sup> currents (cf. Zhang et al., 2009), providing further support for our view that isovaline acts on the G-protein coupling to intracellular cascades.

#### **4.4.4. Unique actions of isovaline**

Unlike the rapidly reversible effects of baclofen, isovaline produced responses that resisted washout on discontinuing the application. Neurons responsive to baclofen did not always respond to isovaline. This observation raises the possibility that isovaline is an agonist only at a subtype of GABA<sub>B</sub> receptors. However, conclusive evidence for

pharmacologically distinct types of GABA<sub>B</sub> receptors is elusive (Pham and Lacaille, 1996; Zhang et al., 1997, but cf. Bettler and Tiao, 2006). Certain analgesic conotoxins also produce GABA<sub>B</sub> receptor-mediated increases in K<sup>+</sup> conductance that persist, apparently by activating Src kinase (Callaghan et al., 2008; cf. Diverse-Pierliussi et al., 1997). Indeed, phosphorylation by Src kinase enhances the magnitude of inwardly rectifying (Yue et al., 2009) and transient outward K<sup>+</sup> currents (Gomes et al., 2008). An absence of essential downstream effectors could account for the lack of isovaline responses in some neurons.

The persistent effects of isovaline are unlikely to involve simply by enhancing the release of GABA from glia or neurons in the slice. Firstly, the effect of isovaline was independent of extracellular [Ca<sup>2+</sup>] similar to baclofen but not GABA, which requires Ca<sup>2+</sup> for GABA<sub>B</sub> receptor activation (Galvez *et al.*, 2000b). Secondly, GABA release would activate GABA<sub>A</sub> receptors in thalamocortical neurons, but the isovaline response does not include a significant Cl<sup>-</sup> component or susceptibility to GABA<sub>A</sub> receptor blockade. Thirdly, application of antagonists rapidly terminates GABA<sub>B</sub> receptor activation by GABA or baclofen (Labouebe et al., 2007), but was ineffective in curtailing an established response to isovaline. The persistence of isovaline responses may be attributable to avid binding to a site that recognizes baclofen, actions on Src kinase or other downstream components of the G-protein system.

In summary, we have shown that the novel amino acid isovaline mediated a long-lasting inhibition of thalamocortical neurons through metabotropic, likely GABA<sub>B</sub> receptors.

Isovaline actions were similar to the GABA<sub>B</sub> agonist baclofen with regard to steady state currents, sensitivity to block by inhibition of G-proteins and insensitivity to low [Ca<sup>2+</sup>]. An allosteric modulator of GABA<sub>B</sub> receptors potentiated isovaline action whereas antagonism of GABA<sub>B</sub> receptors occluded its effects. Unique to GABA<sub>B</sub> receptor activation, isovaline had slow response kinetics, activated a voltage-dependent outward K<sup>+</sup> current, and in some neurons, was unable to stimulate baclofen-receptors. Activation of GABA<sub>B</sub> receptors is antinociceptive in some animal models of pain (Potes et al., 2006b) and hence isovaline may produce analgesia (MacLeod et al., 2010) through GABA<sub>B</sub> receptor activation.

## Figures

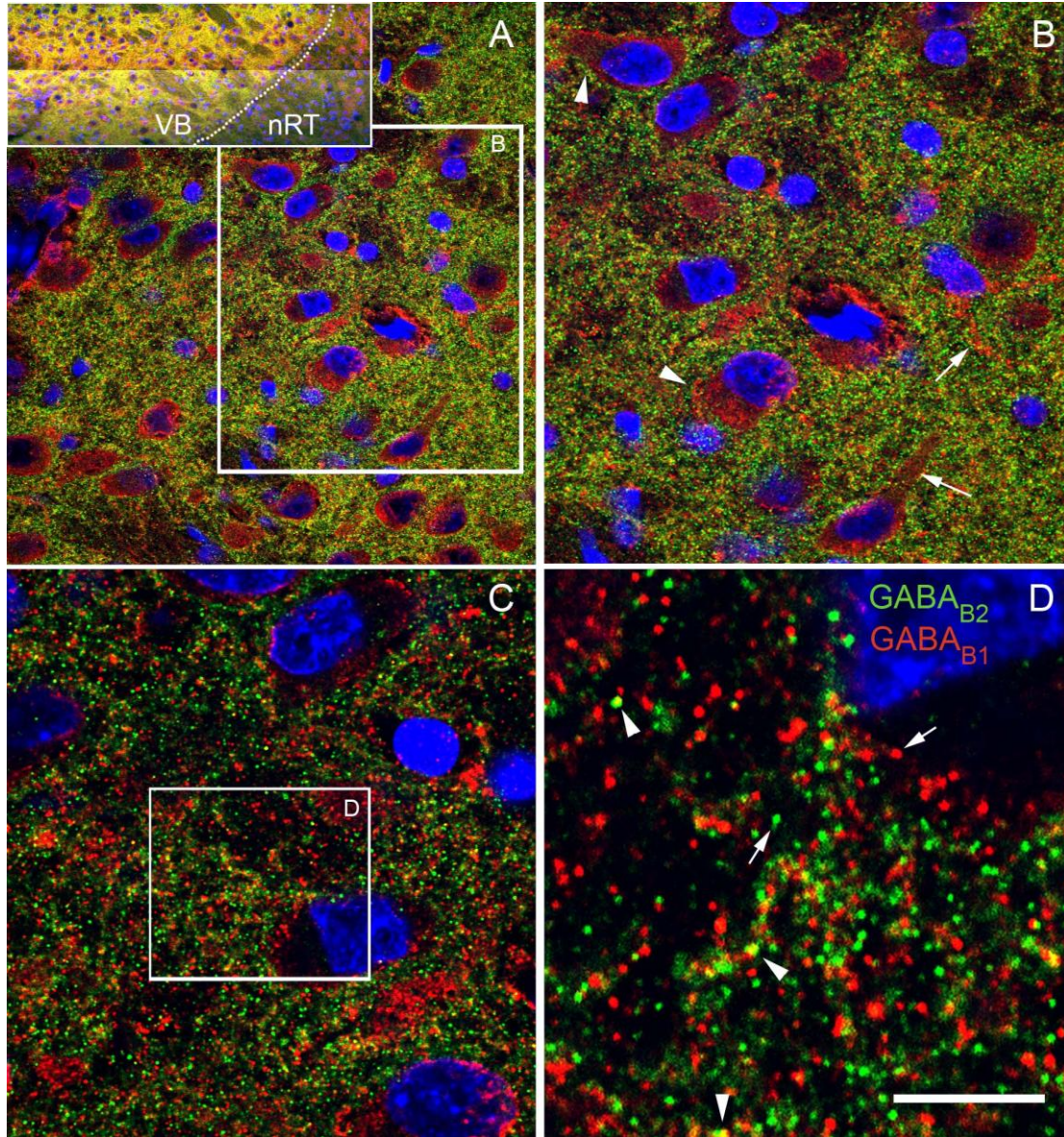


**Figure 4.1. GABA<sub>B1</sub> and GABA<sub>B2</sub> receptor subunits are present in ventrobasal thalamus.** (A) The rectangular insert shows a low power photomicrograph of a sagittal brain slice containing ventrobasal nuclei (VB) and the nucleus reticularis (nRT). Both regions exhibited immunoreactivity to antibodies against the GABA<sub>B1</sub> (red) and GABA<sub>B2</sub> (green) receptor subunits. Staining for both subunits was more evident in VB than in nRT. The main image in (A) shows a region of VB thalamus at higher magnification and

reveals extensive staining for both subunits. (B) Square insert from (A) is shown at higher power and reveals extensive GABA<sub>B1</sub> subunit staining in proximal dendrites (arrows) and somata (arrowheads). (C) A region from the field in (B) is shown at higher power. Note extensive labelling for both GABA<sub>B1</sub> and GABA<sub>B2</sub> subunits. (D) The insert in C is shown a high magnification, revealing the occurrence of some co-localized staining for GABA<sub>B1</sub> and GABA<sub>B2</sub> subunits (yellow, arrowheads) as well as for spatially segregated GABA<sub>B1</sub> and GABA<sub>B2</sub> subunits (arrows). The scale bar was 270  $\mu\text{m}$  for insert in (A), 45  $\mu\text{m}$  for the main panel in (A), 23  $\mu\text{m}$  for (B), 15  $\mu\text{m}$  for (C) and 5  $\mu\text{m}$  for (D). Nuclei were counter-stained with DAPI. Note that panel D is rotated 90° counter-clockwise from the box in panel C.

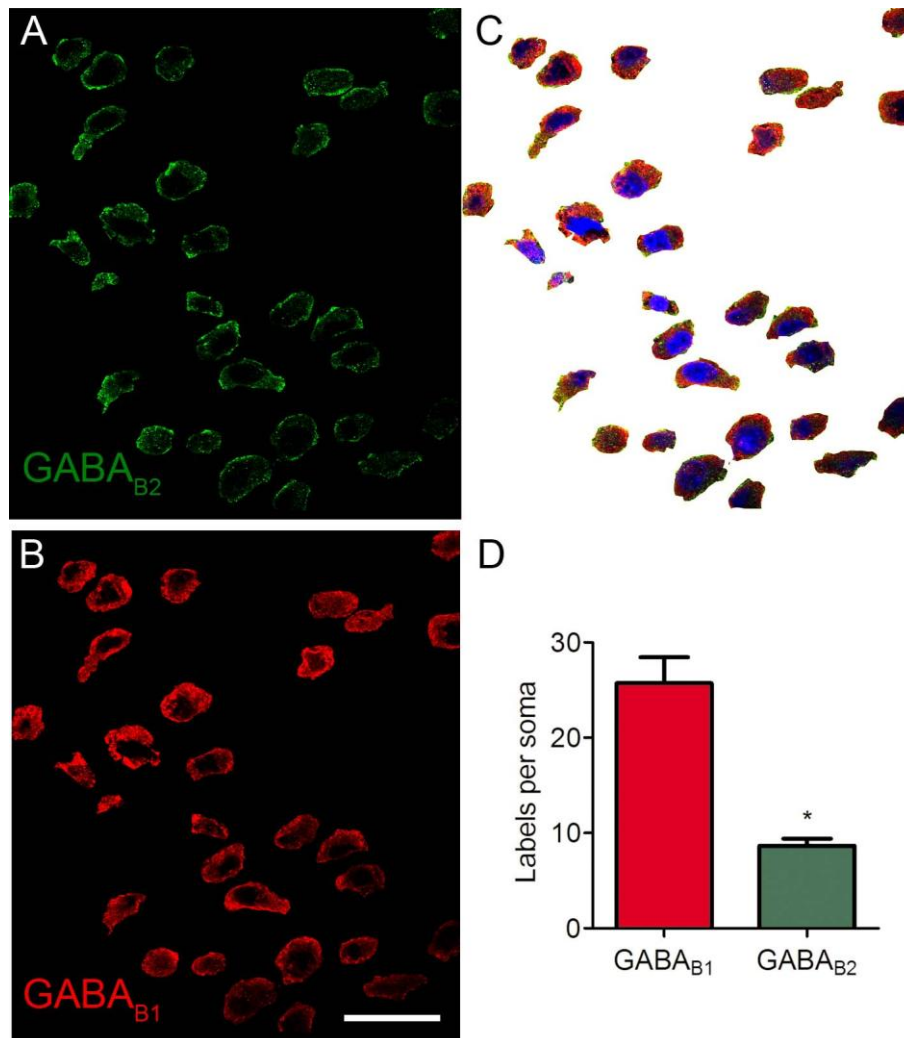


**Figure 4.2. Somata show more labelling for B1 subunits than for B2 subunits.** (A) Somata in an area of VB were cropped from background using digital image processing. Staining of these somata for GABA<sub>B2</sub> and GABA<sub>B1</sub> subunits is shown in (B) and (C) respectively. (D) The somata showed higher fluorescence label counts for GABA<sub>B1</sub> than for GABA<sub>B2</sub> subunits (\*  $p < 0.05$ , t-test,  $n = 30$  somata). Scale bar in (B) represents 25  $\mu\text{m}$  in (A-C).

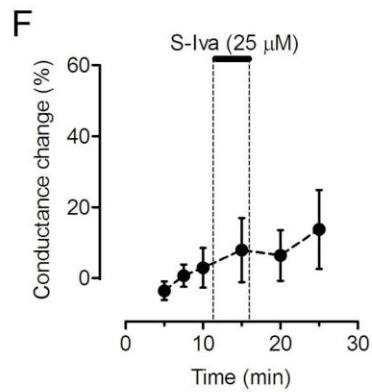
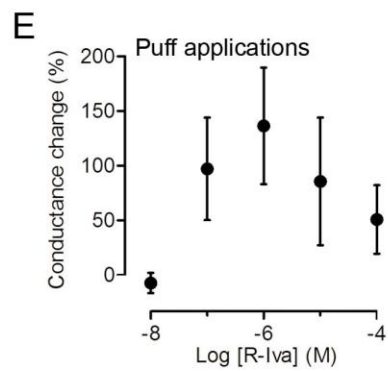
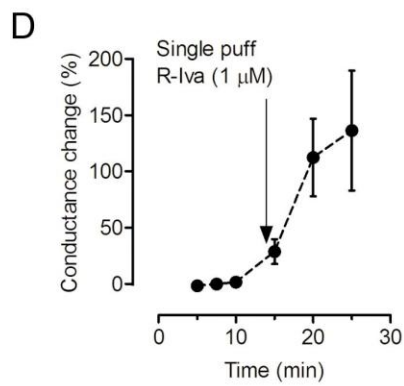
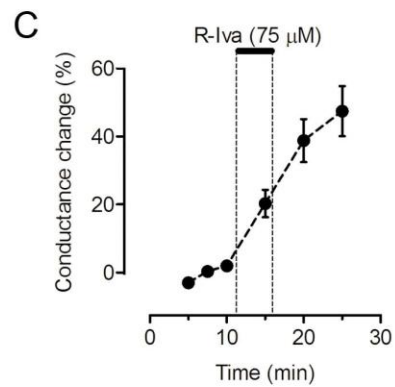
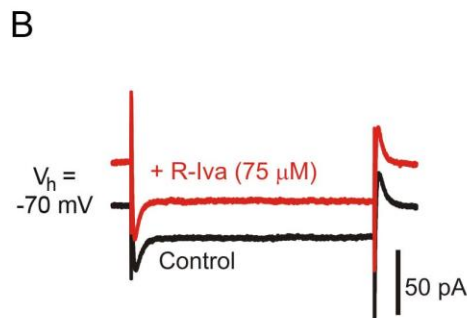
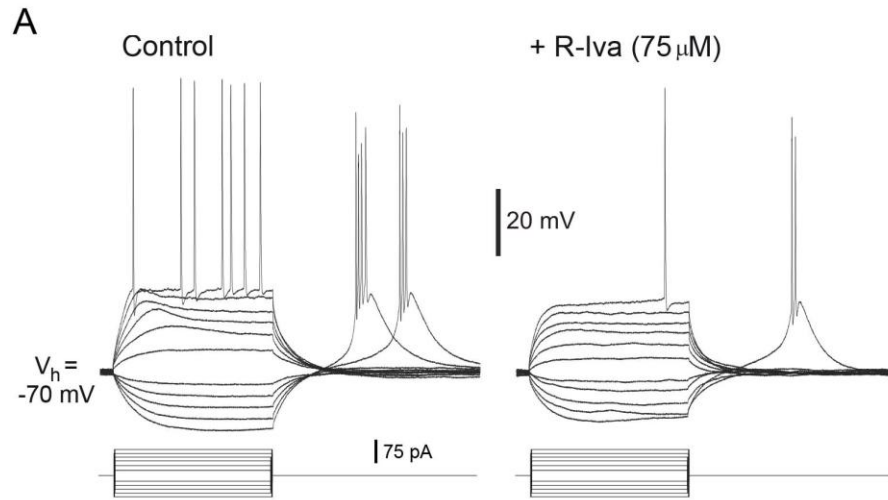


**Figure 4.3. Bath application of isovaline inhibits action potential firing by causing a persistent increase in membrane conductance.** (A) Current-clamp recording from a VB neuron showed that tonic and low-threshold spike (LTS) firing were inhibited by application of isovaline (R-Iva). Firing was elicited by application of 400 ms duration current pulses and the neuron was held at  $V_h = -70$  mV with DC current. Injected current traces are shown below voltage records. (B) In a second neuron voltage-clamped to  $-70$  mV, application of isovaline (red trace) increased outward membrane current and increased current needed to step the membrane to  $-75$  mV (400 ms command pulse), compared to control (black trace). Traces each represent an average of 10 sweeps. (C) The conductance increase caused by bath application of isovaline persisted during reperfusion of the slice with normal aCSF (data from  $n = 20$  neurons). (D) Local application of isovaline by pressure ejection (puff) also caused a persistent increase in conductance (data from  $n = 3$  neurons). (E) The dose-response curve for local application of isovaline showed a maximal response near  $1 \mu\text{M}$  ( $n = 15$  neurons). (E) The action of isovaline is isomer-specific, as S-isovaline (S-Iva) was not able to substantially increase conductance at any dose tested (10 to  $250 \mu\text{M}$ ). Here, we show the mean of 3 neurons tested at  $25 \mu\text{M}$ .

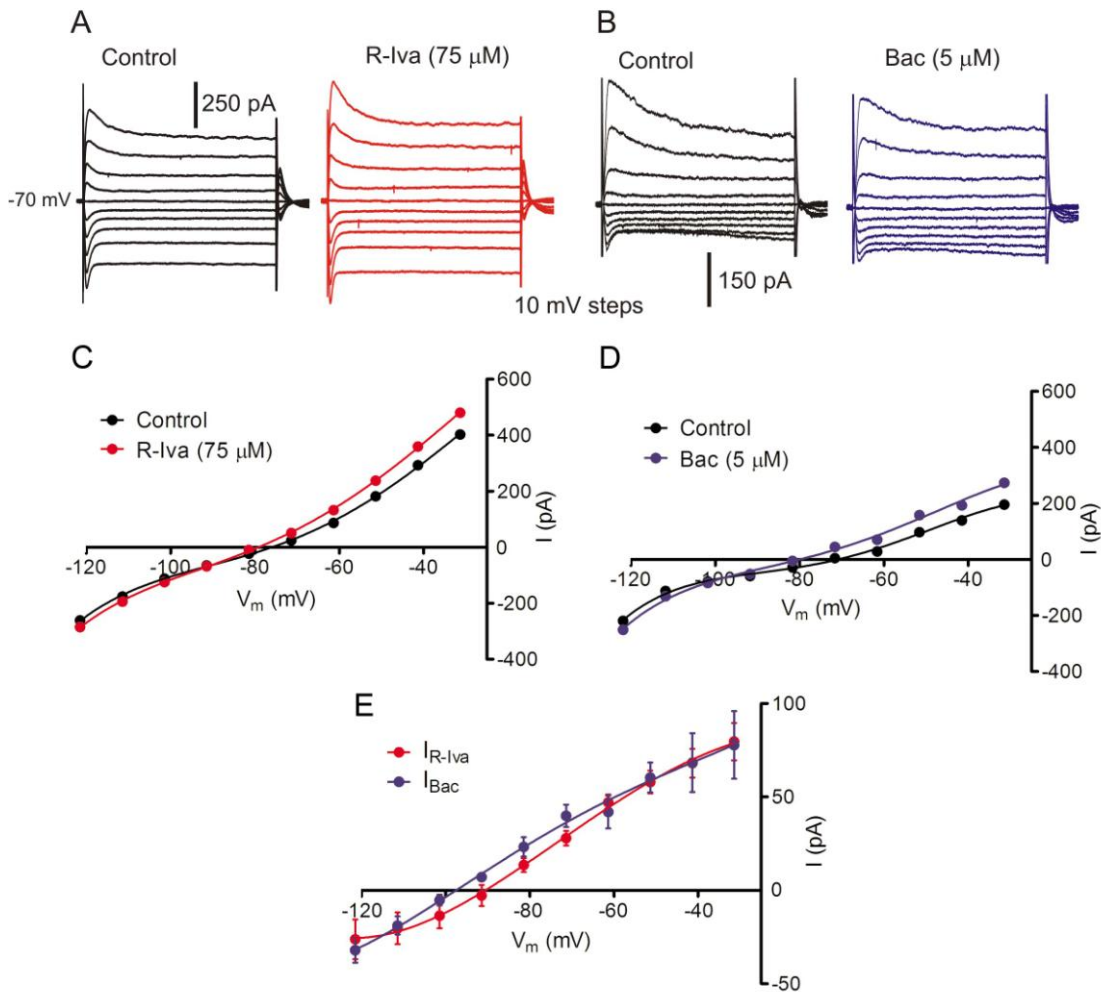


**Figure 4.4. Steady-state current-voltage relationships for isovaline and baclofen are similar.** (A,B) Current traces were obtained from two neurons by applying voltage commands from -120 mV to -30 mV in 10 mV increments, delivered from a holding potential of -70 mV. Application of isovaline (A) or baclofen (B) increased both inward and outward currents. The effects of isovaline and baclofen on the holding current were subtracted from these traces. (C) Steady-state current-voltage relationship for 18 neurons (error bars omitted for clarity) indicated that isovaline (red) increased outward current at potentials depolarized to  $E_K$  (-103 mV), and slightly increased inward current at

potentials hyperpolarized to  $E_K$ . (D) Application of baclofen to 9 other neurons (blue) also increased outward current at potentials depolarized to  $E_K$  and inward current at potentials hyperpolarized from  $E_K$ . (E) Current-voltage relationships for  $I_{R-Iva}$  (R-Iva – Control difference current, red) and  $I_{Bac}$  (Bac – Control difference current, blue) were similar to each other.

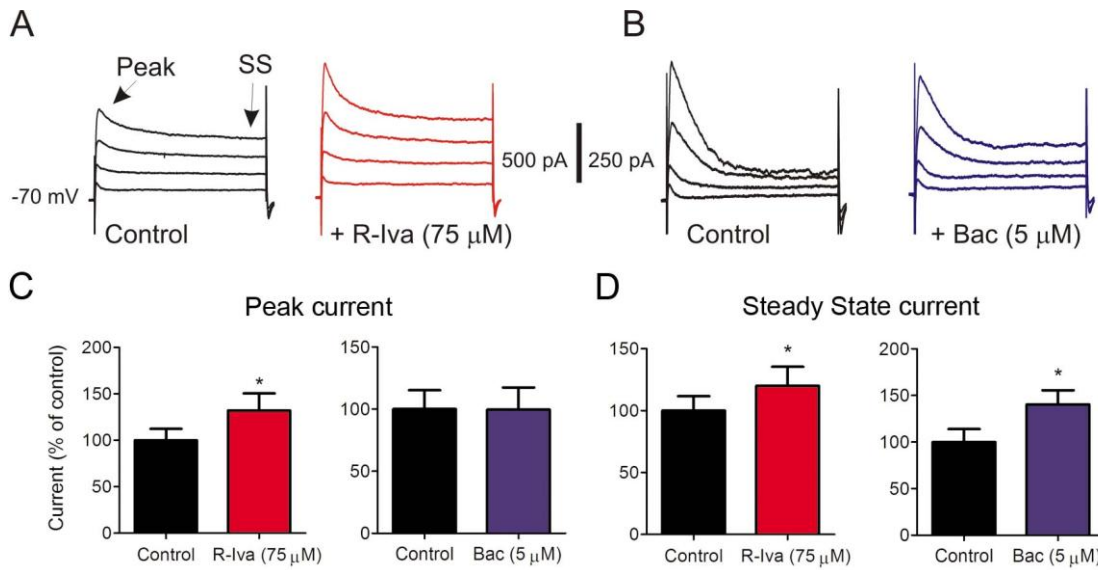


**Figure 4.5. Isovaline and baclofen differ in their effects on peak and steady state outward currents.** (A) Current traces in response to 10 mV depolarizing steps (400 ms duration) to -30 mV from a holding potential of -70 mV before (Control, left) and after application of isovaline (right, red traces). Note that both peak (arrow, peak) and steady state (arrow, SS) increased after application of isovaline. (B) Current traces in response to the same voltage steps as in (A) before (Control, left) and after application of baclofen (right, blue traces). Baclofen application increased steady state but not peak current. (C) Peak current amplitude on stepping from -70 to -30 mV was increased by isovaline (R-Iva, \* $p < 0.05$ , paired t-test,  $n = 4$  neurons) but was unchanged by baclofen (Bac,  $n = 6$  neurons). (D) Steady state current amplitude on stepping from -70 to -30 mV was increased by both isovaline (R-Iva, \* $p < 0.05$ , paired t-test,  $n = 4$  neurons) and baclofen (Bac, \* $p < 0.05$ , paired t-test,  $n = 6$  neurons).

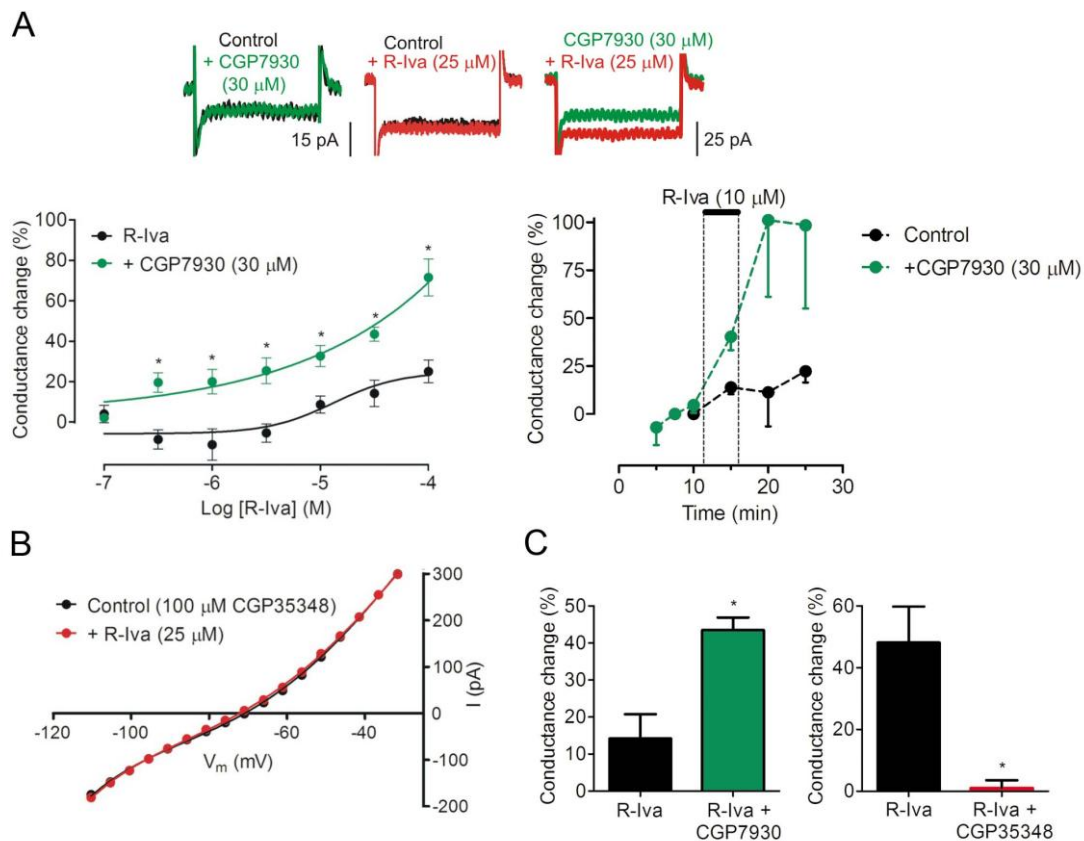


**Figure 4.6. Potential involvement of GABA<sub>B</sub> receptors in isovaline responses.** (A; top left) Application of CGP7930 (green trace) did not itself alter the conductance of a neuron compared to control (black trace). Conductance was measured as in Fig. 4.3B. Top, middle, application of isovaline (red trace) to a second neuron increased conductance. Top, right, co-application of CGP7930 and isovaline to a third neuron caused a large conductance increase. (Left) The graph shows that cumulative co-application of isovaline with CGP7930 to 3 neurons caused a significantly greater increase in conductance than caused by application of isovaline alone to 3 other neurons (\*  $p < 0.05$ , ANOVA). Both data groups were fitted with sigmoid curves. (Right)

CGP7930 increased the conductance change caused by 10  $\mu$ M R-Iva by a factor of 10 after 5 minutes of washing (from  $11 \pm 17$ ,  $n = 4$ ; to  $101 \pm 34$ ,  $n = 4$ ; right). (B) Current-voltage plots showed that co-application of isovaline with CGP35348 prevented the increase in conductance caused by isovaline ( $V_h = -70$  mV,  $n = 9$  neurons). Conductance increase after CGP35348 was calculated the same way as CGP7930, with a -5 mV hyperpolarizing pulse from -70 mV. (C) Summary bar graphs illustrating that CGP7930 potentiated the conductance increase due to 25  $\mu$ M isovaline while the drug was on (left,  $p < 0.05$ ,  $n = 3$ ), and that CGP35348 blocked the conductance increase due to 25  $\mu$ M isovaline at the peak of the conductance increase, 10 minutes after washing (right,  $p < 0.05$ ,  $n = 9$ ).

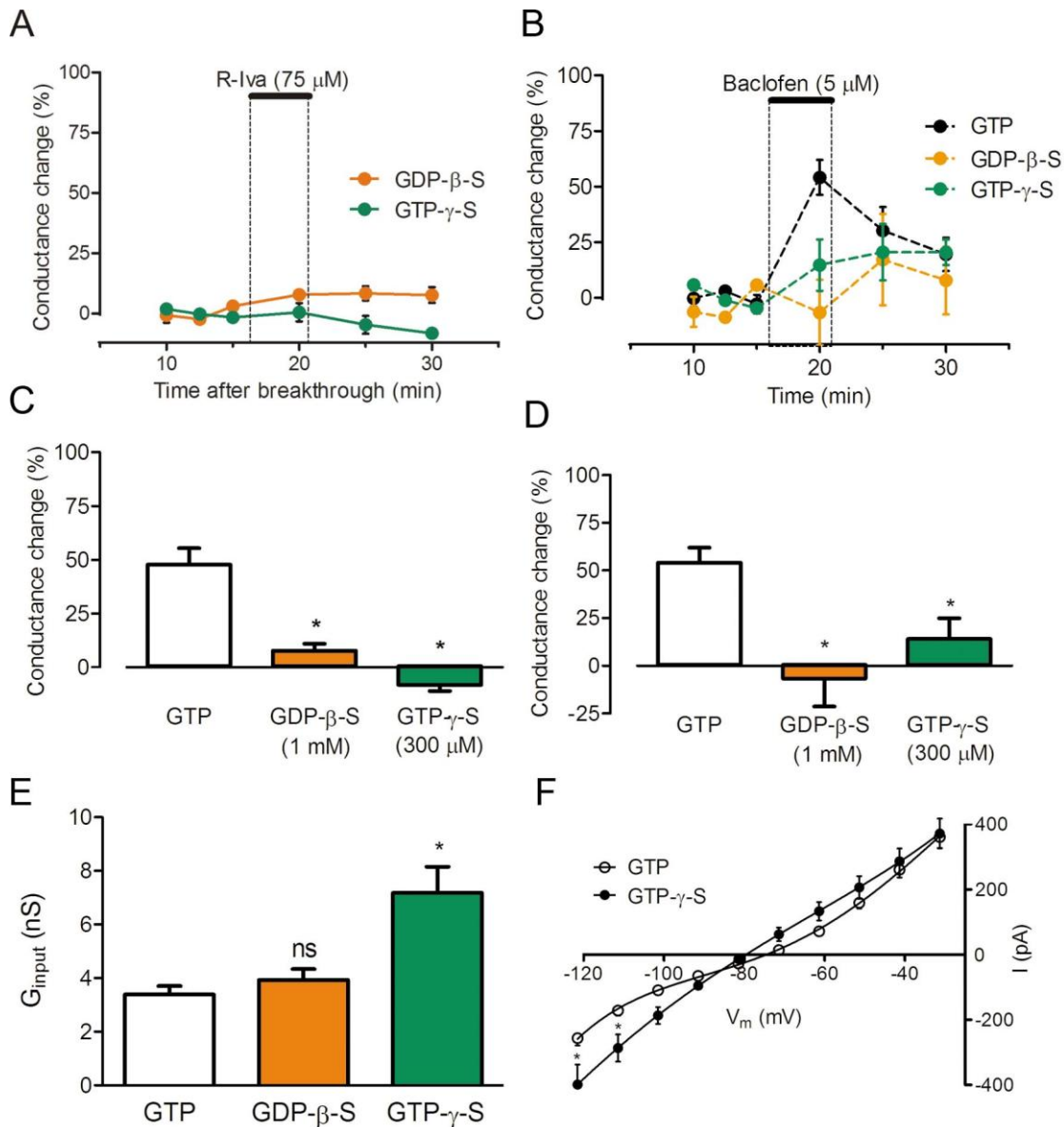


**Figure 4.7. Isovaline actions require G-protein activation.** (A) When intracellular GTP was replaced with GDP- $\beta$ -S (orange line;  $n = 8$ ) or GTP- $\gamma$ -S (green line;  $n = 5$ ), application of isovaline failed to increase conductance (cf: Fig. 3C). (B) Similarly, baclofen-induced conductance increase with GTP (black line,  $n = 6$ ) was prevented by inclusion of both GDP- $\beta$ -S (orange line,  $n = 3$ ) or GTP- $\gamma$ -S (green line,  $n = 3$ ). (C) Bar graphs illustrating the block of isovaline action by GDP- $\beta$ -S or GTP- $\gamma$ -S (\* less than seen

with intracellular GTP,  $n = 20$ ; \*  $p < 0.05$ , ANOVA). (D) Bar graphs illustrating the block of baclofen action by GDP-b-S or GTP-g-S (\* less than seen with intracellular GTP). (E) Bar graph illustrating the increase in input conductance caused by GTP- $\gamma$ -S ( $n = 5$ ) compared to GTP controls ( $n = 20$ ; \*  $p < 0.05$ ; ANOVA with Bonferroni's post-hoc test), prior to application of any ligand. (F) GTP- $\gamma$ -S ( $n = 5$ ) increased the amount of inward current at -110 and -120 mV compared to 20 GTP control neurons (\*  $p < 0.05$ , ANOVA with Bonferroni's post-hoc test).

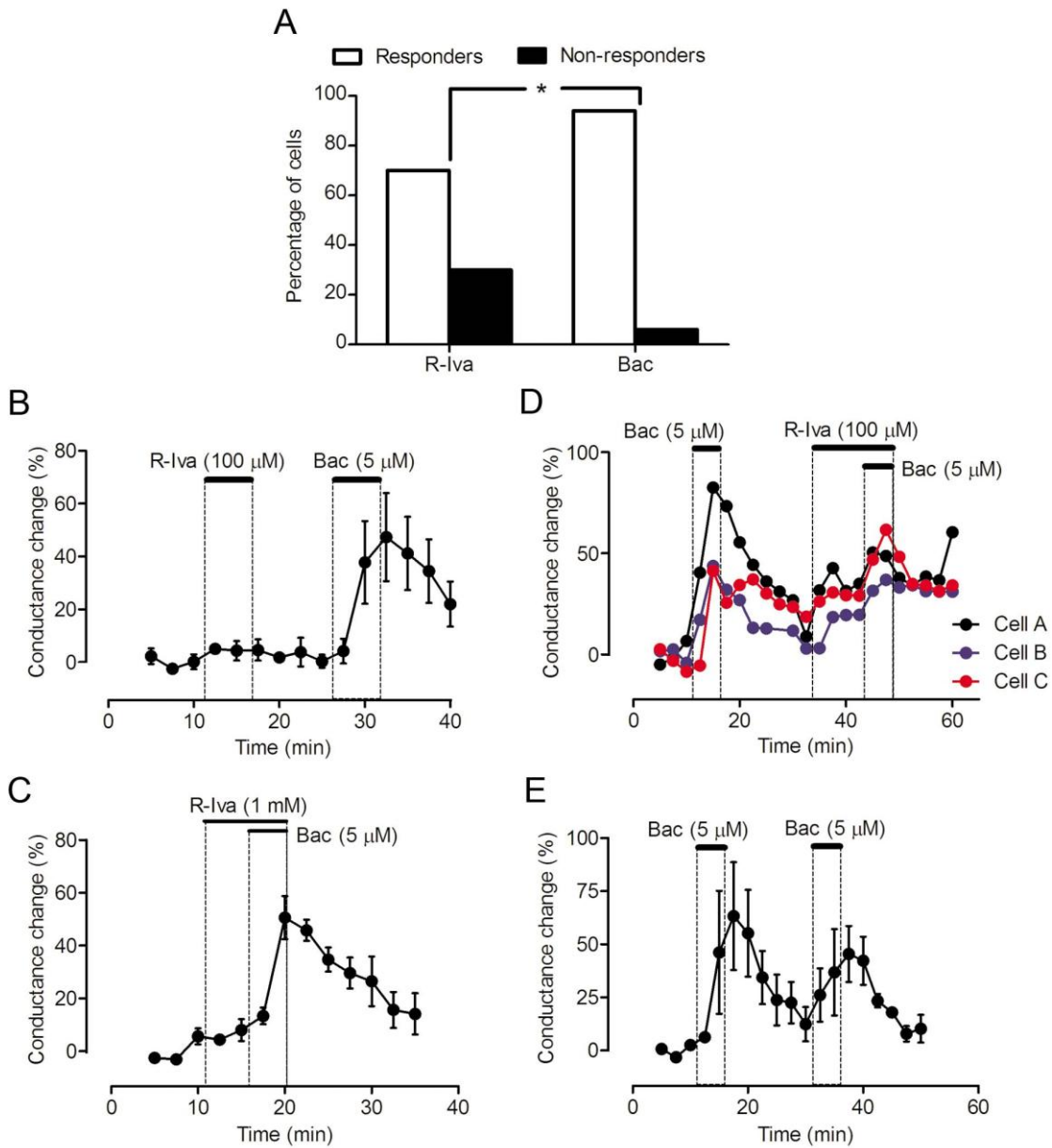


**Figure 4.8. Isovaline and baclofen may activate different receptors.** (A) The fraction of neurons that responded to isovaline was lower than that responding to baclofen (\* $p < 0.05$ , Fisher's exact test). (B) Three neurons that did not respond to isovaline (R-Iva, 100 μM) at an optimum concentration showed a vigorous response to baclofen (Bac, 5 μM). (C) Three additional neurons unresponsive to a high concentration

of isovaline (R-Iva, 1 mM) responded to the co-application of baclofen (Bac, 5  $\mu$ M). (D) Three individual neurons that responded to an initial application of baclofen (Bac, 5  $\mu$ M) responded to an application of isovaline (R-Iva, 100  $\mu$ M). A subsequent co-application of baclofen (Bac, 5  $\mu$ M) resulted in a conductance increase that was smaller than the initial conductance increase caused by baclofen, and did not recover. (E) A second application of baclofen was able to elicit a response that was, at its peak, not significantly different from the peak value of the first baclofen response ( $n = 3$ ;  $p > 0.05$ ; student's t-test).

**Table 4.1: Effects of receptor antagonists on the conductance increase caused by 75**

**μM R-Iva.** \* represents a difference from R-Iva application without an antagonist,  $p <$

0.05, ANOVA.

<b>Antagonist</b>	<b>Conductance change, %</b>	<b>n (cells)</b>
None (Control)	$47 \pm 8$	20
CGP35348 (100 μM)	$1 \pm 2$ *	9
Naloxone (1 μM)	$50 \pm 10$	3
Picrotoxin (50 μM)	$43 \pm 8$	4
Strychnine (20 μM)	$40 \pm 14$	5
Curare (50 μM)	$44 \pm 13$	4

#### **4.5. References**

Andreou A.P., Shields, K.G., Goadsby, P.J. GABA and valproate modulate trigeminovascular nociceptive transmission in the thalamus. *Neurobiol. Dis.* 37: 314-323, 2010.

Bettler B., Kaupmann K., Mossbacher J., Gassmann M. Molecular structure and physiological functions of GABA<sub>B</sub> receptors. *Physiol. Rev.* 84: 835-867, 2004.

Bettler B., Tiao J.Y.-H. Molecular diversity, trafficking and subcellular localization of GABA<sub>B</sub> receptors. *Pharmacol. Ther.* 110: 533-543, 2006.

Bowery N.G. GABA<sub>B</sub> receptor: a site of therapeutic benefit. *Curr. Opin. Pharmacol.* 6: 37-43, 2006.

Brunton J., Charpak S. mu-Opioid peptides inhibit thalamic neurons. *J. Neurosci.* 18: 1671-1678, 1998.

Callaghan B, Haythornthwaite A, Berecki G, Clark RJ, Craik DJ, Adams DJ. Analgesic alpha-conotoxins Vc1.1 and Rg1A inhibit N-type calcium channels in rat sensory neurons via GABA<sub>B</sub> receptor activation. *J Neurosci.* 28(43):10943-51. 2008.

Calver A.R., Medhurst A.D., Robbins M.J., Pangalos M.N. the expression of GABA (B1) and GABA (B2) receptor subunits in the CNS differs from that in peripheral tissues. *Neurosci.* 100: 155-157, 2000.

Chen Y, Phillips K, Minton G, Sher E. GABA(B) receptor modulators potentiate baclofen-induced depression of dopamine neuron activity in the rat ventral tegmental area. *Br J Pharmacol.* 144(7):926-32. 2005.

Christiansen B, Hansen KB, Wellendorph P, Bräuner-Osborne H. Pharmacological characterization of mouse GPRC6A, an L-alpha-amino-acid receptor modulated by divalent cations. *Br J Pharmacol.* 150(6):798-807. 2007.

Cooke J.E., Mathers D.A., Puil E. Isovaline causes inhibition by increasing potassium conductance in thalamic neurons. *Neurosci.* 164: 1235-1243, 2009.

David M., Richer, M., Mamarbachi A.M., Villeneuve L.R., Dupre D.J., Hebert T.E. Interactions between GABA-B1 receptors and Kir 3 inwardly rectifying potassium channels. *Cell. Signall.* 18: 2172-2181, 2006.

Deng P.-Y., Xiao, Z., Yang, C., Rojanathammanee, L., Grisanti, L., Watt, J., Geiger, J.D., Liu, R., Porter, J.E., Lei, S. GABA<sub>B</sub> receptor activation inhibits neuronal excitability and spatial learning in the entorhinal cortex by activating TREK-2 K<sup>+</sup> channels. *Neuron* 63: 230-243, 2009.

Diversé-Pierluissi M, Remmers AE, Neubig RR, Dunlap K. Novel form of crosstalk between G protein and tyrosine kinase pathways. *Proc Natl Acad Sci U S A.* 94(10):5417-21. 1997.

Galvez T., Parmentier M.-L., Joly C., Malitschek B., Kaupmann K., Kuhn R., Bittiger H., Froestl W., Bettler B., Pin J.-P. Mutagenesis and modeling of the GABA<sub>B</sub> receptor extracellular domain support a venus flytrap mechanism for ligand binding. *J. Biol. Chem.* 274: 13362-13369, 1999.

Galvez T., Urwyler S., Prezeau L., Mosbacher J., Joly C, Malischek B., Heid J., Brabet I., Froestl W., Bettler B., Kaupmann K., Pin J.P. Ca<sup>2+</sup> requirement for high-affinity  $\gamma$ -aminobutyric acid (GABA) binding at GABA<sub>B</sub> receptors: involvement of serine 269 of the GABA<sub>B</sub>R1 subunit. *Mol. Pharmacol.* 57: 419-426, 2000b.

Gjoni T., Urwyler S. Changes in the properties of allosteric and orthosteric GABA<sub>B</sub> receptor ligands after a continuous, desensitizing agonist pretreatment. *Eur. J. Pharmacol.* 603: 37-41, 2009.

Gomes P, Saito T, Del Corso C, Alioua A, Eghbali M, Toro L, Stefani E. Identification of a functional interaction between Kv4.3 channels and c-Src tyrosine kinase. *Biochim Biophys Acta.* 1783(10):1884-92. 2008.

Guilbaud G., Peschanski M., Gautron M., Binder D. Neurons responding to noxious stimulations in VB complex and caudal adjacent regions in the thalamus of the rat. *Pain* 8: 303-318, 1980.

Kaupmann K, Malitschek B, Schuler V, Heid J, Froestl W, Beck P, Mosbacher J, Bischoff S, Kulik A, Shigemoto R, Karschin A, Bettler B. GABA(B)-receptor subtypes assemble into functional heteromeric complexes. *Nature*. 396(6712):683-7. 1998.

Kulik A., Nakadate K., Nyiri G., Notomi T., Malitschek B., Bettler B. Distinct localization of GABA<sub>B</sub> receptors relative to synaptic sites in the rat cerebellum and ventrobasal thalamus. *Eur. J. Neurosci*, 15: 291-307, 2002.

Labouebe G., Lomazzi M., Cruz H.G., Creton C., Lujan R., Li M., Yanagawa Y., Obata K., Watanabe M., Wickman K., Boyer S.B., Slesinger P.A., Luscher C. RGS2 modulates coupling between GABA<sub>B</sub> receptors and GIRK channels in dopamine neurons of the ventral tegmental area. *Nat. Neurosci*. 10: 1559-1568, 2007.

MacLeod BA, Wang JT, Chung CC, Ries CR, Schwarz SK, Puil E. Analgesic properties of the novel amino acid, isovaline. *Anesth Analg*. 110(4):1206-14. 2010.

Pham TM, Lacaille JC. Multiple postsynaptic actions of GABA via GABA<sub>B</sub> receptors on CA1 pyramidal cells of rat hippocampal slices. *J Neurophysiol*. 76(1):69-80. 1996.

Potes C.S., Neto F.L., Castro-Lopes J.M. Inhibition of pain behavior by GABA<sub>B</sub> receptors in the thalamic ventrobasal complex: Effect on normal rats subjected to the formalin test of nociception. *Brain Res.* 1115: 37-47, 2006a.

Potes, C.S., Neto F.L., Castro-Lopes J.M. Administration of baclofen, a  $\gamma$ -aminobutyric acid type B agonist in the thalamic ventrobasal complex, attenuates allodynia in monoarthritic rats subjected to the ankle-bend test. *J. Neurosci. Res.* 83: 515-523, 2006b.

Price, D.D. Unpleasant pain evoked by thalamic stimulation. *Nat. Med.* 1: 885-887, 1995.

Saint, D., Thomas, T., Gage, P.W. GABA<sub>B</sub> agonists modulate a transient potassium current in cultured mammalian hippocampal neurons. *Neurosci. Lett.* 118: 9-13, 1990.

Thompson SM, Gähwiler BH. Comparison of the actions of baclofen at pre- and postsynaptic receptors in the rat hippocampus in vitro. *J Physiol.* 451:329-45. 1992.

Ulrich D., Huguenard J.R. GABA<sub>B</sub> receptor-mediated responses in GABAergic projection neurones of rat reticularis thalami in vitro. *J. Physiol.* 493: 845-854, 1996.

Urwyler S., Mosbacher J., Lingenhoel K., Heid J., Hofstetter K., Froestl W., Bettler B., Kaupmann K. Positive allosteric modulation of native and recombinant  $\gamma$ -aminobutyric acid<sub>B</sub> receptors by 2,6-Di-tert-butyl-4-(3-hydroxy-2,2-dimethyl-propyl)-phenol (CGP7930) and its aldehyde analog CGP13501. *Mol. Pharmacol.* 60: 963-971, 2001.

Urwyler S., Gjoni T., Kaupmann K., Pozza M.F., Mosbacher J. Selected amino acids, dipeptides and arylalkylamine derivatives do not act as allosteric modulators at GABA<sub>B</sub> receptors. *Eur. J. Pharmacol.* 483: 147-153, 2004.

Yue P, Lin DH, Pan CY, Leng Q, Giebisch G, Lifton RP, Wang WH. Src family protein tyrosine kinase (PTK) modulates the effect of SGK1 and WNK4 on ROMK channels. *Proc Natl Acad Sci U S A.* 106(35):15061-6. 2009.

Zhang J, Shen W, Slaughter MM. Two metabotropic gamma-aminobutyric acid receptors differentially modulate calcium currents in retinal ganglion cells. *J Gen Physiol.* 110(1):45-58. 1997.

Zhang M, Fei XW, He YL, Yang G, Mei YA. Bradykinin inhibits the transient outward K<sup>+</sup> current in mouse Schwann cells via the cAMP/PKA pathway. *Am J Physiol Cell Physiol.* 296(6):C1364-72. 2009.

## 5. GENERAL DISCUSSION

The broad theme encompassing all 3 manuscripts of this thesis is the actions of amino acids on inhibitory neurotransmitter receptors in the ventrobasal nuclei of the rat thalamus. The first manuscript of this thesis proposes that the difference in antagonism of mixed and purely GABA<sub>A</sub>ergic IPSCs by the  $\beta$ -amino acid antagonist TAG is due to the subunit composition of GABA<sub>A</sub> receptors. Furthermore, we propose a role for endogenous  $\beta$ -amino acids separate from glycine in synaptic transmission in ventrobasal thalamus. The second and third manuscripts of this thesis examine the actions of the antinociceptive amino acid, isovaline, on neurons of VB thalamus. We determine that isovaline inhibits firing of action potentials by activating a potassium conductance. Next, we provide evidence that the long-lasting actions of isovaline are attributable to activation of a G-protein coupled receptors, likely GABA<sub>B</sub> receptors.

This discussion will address these findings, their implications and future studies that I believe would advance the field. In particular, I will focus on the actions of isovaline, as it has formed the bulk of my PhD work. The exact locus(i) of action of this amino acid remains unresolved, and I dedicate a substantial portion of this discussion to hypothesizing where isovaline is acting to produce its unique effects.

### **5.1. TAG actions on IPSCs of VB thalamus: GABA<sub>A</sub> $\alpha$ 4 and glycine receptor co-localization**

The first manuscript of this thesis dealt with differential inhibition of purely GABA<sub>A</sub>ergic IPSCs compared with the GABA<sub>A</sub>ergic component of mixed IPSCs. We found that

GABA<sub>A</sub>ergic IPSCs had distinct kinetic properties when they were pure compared to the GABA<sub>A</sub>ergic component of IPSCs mixed with a glycinergic component in neurons of ventrobasal thalamus. Knowing that specific subunit composition of receptors confers distinct kinetic properties as well as agonist recognition (Keramidas and Harrison, 2008), we wondered if the different kinetic properties of GABA<sub>A</sub>ergic IPSCs were due to heterogeneity of GABA<sub>A</sub> receptor subunits.

GABA<sub>A</sub> receptor subtypes composed of  $\alpha 1\beta 2\gamma 2$  are located synaptically in neurons of VB thalamus (Jia et al., 2005), whereas  $\alpha 4\beta 2\delta$  subtypes are more sensitive to the  $\beta$ -amino acid taurine than  $\alpha 1\beta 2\gamma 2$  subtypes, and are located extrasynaptically ~75% of the time (Jia et al., 2008). We reasoned that the synaptic  $\alpha 4\beta 2\delta$  subtypes might be co-localized with glycine receptors and thus, be sensitive to TAG blockade. On the other hand, purely GABA<sub>A</sub>ergic IPSCs would result from activation of predominantly  $\alpha 1\beta 2\gamma 2$  subtype, and be less sensitive to TAG blockade.

My contribution to this study was the immunohistochemical examinations, which were conducted in coordination with the other experiments to identify whether synaptic GABA<sub>A</sub> $\alpha 4$  subunits were co-localized with glycine receptors. This would be expected if  $\alpha 4$  subunits are mediating the TAG-sensitive GABA<sub>A</sub>ergic component of mixed IPSCs. We initially screened for the anchoring protein gephyrin, which we found in VB thalamus (see: Appendix A). One of the first things we noticed in the  $\alpha 4$  immunostaining was the relatively high number of  $\alpha 4$  subunits that were apposed to presynaptic terminals. We found that just over half (54%) of  $\alpha 4$  subunits were co-localized with

presynaptic terminals and were therefore inferred to be synaptic. This is higher than the 23% found by Jia et al. (2005).

There are 2 explanations for the discrepancy in  $\alpha 4$  distribution between the two studies. First, the cell types between the two studies were different. While we performed studies on slices of postnatal day 12 rat brain, Jia et al. (2005) used cultures of thalamic cells from embryonic day 18 mice, which were grown in culture for a minimum of 11 days. Second, the ability of taurine to generate currents via extrasynaptic  $\alpha 4$  subunits is very low in young mice ( $\sim$ P10) compared to adult (Jia et al., 2008). Therefore, it may be that in young rats, there are fewer extrasynaptic  $\alpha 4$  subunits, but more synaptic  $\alpha 4$  subunits. Indeed, our own lab has shown that responses to application of taurine to neurons of VB thalamus are completely blocked by strychnine (Ghavanini et al., 2005), suggesting that, at least in juvenile animals, there are few taurine-sensitive  $\alpha 4$  GABA<sub>A</sub> receptors and that the taurine activates glycine receptors. It could be that there is a developmental shift in  $\alpha 4$  expression from synaptic to extrasynaptic, which could have important implications for  $\alpha 4$ -containing GABA<sub>A</sub> receptors in the establishment of inhibitory neural networks of the thalamus (see: Section 5.1.2.2). We attempted to use the novel technology of quantum dots to visualize the trafficking of receptors in the membrane of the living brain slice, but were met with technical limitations (see: Appendix B).

The immunohistochemical data support the idea that at least some of the TAG antagonism of the GABA<sub>A</sub>ergic component of mixed IPSCs is due to activation of GABA<sub>A</sub> receptors containing the  $\alpha 4$  subunit, as they were frequently co-localized with

glycine receptors when synaptic (76%). The simplest explanation for our observations is that TAG blocked GABA action on  $\alpha 4$ -containing receptors.

### **5.1.1. Implications of GABA<sub>A</sub> $\alpha 4$ -glycine co-localization**

The functional consequences of co-localization of  $\alpha 4$ -containing GABA<sub>A</sub> receptors and glycine receptors are not immediately clear. Knowing that  $\alpha 4$  subunit-containing GABA<sub>A</sub> receptors open for longer periods than do  $\alpha 1$ -containing GABA<sub>A</sub> receptors (Keramidas and Harrison, 2008), we could suggest that the kinetics of inhibitory neurotransmission in the thalamus could be altered through the  $\alpha 4$  subunit. Activation of  $\alpha 4$  subunit-containing GABA<sub>A</sub> receptors would shift neurons towards burst firing (Sohal et al., 2006), which may have implications for processing pain information (Guilbaud et al., 1980), sensitivity to alcohol (Jia et al., 2007), as well as anxiety and learning behaviours during development (Shen et al., 2007; Shen et al., 2010). There is interest in designing pharmacological agents that are GABA<sub>A</sub>-subtype specific, particularly in the interest of developing novel analgesic compounds (cf. Zeilhofer et al., 2009). It may be that the  $\alpha 4$  subunit will be a target of analgesic compounds in the future.

### **5.1.2. Future studies**

#### 5.1.2.1 GABA<sub>A</sub> $\alpha 4$ subunit: site of action of TAG?

We have used immunohistochemistry and electrophysiology to provide evidence that the amino acid antagonist TAG is acting at the atypical,  $\alpha 4$ -containing GABA<sub>A</sub> receptor. To determine conclusively whether TAG is, in fact, acting on  $\alpha 4$  subunits, an experiment involving a recombinant cell line could be performed. Specifically, GABA<sub>A</sub> receptors

with either  $\alpha 1$  or  $\alpha 4$  subunits could be expressed in the cells. Then the ability of TAG to antagonize the actions of GABA, and  $\beta$ -amino acids including taurine, could be tested.

Next, it would be interesting to use knock-out mice lacking the  $\alpha 4$  subunit to evaluate 1) whether there are pure and mixed IPSCs present, and 2) whether there are TAG-sensitive components to one or both of pure and mixed IPSCs. If the proposed action of TAG is correct (that is, TAG is blocking endogenous GABA action on  $\alpha 4$  subunits of GABA<sub>A</sub> receptors), we would expect TAG to have virtually no effect on GABA<sub>A</sub>ergic IPSCs of  $\alpha 4$  knock-out mice. If mixed IPSCs are in fact due to activation of glycine and  $\alpha 4$  subunit-containing GABA<sub>A</sub> receptors, we would expect to see little to no mixed IPSCs in  $\alpha 4$  knock-out mice. At this point, I am not aware of a knock-out mouse for the  $\alpha 4$  subunit, but there is an  $\alpha 1$  subunit knock-out mouse (Vicini et al., 2001).

#### 5.1.2.2. Developmental switch from synaptic to extrasynaptic?

Another issue worth exploring is the possible developmental change in the location of synaptic versus extrasynaptic  $\alpha 4$  subunits, and whether this correlates to TAG sensitivity. As mentioned above, extrasynaptic taurine sensitivity is much lower in younger (~P10) animals than in adults (Jia et al., 2008). We found that in young animals, we get less (i.e. ~50%) extrasynaptic  $\alpha 4$  expression than Jia et al. (i.e., ~75%; 2005). It is possible that the lower rates of activation of taurine in younger animals are due to a relative decrease in the amount of extrasynaptic  $\alpha 4$  subunits when compared with adults. That is, young animals may have more synaptic  $\alpha 4$  and few extrasynaptic  $\alpha 4$  subunits, whereas adults would have more extrasynaptic  $\alpha 4$  with fewer synaptic  $\alpha 4$  subunits.

To identify whether there are more synaptic  $\alpha 4$  subunits in younger animals, we could employ a technique similar to that we used in Manuscript #1 in which thin sections are made from brains of rats of different ages. For example, we would use sections from postnatal day 1, 5, 10, 15, 20 and adult, use antibodies against the  $\alpha 4$  subunit and a synaptic marker to identify the percentage of subunits that are synaptic versus extrasynaptic at each developmental time point. Using this technique, we could observe whether there is a developmental shift from synaptic to extrasynaptic location of  $\alpha 4$  subunits.

An important caveat with images taken from brain slices is that receptors on membranes of both the cell surface and intracellular components (like the endoplasmic reticulum) would be labelled. To circumvent this problem, a similar experiment could be conducted using neurons cultured from embryonic rats, as done by Jia et al. (2008). Incubating neurons for different times and monitoring the location of  $\alpha 4$  subunits would indicate whether  $\alpha 4$  subunits change location during maturation. The combination of these two imaging approaches should give a reasonable idea as to whether there is a developmental shift in the proportion of  $\alpha 4$  subunits.

## **5.2. Isovaline: actions of an analgesic amino acid**

The latter two manuscripts of this thesis show for the first time the inhibitory action of the analgesic amino acid isovaline on neurons of ventrobasal thalamus. Application of isovaline resulted in an increase in input conductance with a concomitant

hyperpolarization of the neuronal membrane. The combination of increase in conductance with hyperpolarization could only be attributable to activation of  $K^+$  or  $Cl^-$  conductance; however we set our  $E_{Cl}$  to a more depolarized level (-53 mV) than the resting membrane potential ( $\sim -70$  mV), which means that  $K^+$  is the only ion that could be involved in isovaline action.

The reversal potential obtained for isovaline ( $E_{R-Iva}$ ) was close to, albeit slightly depolarized from, the reversal potential for  $K^+$  ( $E_K$ ). While it is possible that there is an underlying ‘leak’ conductance permeable to  $Ca^{2+}$  or  $Na^+$  present at -70 mV, it is likely that the difference between  $E_{R-Iva}$  and  $E_K$  is due to a technical limitation such as a space clamp problem. That is, if the conductance is activated in the distal dendrites of the neuron, we may not be able to have an effective voltage clamp on this region. When we changed the extracellular  $[K^+]$ , we observed a similar change in  $E_{R-Iva}$  that followed a Nernstian pattern. These data support that isovaline activates a  $K^+$  conductance.

Observations with blockers for  $K^+$  channels also indicated a major role for  $K^+$ . Intracellular  $Cs^+$ , which blocks rectifying and leak  $K^+$  conductances (Golshani et al., 1998), suppressed isovaline action. Extracellular application of  $Cs^+$  or  $Ba^{2+}$ , which block inwardly rectifying and leak currents (McCormick and Pape, 1990), also prevented isovaline action. The hyperpolarization-activated current,  $I_h$ , was not apparently involved in the isovaline response, as pre-incubation of the slice with the  $I_h$  antagonist ZD7288 did not have any effect on isovaline actions. The outward current activated by isovaline was significantly reduced by 4-AP (1 mM), which blocks the slow transient ‘A-type’  $K^+$

current (Ficker and Heinemann, 1992). The chloride channel blocker picrotoxin had no effect on isovaline-induced currents. Taken together, these data suggest that isovaline activates a  $K^+$  conductance, and does not involve  $Cl^-$ , precluding any involvement of glycine or  $GABA_A$  receptors.

We next examined whether isovaline was acting on metabotropic  $GABA_B$  receptors because of the chemical similarity between isovaline and GABA, and because the activation of a long-lasting potassium conductance was consistent with a metabotropic receptor. We found that the steady state current-voltage relationship of isovaline was similar to that of the  $GABA_B$  agonist, baclofen. Consistent with this,  $E_{R-Iva}$  was not different from the reversal potential for baclofen,  $E_{Bac}$ . Baclofen and isovaline actions were also similar with regard to their independence of a  $Ca^{2+}$  requirement. Galvez et al. (2000b) showed that GABA requires  $Ca^{2+}$  in the aCSF in order to activate  $GABA_B$  receptors, whereas baclofen does not. Similar to baclofen, isovaline was able to elicit a response in aCSF with nominally zero extracellular  $[Ca^{2+}]$ . Multiple similarities with the  $GABA_B$  agonist baclofen indicated that isovaline activates  $GABA_B$  receptors.

The actions of isovaline were susceptible to modulation by pharmacological tools that target  $GABA_B$  receptors. When we co-applied isovaline with the  $GABA_B$  antagonist CGP35348, we did not observe any increase in conductance. Furthermore, pre-treatment with the positive allosteric modulator of  $GABA_B$  receptors, CGP7930, enhanced the magnitude of the conductance increases observed with low doses of isovaline.

Consistent with an action on G-protein coupled metabotropic receptors, the effects of

isovaline were prevented by replacing intracellular GTP with non-hydrolyzable analogues GTP- $\gamma$ -S and GDP- $\beta$ -S in the pipette. While our data strongly implicate activation of GABA<sub>B</sub> receptors, isovaline may work on another G-protein coupled receptor that is potentiated by CGP7930 and blocked by CGP35348 (see: section 5.3.2. below).

Importantly, isovaline does not activate all GABA<sub>B</sub> receptor-containing neurons. In addition, higher doses (1 mM) of isovaline did not occlude the actions of baclofen. The reason(s) for these observations are unclear. If isovaline acts intracellularly, on Src kinase or PKA for example, there would be state-dependent effects of isovaline action. That is, the presence, amount and phosphorylation state (for example) of Src or PKA (or others) would determine whether isovaline would be able to elicit its effects (see: Section 5.3 below for more information).

Ours is not the first study to show that amino acids other than GABA are capable of acting on GABA<sub>B</sub> receptors. Kerr and Ong (2003) showed that L-amino acids, including L-leucine, L-isoleucine and L-valine, potentiate responses of GABA<sub>B</sub> receptors without activating them directly. Specifically, they found that when they applied the amino acids to neocortical neurons, they did not observe any hyperpolarization of the membrane. Co-application of the L-amino acids with baclofen increased the magnitude of the hyperpolarization, more than doubling the effect of baclofen alone. Importantly, the actions of the L-amino acids were quite long, with a 3 minute application prolonging the baclofen-induced hyperpolarization for up to 20 minutes.

However it has since been shown that, unlike CGP7930, L-leucine, L-isoleucine and L-valine do not act as true allosteric modulators at GABA<sub>B</sub> receptors, because they were not able to increase GABA<sub>B</sub>-mediated GTP- $\gamma$ -S binding in native or recombinant cell systems (Urwyler et al., 2004). Speculation has arisen as to the mechanism of the L-amino acid-induced potentiation of baclofen responses observed by Kerr and Ong (2003; cf: Urwyler et al., 2004). Specifically, it was mentioned that the L-amino acids might be altering neural networks by acting on other cells possibly releasing GABA. An additional theory proposed by Urwyler et al. (2004) was that the L-amino acids might be activating intracellular effector proteins such as adenylyl cyclase.

### **5.3. Isovaline: possible mechanisms of action**

This thesis showed that isovaline inhibits neurons of ventrobasal thalamus by activating a long-lasting potassium conductance, an action mediated by a metabotropic receptor. However, the precise mechanism of action of isovaline remains to be elucidated. The as yet undetermined site of isovaline action is likely responsible for the unique features of isovaline, including an increasing effect upon washout, activation of an I<sub>A</sub> current, a larger (compared to baclofen) proportion of neurons not responsive to isovaline, and failure to elicit a response from some GABA<sub>B</sub> receptors sensitive to baclofen.

Blockade of isovaline action by non-hydrolysable analogues of GTP indicate that isovaline acts through a G-protein coupled receptor. The occlusion of isovaline action by a GABA<sub>B</sub> antagonist, and the potentiation of isovaline by a GABA<sub>B</sub> modulator suggest

that isovaline is acting in one of two ways: (1) isovaline actions are mediated by GABA<sub>B</sub> receptors, and (2) isovaline activates some other G-protein coupled receptor that is sensitive to potentiation by CGP7930 and blockade by CGP35348.

### **5.3.1. Isovaline actions mediated by GABA<sub>B</sub> receptors**

GABA<sub>B</sub> receptors are heterodimers consisting of GABA<sub>B1</sub> and GABA<sub>B2</sub> subunits, each of which consists of a heptathelical transmembrane domain and extracellular ‘Venus fly-trap’ (Galvez et al., 1999). The GABA<sub>B1</sub> subunit contains the agonist binding site, whereas the GABA<sub>B2</sub> subunit couples the receptor to G-proteins which inhibit adenylyl cyclase via G<sub>ai/o</sub> subunits (Kaupmann *et al.*, 1998; Galvez *et al.*, 1999; Bettler and Tiao, 2006). Agonists of GABA<sub>B</sub> receptors activate G-protein-coupled inwardly rectifying K<sup>+</sup> (GIRK) channels (Bettler *et al.*, 2004), as well as outwardly rectifying and leak K<sup>+</sup> channels (Saint *et al.*, 1990; Deng *et al.*, 2009). The receptors coupled to K<sup>+</sup> channels are less commonly present at presynaptic sites (cf. Thompson and Gahwiler, 1992). In ventrobasal neurons that modulate nociceptive and other sensory inputs (Guilbaud *et al.*, 1980; Price, 1995), the postsynaptic GABA<sub>B</sub> receptors are coupled to K<sup>+</sup> channels (Ulrich and Huguenard, 1996).

In the following Sections, I propose several hypotheses that may describe isovaline’s unique actions on GABA<sub>B</sub> receptors. Hypotheses are arranged according to proposed location of action, starting at extracellular, then intracellular regions. Please see Figure 5.1 for visual aid.

### 5.3.1.1. Proposed sites of isovaline action: extracellular loci

#### *5.3.1.1.1. Isovaline may increase release of GABA from surrounding cells*

One hypothesis is that isovaline might release GABA from cells surrounding the recorded neuron, as proposed for the potentiating effects of other  $\alpha$ -amino acids on GABA<sub>B</sub> responses (Urwyler et al., 2004; Kerr and Ong, 2003). The constant release of GABA onto the recorded neuron would give a persistent effect, as was observed. If isovaline failed to release GABA in some local networks, the recorded neuron would appear as a non-responder, but would still have GABA<sub>B</sub> receptors available for activation by baclofen. Against this hypothesis is the lack of any GABA<sub>A</sub> component to the isovaline-induced action, and the inability of CGP35348 to terminate an ongoing response. There is also no Ca<sup>2+</sup> requirement for isovaline's actions, which further precludes this theory, as GABA needs Ca<sup>2+</sup> present to activate the GABA<sub>B</sub> receptor (Galvez et al., 2000b).

#### *5.3.1.1.2. Isovaline may bind to the LIV-BP of GABA<sub>B1</sub> subunits with high affinity, preventing the 'fly-trap' from re-opening*

The agonist binding site of the GABA<sub>B1</sub> subunit contains a conserved domain that consists of a leucine-isoleucine-valine binding protein (LIV-BP; Galvez et al., 2000a). Mapping the structure of R-isovaline into the LIV-BP of the GABA<sub>B1</sub> subunit supports the idea that R-isovaline fits into the LIV-BP in an energetically favourable way (Dr. Richard Wall, personal communication). Importantly, these same mapping studies suggest that the S-isomer of isovaline is not predicted to fit into the LIV-BP in an

energetically favourable way, which corroborates our preliminary finding that S-isovaline does not increase input conductance when applied to neurons of VB thalamus.

If R-isovaline activates GABA<sub>B</sub> receptors by binding to the GABA<sub>B1</sub> subunit with high affinity, it is conceivable that once isovaline has bound to the LIV-BP, it may not be easily removed from the receptor. There is one particular residue, Ser<sup>246</sup>, which is evolutionarily conserved and is an important component of the LIV-BP, forming H-bonds with carboxylic groups of leucine and acetamide (Galvez et al., 2000b). It is possible that the carboxylic group of isovaline also bonds with this Ser<sup>246</sup> domain with high affinity. This hypothesis would account for the prolonged action of isovaline. Against this idea is that high doses of isovaline do not activate GABA<sub>B</sub> receptors, and concurrent application of a high dose (1 mM) of isovaline and baclofen (5 μM) results in a baclofen-induced activation that is not discernibly different from baclofen applied alone. This model also does not explain the existence of non-responder neurons (those that do not show an increase input conductance > 10%), which can in turn be activated by baclofen.

To test the theory that isovaline binds with high affinity to the LIV-BP region of the GABA<sub>B1</sub> subunit, we could use recombinant cell lines in which the LIV-BP has been modified by changing one critical residue (i.e., Ser<sup>246</sup>) with another. If isovaline were still able to elicit its long-lasting effects with mutated LIV-BP proteins, this suggests that it does not bind with high affinity to this region of the GABA<sub>B</sub> subunit.

*5.3.1.1.3. Isovaline may cause conformational changes in GABA<sub>B</sub> receptors that confer constitutive activity*

The allosteric modulator of GABA<sub>B</sub> receptors, CGP7930, has been shown to decrease cAMP levels alone by binding to its allosteric site on the GABA<sub>B2</sub> subunit (Binet et al., 2004). This action is not due to potentiation of ambient GABA in the slice, as the effect is seen in the absence of the GABA<sub>B1</sub> subunit, which is required for binding of ligands (Binet et al., 2004). CGP7930 appears to bind to the heptathelical domain of the GABA<sub>B2</sub> subunit, causing a conformational shift. This shift is sufficient to activate the G-protein associated with this subunit, leading to the drop in cAMP. While the inhibition of cAMP is done with low efficacy, this example might hold true for isovaline. That is, isovaline might bind to a site on either GABA<sub>B1</sub> or GABA<sub>B2</sub> subunit, changing the configuration of the receptor and rendering it constitutively active.

To test this hypothesis, a biochemical assay similar to that mentioned above could be employed to identify whether isovaline is able to decrease cAMP levels through GABA<sub>B</sub> receptors in the presence of an antagonist known to prevent agonist binding to the ligand-binding domain of the GABA<sub>B1</sub> subunit. Specifically, recombinant cell lines could be used with expression of GABA<sub>B1</sub> and GABA<sub>B2</sub> subunit heterodimers. Each subunit could then be expressed individually to identify whether isovaline is capable of causing cAMP decreases by acting on one particular subunit. Following this, the subunits could be broken down into heptathelical domains and 'Venus fly-trap' domains, to identify the specific locus of action, such as the action of CGP7930 on the heptathelical domain.

### 5.3.1.2. Proposed sites of isovaline action: intracellular loci

#### *5.3.1.2.1. Isovaline may inhibit the GTPase activity of the G $\alpha$ subunit*

Once a ligand or agonist has bound to a G-protein coupled receptor, the receptor induces a conformation change in the G-protein which exposes a region of the  $\alpha$ -subunit that promotes exchange of GTP for GDP (Brown and Sihra, 2008). The  $\beta\gamma$  and  $\alpha$  subunits are then able to activate or inhibit effector proteins. For example, G $\beta\gamma$  activates inwardly rectifying potassium channels (Bettler and Tiao, 2006), while G $\alpha$  inhibits adenylate cyclase (Hill, 1985). Termination of the G-protein cascade occurs when GTP is hydrolysed to GDP by an intrinsic GTPase activity in the  $\alpha$  subunit (Brown and Sihra, 2008). The GDP-bound  $\alpha$  subunit can then re-associate with the  $\beta\gamma$  subunit to restore a normal, inactive state.

After isovaline has initiated GABA<sub>B</sub> receptor activation, it is possible that it also prevents hydrolysis of GTP to GDP by inhibiting the GTPase activity of the  $\alpha$  subunit. To accomplish this feat, isovaline would have to gain access to the inside of the cell. The most likely route for an amino acid would be through one of the many amino acid transporters, and both enantiomers of isovaline are actively transported across the gut (Christensen, 1962), suggesting that similar transport may occur into a thalamocortical neuron.

In order to identify whether isovaline is acting on G $\alpha$  subunits specifically, these subunits should be expressed in a cell line in an assay to identify GTPase activity. There is an assay that uses fluorescent-tagged phosphate-binding protein, which scavenges free

phosphate as an indication of GTPase activity (in the absence of other phosphorylation reactions; Shutes and Der, 2005). This allows for real-time assessment of GTPase activity. If isovaline application to the intracellular region results in a decrease of GTPase activity as revealed by fluctuations in the fluorescent signal, this would confirm its actions on G $\alpha$  subunit.

#### *5.3.1.2.2. Isovaline may inhibit regulators of G-protein signalling proteins*

Regulator of G protein Signalling (RGS) proteins are involved in accelerating both activation and inactivation of G-protein coupled receptors, by promoting GTP hydrolysis via the  $\alpha$  subunit of G proteins (see: General Introduction, section 1.2.2.3; Lambert et al., 2010). The application of RGS4 from the recording electrode has been shown to decrease the time constant of activation of muscarinic receptors by 50%, and that of deactivation by 75% (Fowler et al., 2007). While RGS proteins enhance the kinetics of activation and inactivation, they are not required for activation or inactivation; blocking RGS proteins does not result in non-decaying responses (Labouebe et al., 2007). There are up to 12 different RGS proteins, which vary according to anatomical location (Gold et al., 1997). Of the 12 subtypes, RGS2, 3, 4, 7 and 8 are all found in ventrobasal thalamus (Gold et al., 1997; Ingi and Aoki, 2002).

RGS proteins have been implicated in pain. Up-regulation of RGS4 leads to neuropathic pain and morphine insensitivity of the spinal cord in sciatic nerve-ligation model rats (Garnier et al., 2003). Garzon et al. (2001) showed that blocking expression of RGS2 or 3 reduced morphine-induced analgesia, while inhibition of RGS9 proteins enhanced this

analgesia. GABA<sub>B</sub> receptors are known to be coupled to RGS2 proteins, which couple them to potassium channels (Labouebe et al., 2007). Specifically, Labouebe et al. (2007) showed that RGS2 acts to decrease the efficiency of the Gβγ subunit coupling to the GIRK3 channel. If isovaline inhibited, RGS proteins 2 or 4, for example, analgesia may result, as observed in other models (Garnier et al., 2003). The analgesia presumably would result from prolonged activation of GABA<sub>B</sub> receptors. However, this would not fully account for isovaline's actions, as inhibition of RGS proteins does not prevent inactivation of GABA<sub>B</sub> responses (Fowler et al., 2007).

To test whether isovaline acts, at least in part, by inhibiting RGS proteins, we could conduct experiments in which the RGS inhibitor phosphatidylinositol (3,4,5)-trisphosphate (PtdIns(3,4,5)P<sub>3</sub>)<sup>32</sup> is added to the intracellular environment. Having already blocked RGS actions, isovaline would presumably not be able to further inhibit RGS proteins. In a complementary study, we would want to increase the amount or action of RGS proteins during isovaline application. To do this, we could employ a recombinant cell line in which RGS proteins are greatly over-expressed. In this way, isovaline would likely not be able to inhibit all RGS within the cell. Another option for increasing RGS levels would be to transfect neurons with a virus that leads to increased RGS levels. The benefit of this approach is that one could use the same type of cells (thalamocortical neurons) to test isovaline's ability to inhibit RGS proteins.

#### 5.3.1.2.3. Isovaline may interfere with normal function of intracellular tyrosine kinases

Activation of GABA<sub>B</sub> receptors can lead to activation of the non-receptor tyrosine kinase Src (see: Figure 5.1; Diverse-Pierliussi et al., 1997). Src kinase is known to be activated directly by both G $\alpha$  and G $\beta\gamma$  subunits (Fadool, 1998) and Src activation has been implicated in regulating many types of K<sup>+</sup> channels.

Src associates with potassium channel Kv1.5, which is a delayed rectifier K<sup>+</sup> channel (Holmes et al., 1996). Holmes et al. (1996) found that phosphorylation of Kv1.5 by Src inhibited outward currents evoked by depolarizing current steps in HEK293 cells. Similarly, Fadool et al. (1997) showed that Src inhibited Kv1.3 delayed rectifier K<sup>+</sup> channels by phosphorylating them. The transient outward potassium (I<sub>A</sub>) channel Kv4.3 is also associated with Src (Gomes et al., 2008). When a Src inhibitor peptide is applied intracellularly, the Kv4.3-mediated outward current is abrogated, while intracellular application of recombinant Src increased peak current amplitude (Gomes et al., 2008). Src kinase has also been shown to be involved in mediating inward rectifying K<sup>+</sup> currents. The inward rectifying K<sup>+</sup> channels called ROMK are inhibited by a kinase called WNK4 (lysine deficient kinase 4), which closes the channels when phosphorylated (Yue et al., 2009). Activation of Src phosphorylates WNK4, thereby occluding WNK4's ability to inhibit ROMK channels (Yue et al., 2009). Therefore, Src activation indirectly leads to activation of ROMK inward rectifying channels.

In our studies, observations on blockers of K<sup>+</sup> currents demonstrated a major role for rectifiers in thalamic neurons. Intracellular Cs<sup>+</sup> which blocks rectifying and leak K<sup>+</sup>

currents (cf. Golshani et al., 1998) suppressed the responses to isovaline. Extracellular  $Ba^{2+}$  or  $Cs^{+}$  which blocked the inward rectifier,  $I_{Kir}$ , and leak current (McCormick and Pape, 1990; Wan et al. 2003), also prevented the responses. Isovaline induced appreciable currents at potentials positive to -60 mV indicating involvement of additional  $K^{+}$  currents, such as outward rectifiers. These results were consistent with isovaline actions on several types of  $K^{+}$  channels with voltage-dependent and leak properties.

It was recently shown that the analgesic actions of conotoxins, Vc1.1 and Rg1A, are due to closure of N-type  $Ca^{2+}$  channels through  $GABA_B$  receptor activation (Callaghan et al., 2008). When Src kinase activity was blocked,  $GABA_B$  receptor activation was no longer able to block  $Ca^{2+}$  channels, showing that Src kinase is critical for  $GABA_B$  closure of N-type  $Ca^{2+}$  channels. Src kinase is believed to be associated with the  $Ca^{2+}$  channel itself, and activation of the receptor leads to increased Src activity, through either the  $G\alpha$  or  $G\beta\gamma$  subunit, which can alter the kinetics of activation and the magnitude of the  $Ca^{2+}$  channel currents (Richman et al., 2004).

The modification of intracellular Src tyrosine kinase has also been shown to be involved in antinociception by acting on potassium channels (Gamper et al., 2003). The inhibition of Src increases the magnitude of 'M-currents' in cultured sympathetic neurons, which leads to antinociception (Gamper et al., 2003). Additionally, Src-induced phosphorylation of Kir3.1 inward rectifying  $K^{+}$  channels, caused by  $\kappa$ -opioid receptors, leads to desensitization of the receptors and provides another mechanism for increased

nociception (Clayton et al., 2009). The data showing Src involvement in antinociception further supports the possibility that isovaline may act through Src kinase.

To test whether isovaline increases or inhibits Src action, we can both block or augment Src action inside the cell prior to bath application of isovaline. To block Src activity, we can add the cell permeable Src kinase inhibitor PP2 to the bath for 30 minutes prior to isovaline application (Gomes et al., 2008). To increase Src activity, we can add active recombinant Src kinase to our recording electrode prior to isovaline application (Gomes et al., 2008). Assuming that Src activity would be saturated by the recombinant Src kinase, both inhibition and augmentation of Src kinase activity should occlude isovaline action if Src is involved in isovaline actions.

#### *5.3.1.2.4. Isovaline may inhibit NSF proteins*

The regulatory proteins called *N*-ethylmaleimide-sensitive factor (NSF) proteins are associated with GABA<sub>B</sub> receptors, and are capable of ‘priming’ the receptors such that activation leads to rapid desensitization by protein kinase C (Pontier et al., 2006).

Desensitization via NSF involves internalization of the receptors (Couve et al., 2002).

Inhibition of NSF proteins with a synthetic peptide prevents receptor desensitization during prolonged baclofen exposure (Pontier et al., 2006). While inhibition of NSF proteins would likely prevent desensitization, this is likely not the sole cause of the prolonged conductance increase caused by isovaline. It seems that there would need to be a continued stimulation of GABA<sub>B</sub> receptors in addition to the lack of desensitization in order to obtain the observed prolonged conductance increase.

To test whether isovaline produces its prolonged effects via NSF proteins, we could inhibit NSF proteins with a cell permeable peptide, TAT-Pep27, prior to application of isovaline. The TAT-Pep27 peptide would likely occlude the isovaline-induced inhibition of NSF proteins.

### **5.3.2. Isovaline actions mediated by another G-protein coupled receptor**

We cannot exclude the possibility that isovaline is activating another G-protein coupled receptor that is potentiated and occluded by CGP7930 and CGP35348, respectively.

Family C G-protein-coupled receptors (GPRC6A) are stereoselectively activated by *L*- $\alpha$ -amino acids (Christiansen et al., 2007). To our knowledge, the only antagonist identified for GPRC6A receptors is Calindol, a calcimimetic (Faure et al., 2009), while CGP compounds have not yet been tested on this receptor. However, the selective activation by *R*-isovaline (*D*- enantiomer) over *S*-isovaline (*L*- enantiomer) in our study suggests that coupling to GPRC6A is less likely.

A novel, GABA<sub>B</sub>-like amino acid receptor has been described, although due to the lack of an as yet unidentified second subunit, this GABA<sub>B</sub>-like receptor is not active (Calver et al., 2003). *R*-isovaline could potentially activate this new, GABA<sub>B</sub>-like receptor subunit if/when co-localized with its partner *in vivo*. Again, we are not aware of any study evaluating potentiation or blockade of this receptor with CGP7930 or CGP35348.

#### **5.4. Future studies**

This thesis has identified, for the first time, the mechanism of inhibition of thalamocortical neurons by the novel amino acid, isovaline. However, the precise mechanism by which isovaline exerts its effects has yet to be determined. Future studies should utilize the technology of recombinant cell lines to identify the how isovaline is causing its effects. This will allow a great deal of control to manipulate specific sites involved in the actions on GABA<sub>B</sub> receptors or other signalling molecules.

The first objective should be to confirm that the GABA<sub>B</sub> receptor is the receptor activated by isovaline. Initial experiments with one subtype of GABA<sub>B1</sub> subunit should be followed by experiments to identify whether the other GABA<sub>B1</sub> subunit is also activated by isovaline. For example, start by transfecting GABA<sub>B1A</sub> with GABA<sub>B2</sub> (need a heterodimer) and see if isovaline is able to activate the receptors. Next, proceed with GABA<sub>B1B</sub> and GABA<sub>B2</sub> transfection, because both subtypes are present in VB thalamus (Ulrich and Bettler, 2007). If only one subtype is activated by isovaline, this may be the first demonstration of a pharmacological difference between the two receptor subtypes.

The next step would be to determine whether isovaline acts intracellularly or extracellularly. This could be done by placing isovaline in the recording electrode and observing whether there is an increase in conductance. Regardless of outcome, application of intracellular isovaline should be followed by application of a GABA<sub>B</sub> agonist, for example baclofen, to determine whether intracellular isovaline prolongs the action of the normally reversible agonist.

The brain slice experiments performed in this thesis were all done in ventrobasal thalamus. However, behavioural experiments involving injection of isovaline intrathecally or into the cisterna magna both produced marked analgesia (MacLeod et al., 2010). This suggests that there is a local action of isovaline in the spinal cord and/or brainstem. It would be prudent to determine whether the actions of isovaline are similar in these regions of the nervous system. A similar slice preparation and application of isovaline as was done in this thesis would allow for such an assessment.

#### **5.4.1. Synaptic actions of isovaline**

In addition to the experiments described above, future work should include an assessment of isovaline's ability to modulate synaptic transmission. The cyclic analogue of isovaline, aminocyclobutyric carboxylic acid (ACBC), has even more potent actions as an analgesic than isovaline in the formalin foot test (Wang, 2008). The mechanism of action of ACBC is that of a partial agonist/antagonist, occupying the glycine<sub>B</sub> site of NMDA receptor, and preventing the receptors from being maximally activated (Inanobe et al., 2005). It is possible that isovaline also interacts with the glycine site of NMDA receptors, preventing the receptor from being maximally activated.

This is not to rule out the potential of a synaptic action of isovaline on other neurotransmitter systems; the analgesic action of isovaline suggest that it might be reducing excitatory input through NMDA or non-NMDA receptors (AMPA and kainate

receptors), or it could be augmenting inhibitory neurotransmission through GABA<sub>A</sub> or glycine receptors.

### **5.5. Implications of isovaline action**

Neuronal inhibition via activation of a potassium conductance is known to generate antinociception. Receptors that are coupled to K<sup>+</sup> channels and mediate antinociception include opioid, 5-HT<sub>1A</sub>, and muscarinic cholinergic receptors (Ocana et al., 1990; Robles et al., 1996; Raffa and Martinez, 1995). Indeed, activation of GABA<sub>B</sub> receptors is antinociceptive as well (Potes et al., 2006). It is plausible that the analgesic action of isovaline (MacLeod et al., 2010) is due to its ability to generate a long-lasting potassium conductance.

This thesis has begun the process of identifying the mechanism of action of a novel analgesic amino acid. This is particularly exciting given the effectiveness of isovaline at treating pain, especially phase 2, chronic pain, in combination with a relative paucity of deleterious side effects (MacLeod et al., 2010). I have done immunohistochemistry to show that there are co-localized GABA<sub>B</sub> receptor subunits in the epidermis of the hindpaw, and these peripheral receptors may be the site of action of isovaline in the periphery (see: Appendix C). The search for better analgesic compounds is important given the magnitude of the side effects common with most ‘effective’ analgesics for treatment of chronic pain (Eisenberg et al., 2005).

We now know that isovaline, at the very least, is capable of activating a long-lasting potassium conductance, and that this is mediated by a G-protein coupled receptor, likely GABA<sub>B</sub>. The GABA<sub>B</sub> receptor agonist baclofen is an effective antinociceptive agent, although it has adverse side effects, including the requirement for administration via pump (Slonimski et al., 2004). This suggests that activation of GABA<sub>B</sub> receptors represents a strategy in the treatment of pain, but that current ligands are not ideal. The unique actions of isovaline, including its long-lasting action, may make isovaline a strong candidate to treat chronic pain in particular. The reason(s) for isovaline's lack of adverse side effects are unclear, but may be due to the low potency of the compound (cf. MacLeod et al., 2010).

Once the precise mechanism of action of isovaline has been identified, this can be used as a target by others looking to synthesize drugs designed to have antinociceptive properties with minimal side effects.

## Figures

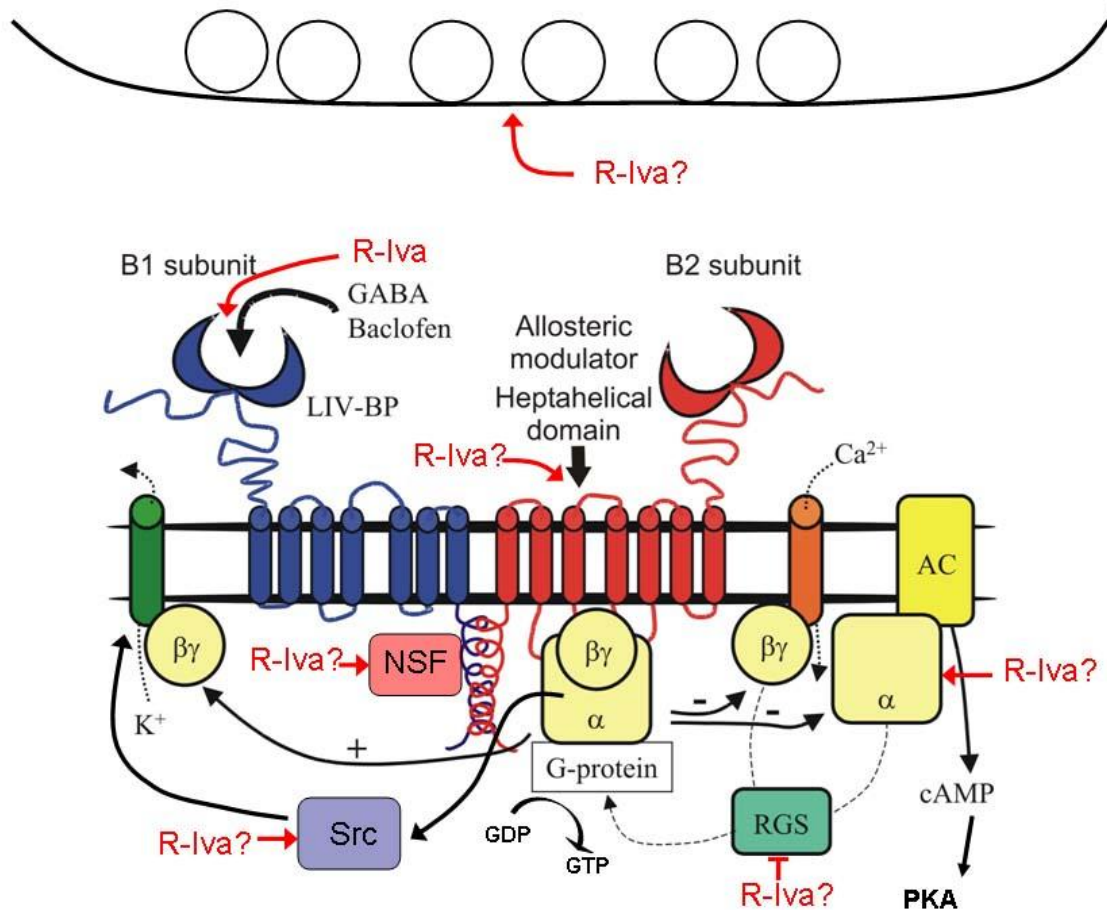


**Figure 5.1. Potential sites of isovaline action.** Isovaline could act extracellularly, increasing release of GABA onto neurons. Isovaline could bind with high affinity to the LIV-BP region of the GABA<sub>B1</sub> subunit. Isovaline could interact with the heptahelical domain known to bind the allosteric modulator CGP7930. Isovaline could interact with NSF proteins, preventing desensitization of the receptor. Isovaline could be inhibiting the GTPase action of the G $\alpha$  subunit, preventing the G-protein complex from re-associating. Isovaline could be activating Src tyrosine kinase, which would presumably activate multiple K<sup>+</sup> channels. Last, isovaline could be inhibiting RGS proteins,

prolonging the activation and inactivation rates of G-proteins. See text for full details (i.e.: section 5.3.1.). Adapted from Bowery and Smart, 2006.

## **5.6. References**

Bettler B., Kaupmann K., Mossbacher J., Gassmann M. Molecular structure and physiological functions of GABA<sub>B</sub> receptors. *Physiol. Rev.* 84: 835-867, 2004.

Bettler B., Tiao J.Y.-H. Molecular diversity, trafficking and subcellular localization of GABA<sub>B</sub> receptors. *Pharmacol. Ther.* 110: 533-543, 2006.

Binet V, Brajon C, Le Corre L, Acher F, Pin JP, Prézeau L. The heptahelical domain of GABA(B2) is activated directly by CGP7930, a positive allosteric modulator of the GABA(B) receptor. *J Biol Chem.* 279(28):29085-91. 2004.

Bowery N.G., Smart T.G. GABA and glycine as neurotransmitters: a brief history. *Br. J. Pharmacol.* 147: S109-S119, 2006.

Brown DA, Sihra TS. Presynaptic signaling by heterotrimeric G-proteins. *Handb Exp Pharmacol.* (184):207-60. 2008.

Callaghan B, Haythornthwaite A, Berecki G, Clark RJ, Craik DJ, Adams DJ. Analgesic alpha-conotoxins Vc1.1 and Rg1A inhibit N-type calcium channels in rat sensory neurons via GABA<sub>B</sub> receptor activation. *J Neurosci.* 28(43):10943-51. 2008.

Calver AR, Michalovich D, Testa TT, Robbins MJ, Jaillard C, Hill J, Szekeres PG, Charles KJ, Jourdain S, Holbrook JD, Boyfield I, Patel N, Medhurst AD, Pangalos MN.

Molecular cloning and characterisation of a novel GABA<sub>B</sub>-related G-protein coupled receptor. *Brain Res Mol Brain Res.* 110(2):305-17. 2003.

Christensen H.N. Intestinal absorption with special reference to amino acids. *Gastroenterol.* 21: 37-42, 1962.

Christiansen B, Hansen KB, Wellendorph P, Bräuner-Osborne H. Pharmacological characterization of mouse GPRC6A, an L-alpha-amino-acid receptor modulated by divalent cations. *Br J Pharmacol.* 150(6):798-807. 2007.

Clayton CC, Xu M, Chavkin C. Tyrosine phosphorylation of Kir3 following kappa-opioid receptor activation of p38 MAPK causes heterologous desensitization. *J Biol Chem.* 284(46):31872-81. 2009.

Couve A, Filippov AK, Connolly CN, Bettler B, Brown DA, Moss SJ. Intracellular retention of recombinant GABA<sub>B</sub> receptors. *J Biol Chem.* 273(41):26361-7. 2002.

Deng P.-Y., Xiao, Z., Yang, C., Rojanathammanee, L., Grisanti, L., Watt, J., Geiger, J.D., Liu, R., Porter, J.E., Lei, S. GABA<sub>B</sub> receptor activation inhibits neuronal excitability and spatial learning in the entorhinal cortex by activating TREK-2 K<sup>+</sup> channels. *Neuron* 63: 230-243, 2009.

Diversé-Pierluissi M, Remmers AE, Neubig RR, Dunlap K. Novel form of crosstalk between G protein and tyrosine kinase pathways. *Proc Natl Acad Sci U S A*. 94(10):5417-21. 1997.

Eisenberg E, McNicol ED, Carr DB. Efficacy and safety of opioid agonists in the treatment of neuropathic pain of nonmalignant origin: systematic review and meta-analysis of randomized controlled trials. *JAMA*. 293(24):3043-52. 2005.

Fadool DA, Holmes TC, Berman K, Dagan D, Levitan IB. Tyrosine phosphorylation modulates current amplitude and kinetics of a neuronal voltage-gated potassium channel. *J Neurophysiol*. 78(3):1563-73. 1997.

Faure H, Gorojankina T, Rice N, Dauban P, Dodd RH, Bräuner-Osborne H, Rognan D, Ruat M. Molecular determinants of non-competitive antagonist binding to the mouse GPRC6A receptor. 46(5-6):323-32. 2009.

Ficker E, Heinemann U. Slow and fast transient potassium currents in cultured rat hippocampal cells. *J Physiol*. 445:431-55. 1992.

Fowler CE, Aryal P, Suen KF, Slesinger PA. Evidence for association of GABA(B) receptors with Kir3 channels and regulators of G protein signalling (RGS4) proteins. *J Physiol*. 580(Pt 1):51-65. 2007.

Garnier M, Zaratin PF, Ficalora G, Valente M, Fontanella L, Rhee MH, Blumer KJ, Scheideler MA. Up-regulation of regulator of G protein signaling 4 expression in a model of neuropathic pain and insensitivity to morphine. *J Pharmacol Exp Ther.* 304(3):1299-306. 2003.

Garzón J, Rodríguez-Díaz M, López-Fando A, Sánchez-Blázquez P. RGS9 proteins facilitate acute tolerance to mu-opioid effects. *Eur J Neurosci.* 13(4):801-11. 2001.

Galvez T., Parmentier M.-L., Joly C., Malitschek B., Kaupmann K., Kuhn R., Bittiger H., Froestl W., Bettler B., Pin J.-P. Mutagenesis and modeling of the GABA<sub>B</sub> receptor extracellular domain support a venus flytrap mechanism for ligand binding. *J. Biol. Chem.* 274: 13362-13369, 1999.

Galvez T., Prezeau L., Milioti G., Franek M., Joly C., Froestl W., Bettler B., Bertrand H.-O., Blahos J., Pin J.-P. Mapping the agonist-binding site of GABA<sub>B</sub> type 1 subunit sheds light on the activation process of GABA<sub>B</sub> receptors. *J. Biol. Chem.* 275: 41166-41174, 2000a.

Galvez T., Urwyler S., Prezeau L., Mosbacher J., Joly C, Malischek B., Heid J., Brabet I., Froestl W., Bettler B., Kaupmann K., Pin J.P. Ca<sup>2+</sup> requirement for high-affinity  $\gamma$ -aminobutyric acid (GABA) binding at GABA<sub>B</sub> receptors: involvement of serine 269 of the GABA<sub>B</sub>R1 subunit. *Mol. Pharmacol.* 57: 419-426, 2000b.

Gamper N, Stockand JD, Shapiro MS. Subunit-specific modulation of KCNQ potassium channels by Src tyrosine kinase. *J Neurosci.* 23(1):84-95. 2003.

Ghavanini, A.A., Mathers, D.A., Puil, E., 2005. Glycinergic inhibition in thalamus revealed by synaptic receptor blockade. *Neuropharmacology* 49, 338-349.

Gold SJ, Ni YG, Dohlman HG, Nestler EJ. Regulators of G-protein signaling (RGS) proteins: region-specific expression of nine subtypes in rat brain. *J Neurosci.* 17(20):8024-37. 1997.

Golshani P, Warren RA, Jones EG. Progression of change in NMDA, non-NMDA, and metabotropic glutamate receptor function at the developing corticothalamic synapse. *J Neurophysiol.* 80(1):143-54. 1998.

Gomes P, Saito T, Del Corso C, Alioua A, Eghbali M, Toro L, Stefani E. Identification of a functional interaction between Kv4.3 channels and c-Src tyrosine kinase. *Biochim Biophys Acta.* 1783(10):1884-92. 2008.

Guilbaud G., Peschanski M., Gautron M., Binder D. Neurons responding to noxious stimulations in VB complex and caudal adjacent regions in the thalamus of the rat. *Pain* 8: 303-318, 1980.

Hill DR. GABA<sub>B</sub> receptor modulation of adenylate cyclase activity in rat brain slices.  
Br J Pharmacol. 84(1):249-57.

Holmes TC, Fadool DA, Ren R, Levitan IB. Association of Src tyrosine kinase with a human potassium channel mediated by SH3 domain. Science. 274(5295):2089-91.

Inanobe A., Furukawa H., Gouaux E. Mechanism of partial agonist action at the NR1 subunit of NMDA receptors. Neuron 47: 71-84, 2005.

Ingi T, Aoki Y. Expression of RGS2, RGS4 and RGS7 in the developing postnatal brain. Eur J Neurosci. 15(5):929-36. 2002.

Jia, F., Pignataro, L., Schofield, C.M., Yue, M., Harrison, N.L., Goldstein, P.A. An extrasynaptic GABA<sub>A</sub> receptor mediates tonic inhibition in thalamic VB neurons. Journal of Neurophysiology 94, 4491-4501. 2005.

Jia F, Pignataro L, Harrison NL. GABA<sub>A</sub> receptors in the thalamus: alpha4 subunit expression and alcohol sensitivity. Alcohol. 41(3):177-85. 2007.

Jia, F., Yue, M., Chandra, D., Keramidas, A., Goldstein, P.A., Homanics, G.E., Harrison, N.L. Taurine is a potent activator of extrasynaptic GABA<sub>A</sub> receptors in the thalamus. Journal of Neuroscience 28, 106-115. 2008.

Kaupmann K, Malitschek B, Schuler V, Heid J, Froestl W, Beck P, Mosbacher J, Bischoff S, Kulik A, Shigemoto R, Karschin A, Bettler B. GABA(B)-receptor subtypes assemble into functional heteromeric complexes. *Nature*. 396(6712):683-7. 1998.

Keramidas, A., Harrison, N.L. (2008). Agonist-dependent single channel current and gating in  $\alpha_4\beta_2\delta$  and  $\alpha_1\beta_2\gamma_{2S}$  receptors. *Journal of General Physiology* 131, 163-181.

Kerr D.I., Ong J. Potentiation of metabotropic GABA<sub>B</sub> receptors by L-amino acids and dipeptides in rat neocortex. *Eur. J. Pharmacol.* 468: 103-108, 2003.

Labouebe G., Lomazzi M., Cruz H.G., Creton C., Lujan R., Li M., Yanagawa Y., Obata K., Watanabe M., Wickman K., Boyer S.B., Slesinger P.A., Luscher C. RGS2 modulates coupling between GABA<sub>B</sub> receptors and GIRK channels in dopamine neurons of the ventral tegmental area. *Nat. Neurosci.* 10: 1559-1568, 2007.

Lambert NA, Johnston CA, Cappell SD, Kuravi S, Kimple AJ, Willard FS, Siderovski DP. Regulators of G-protein signaling accelerate GPCR signaling kinetics and govern sensitivity solely by accelerating GTPase activity. *Proc Natl Acad Sci U S A*. 107(15):7066-71. 2010.

MacLeod BA, Wang JT, Chung CC, Ries CR, Schwarz SK, Puil E. Analgesic properties of the novel amino acid, isovaline. *Anesth Analg.* 110(4):1206-14. 2010.

- McCormick DA, Pape HC. Noradrenergic and serotonergic modulation of a hyperpolarization-activated cation current in thalamic relay neurones. *J Physiol.* 431:319-42. 1990.
- Ocaña M, Del Pozo E, Barrios M, Robles LI, Baeyens JM. An ATP-dependent potassium channel blocker antagonizes morphine analgesia. *Eur J Pharmacol.* 186(2-3):377-8. 1990.
- Pontier SM, Lahaie N, Ginham R, St-Gelais F, Bonin H, Bell DJ, Flynn H, Trudeau LE, McIlhinney J, White JH, Bouvier M. Coordinated action of NSF and PKC regulates GABA<sub>B</sub> receptor signaling efficacy. *EMBO J.* 25(12):2698-709. 2006.
- Potes C.S., Neto F.L., Castro-Lopes J.M. Inhibition of pain behavior by GABA<sub>B</sub> receptors in the thalamic ventrobasal complex: Effect on normal rats subjected to the formalin test of nociception. *Brain Res.* 1115: 37-47, 2006.
- Price, D.D. Unpleasant pain evoked by thalamic stimulation. *Nat. Med.* 1: 885-887, 1995.
- Raffa RB, Martinez RP. The 'glibenclamide-shift' of centrally-acting antinociceptive agents in mice. *Brain Res.* 677(2):277-82. 1995.
- Richman RW, Tombler E, Lau KK, Anantharam A, Rodriguez J, O'Bryan JP, Diversé-Pierluissi MA. N-type Ca<sup>2+</sup> channels as scaffold proteins in the assembly of signaling molecules for GABA<sub>B</sub> receptor effects. *J Biol Chem.* 279(23):24649-58. 2004.

Robles LI, Barrios M, Del Pozo E, Dordal A, Baeyens JM. Effects of K<sup>+</sup> channel blockers and openers on antinociception induced by agonists of 5-HT<sub>1A</sub> receptors. *Eur J Pharmacol.* 295(2-3):181-8. 1996.

Romei C, Luccini E, Raiteri M, Raiteri L. GABA(B) presynaptic receptors modulate glycine exocytosis from mouse spinal cord and hippocampus glycinergic nerve endings. *Pharmacol Res.* 59(3):154-9. 2009.

Saint, D., Thomas, T., Gage, P.W. GABA<sub>B</sub> agonists modulate a transient potassium current in cultured mammalian hippocampal neurons. *Neurosci. Lett.* 118: 9-13, 1990.

Shen H, Gong QH, Aoki C, Yuan M, Ruderman Y, Dattilo M, Williams K, Smith SS. Reversal of neurosteroid effects at alpha4beta2delta GABA<sub>A</sub> receptors triggers anxiety at puberty. *Nat Neurosci.* 10(4):469-77. 2007.

Shen H, Sabaliauskas N, Sherpa A, Fenton AA, Stelzer A, Aoki C, Smith SS. A critical role for alpha4betadelta GABA<sub>A</sub> receptors in shaping learning deficits at puberty in mice. *Science.* 327(5972):1515-8.

Shutes A, Der CJ. Real-time in vitro measurement of GTP hydrolysis. *Methods.* 37(2):183-89. 2005.

Slonimski M, Abram SE, Zuniga RE. Intrathecal baclofen in pain management. *Reg Anesth Pain Med.* 29(3):269-76. 2004.

Sohal, V.S., Pangratz-Fuehrer, S., Rudolph, U., Huguenard, J.R. Intrinsic and synaptic dynamics interact to generate emergent patterns of rhythmic bursting in thalamocortical neurons. *Journal of Neuroscience* 26, 4247-4255. 2006

Thompson, S.M., Gahwiler, B.H. Comparison of the actions of baclofen at pre- and postsynaptic receptors in the rat hippocampus in vitro. *J. Physiol.* 451: 329-345, 1992.

Ulrich D, Bettler B. GABA(B) receptors: synaptic functions and mechanisms of diversity. *Curr Opin Neurobiol.* 17(3):298-303. 2007.

Ulrich D., Huguenard J.R. GABA<sub>B</sub> receptor-mediated responses in GABAergic projection neurones of rat reticularis thalami in vitro. *J. Physiol.* 493: 845-854, 1996.

Urwyler S., Gjoni T., Kaupmann K., Pozza M.F., Mosbacher J. Selected amino acids, dipeptides and arylalkylamine derivatives do not act as allosteric modulators at GABA<sub>B</sub> receptors. *Eur. J. Pharmacol.* 483: 147-153, 2004.

Vicini S, Ferguson C, Prybylowski K, Kralic J, Morrow AL, Homanics GE. GABA(A) receptor alpha1 subunit deletion prevents developmental changes of inhibitory synaptic currents in cerebellar neurons. *J Neurosci.* 21(9):3009-16. 2001.

Wan X, Mathers DA, Puil E. Pentobarbital modulates intrinsic and GABA-receptor conductances in thalamocortical inhibition. *Neuroscience*. 121(4):947-58. 2003.

Wang T. Isovaline: a new analgesic. M.Sc. thesis, University of British Columbia, 2008.

Yue P, Lin DH, Pan CY, Leng Q, Giebisch G, Lifton RP, Wang WH. Src family protein tyrosine kinase (PTK) modulates the effect of SGK1 and WNK4 on ROMK channels. *Proc Natl Acad Sci U S A*. 106(35):15061-6. 2009.

Zeilhofer HU, Möhler H, Di Lio A. GABAergic analgesia: new insights from mutant mice and subtype-selective agonists. *Trends Pharmacol Sci*. 30(8):397-402. 2009.

## **APPENDIX A: IMMUNOHISTOCHEMICAL IDENTIFICATION OF THE ANCHORING PROTEIN GEPHYRIN IN VENTROBASAL THALAMUS.**

### **Brief background**

Gephyrin is an anchoring that is responsible for localizing both glycine (Prior et al., 1992) and GABA<sub>A</sub> (Cabot et al., 1995) receptors to the cell membrane. Prior to performing immunohistochemistry for glycine  $\alpha_{1/2}$  receptor subunits (see: Manuscript #2), we wanted to verify the presence of gephyrin in VB thalamus.

### **Methods**

#### **Immunohistochemistry**

Immunohistochemistry was performed on sections post-fixed in 4% formaldehyde for 10 min. The sections were permeabilized with 0.1% Triton X-100, blocked with 0.5% bovine serum albumin (BSA) in phosphate buffered saline (PBS) and incubated in primary antibody overnight at 4°C in PBS solution containing 0.1% BSA. The primary antibody was rabbit anti-gephyrin (1:200; Abcam, Cambridge, MA; ab32206). Secondary antibody was chicken anti-rabbit Alexa 488 (Invitrogen, Burlington, ON), and was applied for one hour at room temperature. Sections were followed by 4',6-diamidino-2-phenylindole (DAPI) nuclear counterstain. Sections were coverslipped with Prolong Gold (Invitrogen, Burlington, ON) and allowed to cure overnight before imaging.

Low magnification images were captured using an Axioskop 2 MOT epifluorescence microscope (Zeiss, Jena, Germany), fitted with a SPOT camera (Diagnostic Instruments,

Sterling Heights, MI) and Northern Eclipse software (Empix Imaging, Mississauga, Ontario, Canada). Image brightness was modified slightly using Adobe Photoshop software to enhance visualization.

## **Results**

We used immunohistochemistry to determine whether gephyrin, an anchoring protein required for the stabilization of glycine receptors to the synapse (Prior *et al.*, 1992), was present in VB thalamus. Indeed, we found extensive expression of gephyrin throughout both ventroposteromedial (VPM) and ventroposterolateral (VPL) nuclei of VB thalamus (Fig. A.1). Higher power image in the inset of Fig. A.1 shows gephyrin positive neurons in the VPL, with nuclei counter-stained with DAPI. Negative controls, in which the primary antibody for gephyrin is omitted from the protocol above, did not show any gephyrin staining at all (data not shown).

While the pattern of gephyrin expression in the VPL corresponds to that of glycine receptor expression (see: Figure 2.1), there is much more gephyrin expression than there are glycine receptors in the VPM. Gephyrin in the VPM is likely anchoring GABA<sub>A</sub> receptors (Cabot *et al.*, 1995).

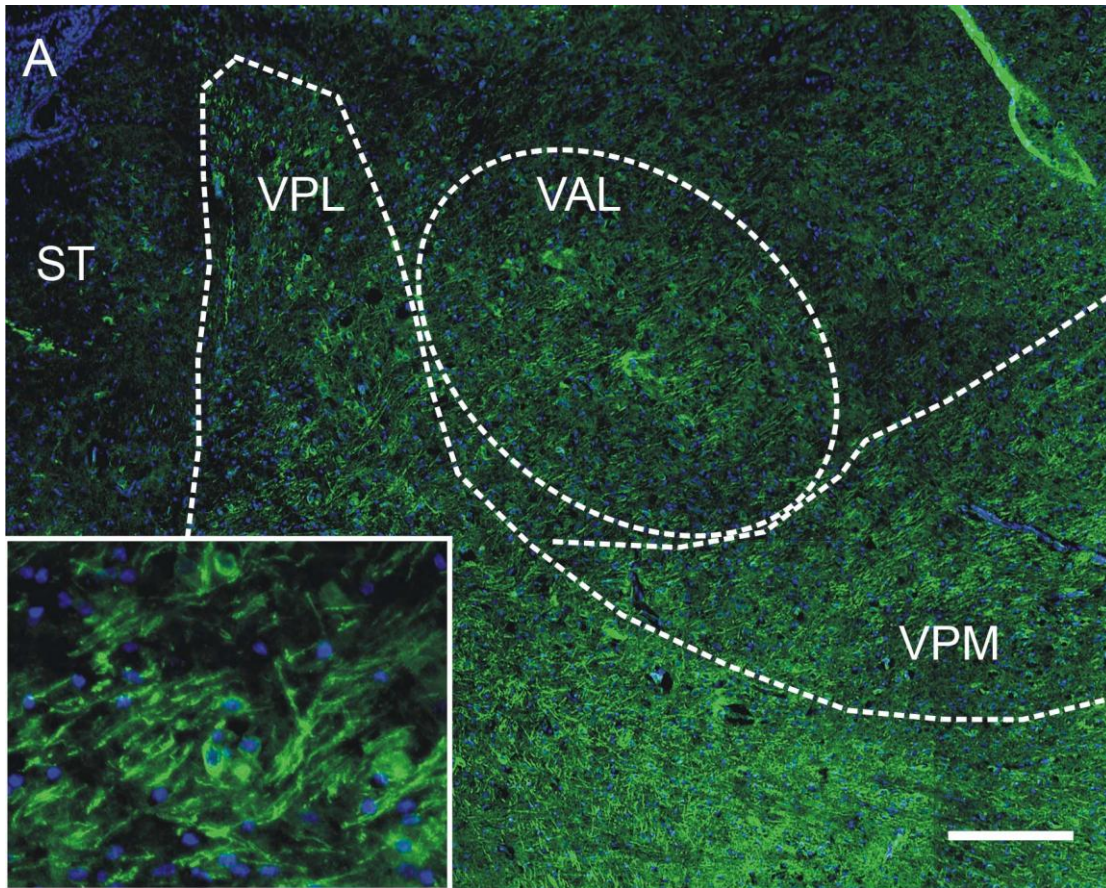


**Figure A.1. Gephyrin is found throughout the ventrobasal thalamus.** (A) Gephyrin (green), which anchors both glycine and GABA<sub>A</sub> receptors to the cell membrane, is expressed throughout the ventroposterolateral (VPL) and ventroposteromedial (VPM) nuclei of the thalamus. The inset shows cells expressing gephyrin at high magnification. Scale bars in (A) are 250  $\mu\text{m}$  for low magnification and 50  $\mu\text{m}$  for inset. ST = stria terminalis. Nuclei are counter-stained with DAPI. VAL = ventro-anterolateral thalamic nucleus.

## **References**

Cabot JB, Bushnell A, Alessi V, Mendell NR. 1995. Postsynaptic gephyrin immunoreactivity exhibits a nearly one-to-one correspondence with gamma-aminobutyric acid-like immunogold-labeled synaptic inputs to sympathetic preganglionic neurons. *J Comp Neurol.* **356**(3):418-32.

Prior, P, Schmitt,B, Crenningloh, C, Pribilla, I, Multhaup, G, Beyreuther, K, Maulet, Y, Werner, P, Tangosch, D, Kirsch, J, Betz H. 1992. Primary structure and alternative splice variants of gephyrin, a putative glycine receptor-tubulin linker protein. *Neuron.* **8**: 1161-1170.

## **APPENDIX B: LIMITATIONS OF QUANTUM DOTS AS FLUOROPHORES FOR VISUALIZING RECEPTORS IN TISSUE**

### **Brief background**

Following our observations of co-localization of GABA<sub>A</sub>α4 subunits and glycine receptors (See section 2), we wondered if there was a change in synaptic location of these receptors developmentally (see Section: 5.1.2.2), or in response to increased synaptic input from afferent fibres. To address these questions, we were interested in using the emerging technology of quantum dot (Qdot) nanocrystals. Qdots are a special type of semiconductor made from cadmium mixed with selenium, and they range from ~ 10 to 40 nm in diameter. Qdots are inherently fluorescent and are able to be conjugated to biological reagents, such as antibodies, for imaging studies. Qdots are extremely photostable, which allows them to be used for imaging over prolonged periods of time (Dahan et al., 2003). Having been used to follow the trafficking of glycine receptors in cultured neurons (Dahan et al., 2003), we wondered if we could use them to following trafficking of glycine and GABA<sub>A</sub>α4 receptors in the living brain slice.

The following appendix outlines our attempts to use Qdots to visualize glycine receptors under various conditions, in an attempt to follow receptor trafficking.

### **Methods**

#### **Tissue preparation**

Sprague-Dawley rats (P12) were anesthetized with pentobarbital (40 mg/kg) and transcardially perfused with cold 0.1% PBS, followed by 4% formaldehyde. Brains were

dissected and post-fixed in 4% formaldehyde for 2 h at 4°C, followed by submersion in 30% sucrose for 24-48 h at 4°C. The tissue was embedded with Tissue-Tek embedding medium (Sakura Finetek, Torrence, CA) and frozen in liquid nitrogen. Sagittal sections were made at 14 µm thickness and stored at -20°C.

### **Immunohistochemistry**

Immunohistochemistry was performed on sections post-fixed in 4% formaldehyde for 10 min. The sections were permeabilized with 0.1% Triton X-100, blocked with 0.5% bovine serum albumin (BSA) in phosphate buffered saline (PBS) and incubated in rabbit anti-glycine receptor  $\alpha 1/2$  subunit (1: 200; Abcam, Cambridge, MA; ab23809) overnight at 4°C in PBS solution containing 0.1% BSA. The secondary antibody, chicken anti-rabbit, was conjugated to either Alexa 488 fluorophore as a positive control (Invitrogen, Burlington, ON), or to Qdot 525 fluorophore. Secondary antibodies were applied for one hour at room temperature in 0.1% BSA.

Sections were all followed by 4',6-diamidino-2-phenylindole (DAPI) nuclear counterstain, except certain preparations containing Qdots. Since Qdots are excited by UV light, the fluorescence filter normally used for DAPI was not ideal for use with Qdots. Sections were all coverslipped with Prolong Gold (Invitrogen, Burlington, ON) and allowed to cure overnight before imaging.

Low magnification images were captured using an Axioskop 2 MOT epifluorescence microscope (Zeiss, Jena, Germany), fitted with a SPOT camera (Diagnostic Instruments,

Sterling Heights, MI) and Northern Eclipse software (Empix Imaging, Mississauga, Ontario, Canada). Image brightness was modified slightly using Adobe Photoshop software to enhance visualization.

### **Immunohistochemistry on living slices**

In a subset of experiments, we wanted to visualize the trafficking of receptors in the living brain slice. As a control, we first wondered whether antibodies against the receptors would be able to permeate the living slice to allow visualization. First, we prepared 300  $\mu\text{m}$  thick brain slices (as in *Slice preparation*). While in aCSF, antibodies against glycine receptor  $\alpha_{1/2}$  subunits were added for one hour, suspended in 0.1% BSA in PBS. After 2 washes of 5 minutes in aCSF, secondary antibodies were added for one hour, also suspended in 0.1% BSA in PBS. The secondary antibodies were either conjugated to an Alexa 488 fluorophore or Qdot 525 fluorophores.

Live slices were then fixed with 4% formaldehyde and embedded with Tissue-Tek embedding medium (Sakura Finetek, Torrance, CA) and frozen in liquid nitrogen. Sections were made perpendicular to the plane of the original slice at 14  $\mu\text{m}$  thickness. Nuclei were counter-stained with DAPI (for Alexa 488) and sections were coverslipped with Prolong Gold (Invitrogen, Burlington, ON). Images were captured using an Axioskop 2 MOT epifluorescence microscope (Zeiss, Jena, Germany), fitted with a SPOT camera (Diagnostic Instruments, Sterling Heights, MI) and Northern Eclipse software (Empix Imaging, Mississauga, Ontario, Canada). Image brightness was modified slightly using Adobe Photoshop software to enhance visualization.

### **Physical dissociation of thalamocortical neurons**

For experiments involving immunocytochemistry on dissociated thalamocortical cells, we first prepared 300  $\mu\text{m}$  thick sagittal sections of postnatal day 9 (p9) Sprague-Dawley rats. The thalami were removed using a razor blade and placed in a coverslip-bottomed petri dish. A glass capillary tube was inserted into the thalamus which was vibrated at 2 Hz for 2 minutes. The thalamus was removed and dissociated cells were given an hour to attach to the bottom of the petri dish. Immunocytochemistry was carried out as for immunohistochemistry on fixed, frozen sections, outlined above.

### **Results**

#### **Quantum dots: methodological limitations to visualization of receptor trafficking in living brain slices**

Having shown a high degree of co-localization of synaptic glycine receptors with a GABA<sub>A</sub> subunit that is more often located extrasynaptically (Jia et al., 2008), we wondered if GABA<sub>A</sub>  $\alpha_4$  subunits were trafficked to synapses during periods of increased stimulation. To test this theory we decided to use stimulation of medial lemniscus, known to elicit both glycinergic and GABA<sub>A</sub>ergic IPSCs (i.e.: Fig. 2.5), in combination with visualization of receptors using the emerging technology of quantum dots.

First, we needed to verify that we could, in fact, visualize fluorophore-conjugated antibodies in living brain slices. To test this, we prepared 300  $\mu\text{m}$  thick sections of p10-15 Sprague-Dawley rats to include ventrobasal thalamus. Sections were placed in

oxygenated aCSF, and incubated with antibodies against glycine receptor  $\alpha 1/2$  subunits for one hour. Following washes with normal aCSF, secondary antibodies were added for one hour. In 3 brain slices, secondary antibodies were conjugated to Alexa 488 fluorophores, while another 3 brain slices received secondary antibodies conjugated to Qdot 525 fluorophores. After washes with normal aCSF, the slices were all fixed with 4% formaldehyde, embedded and sectioned at 14  $\mu\text{m}$  perpendicular to the plane of the brain slice with a cryostat. The nuclear counter-stain DAPI was added to Alexa 488-receiving sections, and the sections were coverslipped. Sections were then examined with a fluorescent microscope.

We found that in brain slices incubated with secondary antibodies conjugated to Alexa 488 fluorophores, glycine receptors were clearly visible throughout the thickness of the 300  $\mu\text{m}$  thick brain slice (Fig. B.1A). By contrast, we found that all brain slices incubated with secondary antibodies conjugated to Qdot 525 fluorophores had no glycine receptors visible above background (Fig. B.1B). These results suggested that, while it is possible for fluorophore-conjugated antibodies to penetrate the living brain slice, Qdot-conjugated antibodies were not detectable.

### **Quantum dots: methodological limitations to visualization in fixed, frozen tissue**

Since we were unable to use Qdots to visualize glycine receptors in 300  $\mu\text{m}$  thick, living tissue, we wondered if they would be able to work on 14  $\mu\text{m}$  sections of fixed, frozen tissue. We made sagittal sections from p12 Sprague Dawley rats and incubated them with antibodies against glycine  $\alpha_{1/2}$  subunits. We then followed with secondary

antibodies conjugated to either Alexa 488 fluorophores or Qdot 525 fluorophores. We examined the brainstem area of the sections, as these areas generally have a high amount of expression of glycine receptors (Ghavanini *et al.*, 2005).

While there was a large amount of glycine receptors visible using the Alexa 488 fluorophore (Fig. B.2A), we were not able to visualize any signal above background using the Qdot 525 fluorophore (Fig.B.2B), compared with negative control in which the primary antibody has been omitted (Fig. B.2C). These results suggested that, while it is possible to visualize glycine receptors using conventional Alexa fluorophores, Qdot-conjugated antibodies are not detectable in fixed, frozen tissue.

### **Quantum dots: detectable using the experimental setup**

Having had successive failures in our attempts to visualize glycine receptors using Qdots, we wondered if our imaging setup was not ideally configured to detect the Qdots. To test whether we were able to visualize Qdots themselves, we placed 1  $\mu$ L of Qdot 525 fluorophores on a glass slide and covered them with a coverslip. Using the filter settings optimized for emission around 525 nm wavelength we found that the quantum dots emitted a large amount of light with minimal exposure time. When we used 10 ms exposure, we were clearly able to resolve Qdots on our slide (Fig. B.3A). As we increased the duration of the exposure to 20 (Fig. B.3B) and 50 ms (Fig. B.3C), there was a large increase in the amount of light given off by the Qdots. Compare these exposure times with that used to visualize the Alexa 488 fluorophore in Fig. B.2A, which was 250

ms. These results suggest that our setup was indeed able to resolve the Qdots, and that the problems we had been having were not due to limitations of our imaging setup.

### **Quantum dots: only on dissociated cells**

A major difference between our approach to visualize receptors with Qdots and the approach used by others is that we were using brain slices while others tend to use dissociated or cultured cells (cf: Dahan et al., 2003). Knowing that our setup was able to resolve Qdots, we decided to test whether we could visualize glycine receptors with Qdots on neurons of ventrobasal thalamus after they had been physically dissociated. To do this, we prepared 300  $\mu\text{m}$  thick sagittal brain slices from p9 Sprague-Dawley rats as previously, and then isolated the thalamus using a razor blade. The thalamus was transferred to a coverslip-bottom petri dish and vibrated at 2 Hz with a glass capillary tube for 2 minutes. The thalamus was removed and any dissociated cells were given one hour to adhere to the bottom of the petri dish. Immunocytochemistry was carried out with the same protocol as in fixed, frozen tissue.

Using the Alexa 488 fluorophore as a positive control, we found glycine receptor expression throughout the somata and proximal dendrites of thalamocortical neurons, with intact presynaptic terminals labelled with VGAT (Fig. B.4A,B). Similarly, using Qdot 525 fluorophores we observed glycine receptor expression throughout the somata and proximal dendrites, with presynaptic terminals labelled with VGAT (Fig. B.4C,D). These results suggest that Qdots are able to visualize receptors of thalamocortical

neurons, but that they are optimally suited for use with cultured or dissociated cells, and not with intact nervous tissue.

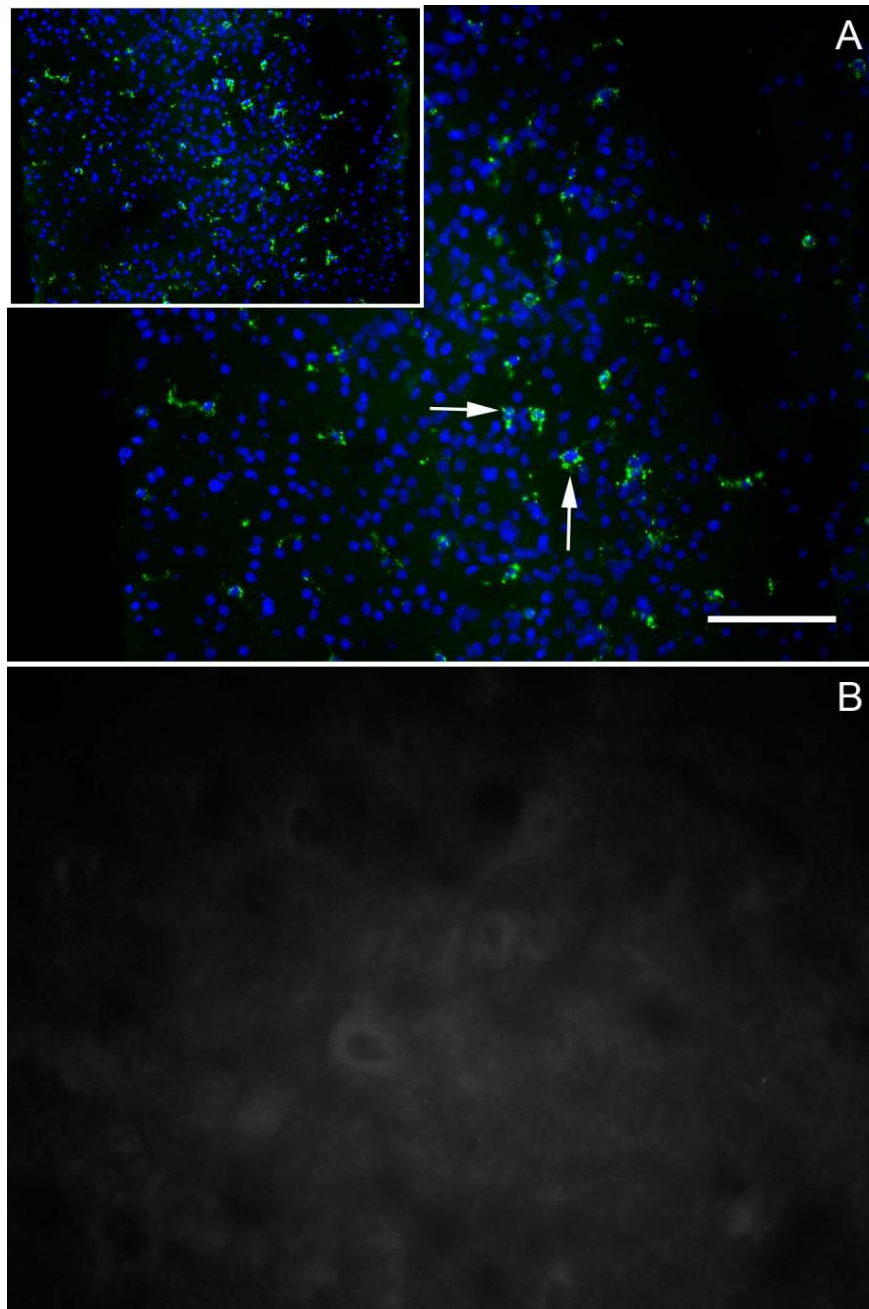


**Figure B.1. Quantum dots (Qdots) do not work in live brain slices.** Brain slices were incubated in primary antibodies directed against glycine receptor  $\alpha_{1/2}$  subunits, followed by secondary antibodies conjugated to (A) Alexa 488 fluorophores, or (B) 525 Qdots. After fixing and embedding, the slices were sectioned perpendicularly at 14  $\mu\text{m}$  and

imaged. (A) Glycine receptors revealed with Alexa 488 were present throughout the brain slice (arrows). Inset shows a lower power image of the same slice. (B) Using the same preparation but with Qdots instead of the Alexa 488 fluorophore, no glycine receptors could be seen anywhere in the slice, even at higher magnification. Nuclei in (A) were counter-stained with DAPI, those in (B) were not (see: Methods). Bar in (A) represents 100  $\mu\text{m}$ , 200  $\mu\text{m}$  in inset and 400  $\mu\text{m}$  in (B).

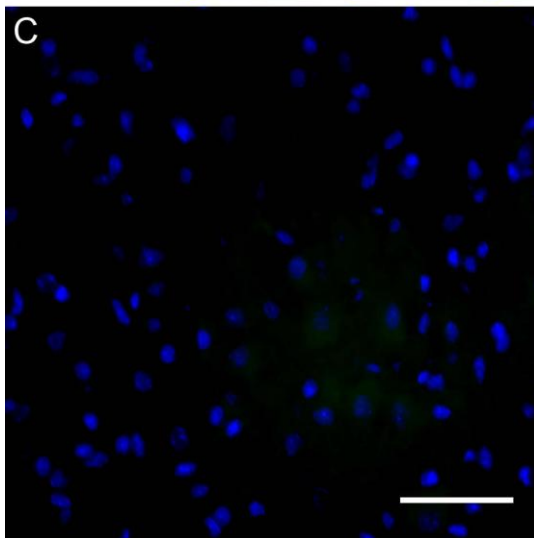
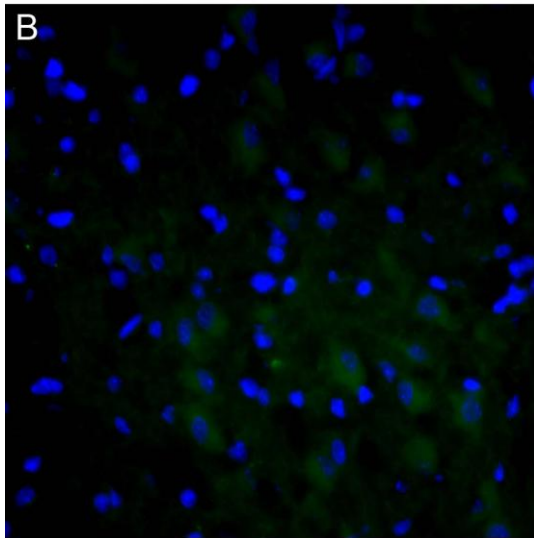
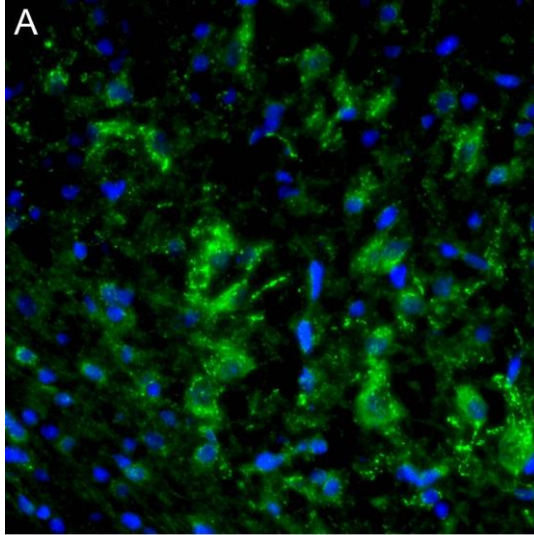


**Figure B.2. Quantum dots (Qdots) do not work on fixed, frozen tissue.** Glycine receptors were visualized in the brainstem of fixed, frozen tissue using secondary antibodies conjugated to either Alexa 488 fluorophores, or Qdot 525. (A) Glycine receptors in the brainstem visualized using an Alexa 488 secondary antibody showed extensive expression of glycine receptors. (B) Glycine receptors in the brainstem visualized using secondary antibodies conjugated to Qdots had no signal detectable over background. (C) Negative control for Qdot 525 in which the primary antibody was omitted. Note the similarity in (B) and (C). Nuclei were counter-stained with DAPI. Scale bar in C is 50  $\mu\text{m}$  for each panel.

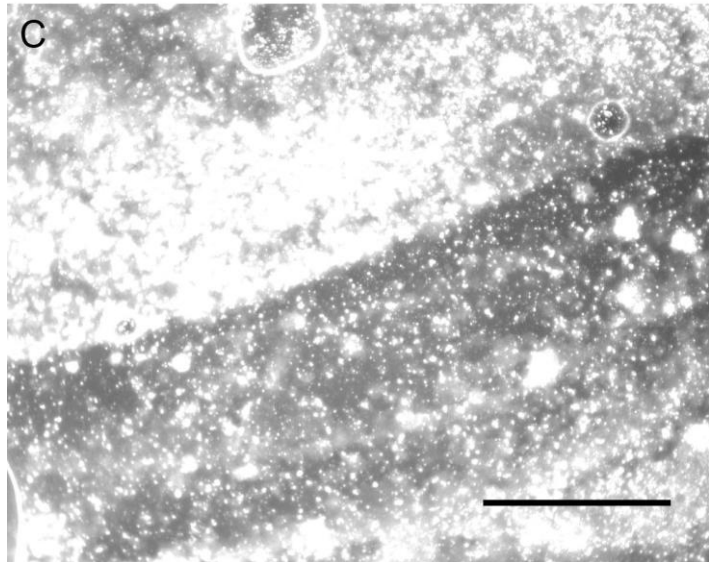
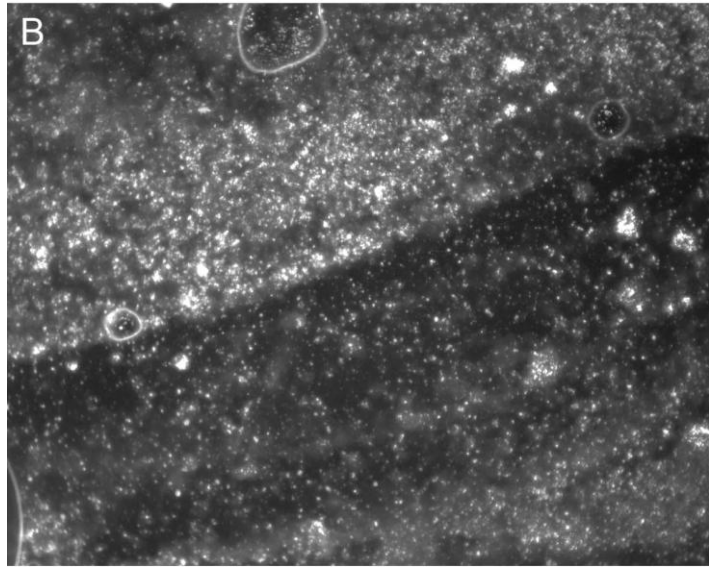
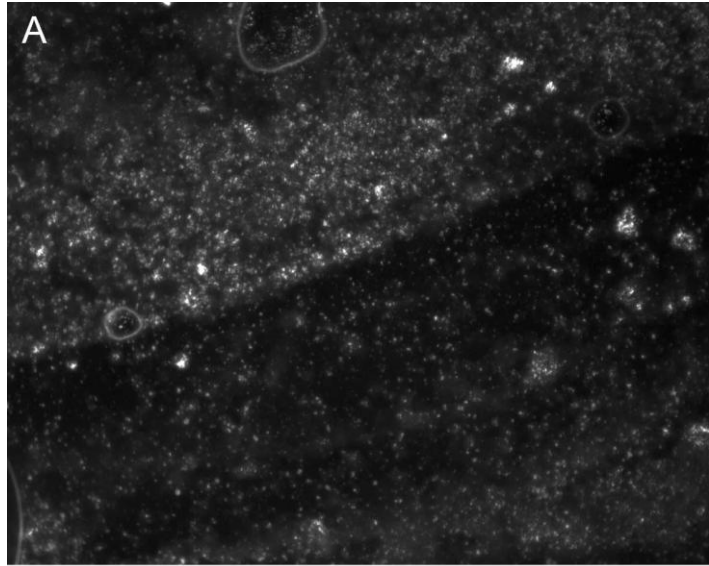


**Figure B.3. The experimental setup used is able to visualize quantum dots (Qdots).**

To verify that the Qdots were working and that we could observe them with our experimental setup, 1  $\mu\text{L}$  of Qdot 525 were placed on a slide and coverslipped. We then exposed the Qdots to ultraviolet light and recorded images at increasing exposure times of (A) 10, (B) 20 and (C) 50 ms. For comparison, the Alexa 488 in Fig. 5(A) was captured with an exposure time of 250 ms. Scale bar in (C) represents 50  $\mu\text{m}$  in all panels.

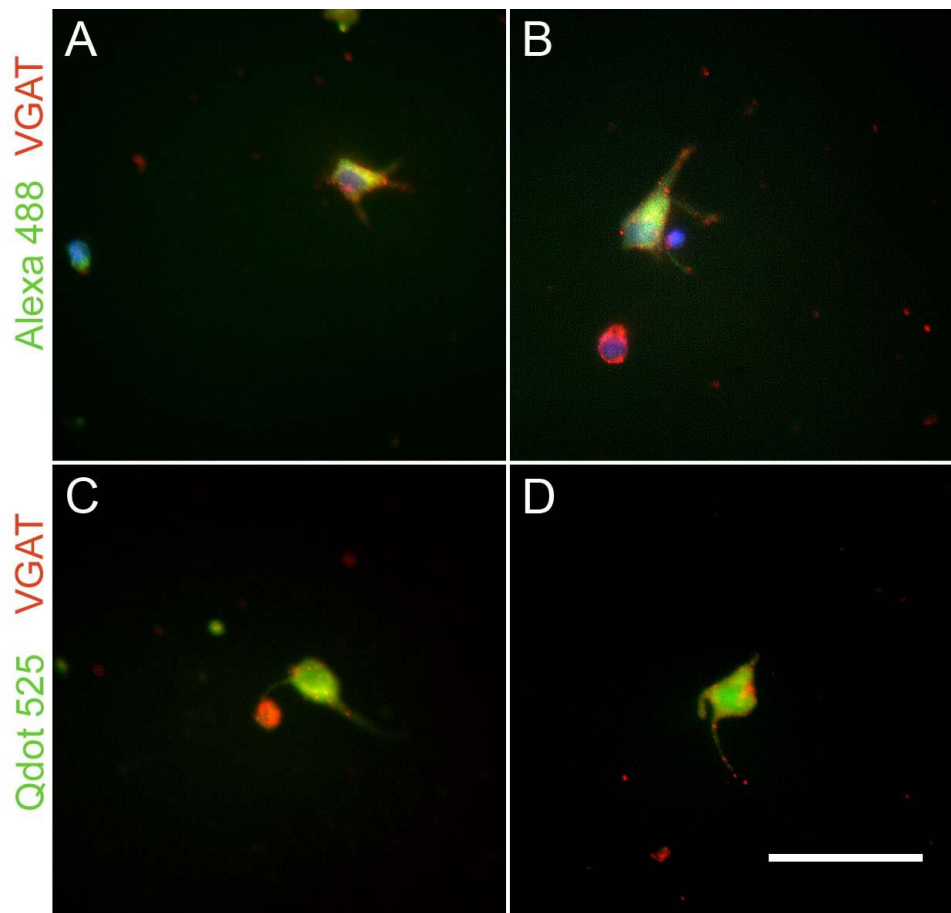


**Figure B.4. Quantum dots are able to visualize glycine receptors in dissociated cells.**

(A, B) Thalamocortical neurons were mechanically dissociated and immunohistochemistry was performed with antibodies against the vesicular inhibitory amino acid transporter (VGAT; red) and glycine<sub>α1/2</sub> (green). The secondary antibodies for glycine<sub>α1/2</sub> were conjugated to an Alexa 488 fluorophore. (C, D) Using the same preparation as in (A) and (B) but with secondary antibodies for glycine<sub>α1/2</sub> conjugated to Qdot 525, showing similar distribution of glycine receptors as with Alexa 488. Nuclei in (A) and (B) are stained with DAPI. Scale bar in (D) is 50 μm and applies to all panels.

## **References**

Dahan M, Lévi S, Luccardini C, Rostaing P, Riveau B, Triller A. 2003. Diffusion dynamics of glycine receptors revealed by single-quantum dot tracking. *Science*. **302**(5644): 442-5.

Ghavanini AA, Mathers DA, Puil E (2005), Glycinergic inhibition in thalamus revealed by synaptic receptor blockade. *Neuropharmacol.* **49**: 338-349.

Jia, F., Yue, M., Chandra, D., Keramidas, A., Goldstein, P.A., Homanics, G.E., Harrison, N.L., 2008. Taurine is a potent activator of extrasynaptic GABA<sub>A</sub> receptors in the thalamus. *Journal of Neuroscience* **28**, 106-115.

## **APPENDIX C: IMMUNOHISTOCHEMISTRY TO IDENTIFY GABA<sub>B</sub> RECEPTORS IN THE EPIDERMIS OF THE MOUSE HIND-PAW**

### **Brief background**

Ongoing studies in the laboratory of a colleague have investigated the analgesic action of isovaline injected into the hindpaw. While studies have shown that the GABA<sub>B</sub> agonist baclofen is effective at treating prostaglandin E2-induced pain (Reis and Duarte, 2006), it is not known whether GABA<sub>B</sub> receptors exist in the skin.

To address this question, we performed immunohistochemistry on a skin-punch biopsy taken from the intraplantar surface of the mouse hind-paw.

### **Methods**

#### **Tissue preparation**

A skin punch of 2 mm diameter was taken from the intraplantar surface of the mouse hind-paw and placed in 4% formalin in PBS for 48 hours. The tissue was then cryoprotected in 30% sucrose for 24 hours. Sections were made perpendicular to the plane of the biopsy at 30 µm using a cryostat, and were kept at -20°C until needed.

#### **Immunohistochemistry**

Immunohistochemistry was performed on sections post-fixed in 4% formaldehyde for 10 min. The sections were permeabilized with 0.1% Triton X-100, blocked with 0.5% bovine serum albumin (BSA) in phosphate buffered saline (PBS) and incubated in primary antibody overnight at 4°C in PBS solution containing 0.1% BSA. The primary

antibodies were as follows, according to the experiment performed: mouse anti-GABA<sub>B</sub>R1 subunit (1:100; ab55051; Abcam, Cambridge, MA), rabbit anti-GABA<sub>B</sub>R2 subunit (1:100; ab75838; Abcam, Cambridge, MA), and chicken anti-MAP-2 (1:100; ab75713; Abcam, Cambridge, MA).

Sections were incubated in goat anti-mouse Alexa 546, goat anti-rabbit Alexa 488, and goat anti-chicken 633 secondary antibodies for 1 h at room temperature (Invitrogen, Burlington, ON) followed by 4',6-diamidino-2-phenylindole (DAPI) nuclear counterstain. Sections were coverslipped with Prolong Gold (Invitrogen, Burlington, ON) and allowed to cure overnight before imaging.

Images were captured using an Olympus Fluoview 1000 confocal microscope (10x and 60x/1.4 oil Plan-Apochromat objectives). Image brightness was modified slightly using Adobe Photoshop software to enhance visualization.

## **Results**

### **Immunocytochemistry of GABA<sub>B</sub> receptors in the epidermis of the mouse hind-paw**

Baclofen is known to produce analgesia on GABA<sub>B</sub> receptors in the periphery in animal models of pain that involve injection of prostaglandin E2 into the intraplantar region of the hindpaw (Reis and Duarte, 2006). However, no histology has ever shown the presence of GABA<sub>B</sub> receptors in the dermal or epidermal tissue of the hind-paw. For this reason, we performed immunohistochemistry on the dermal and epidermal tissue of the mouse hind-paw using antibodies directed against both GABA<sub>B</sub> receptor subunits and the

neuronal marker MAP-2. We found that both GABA<sub>B2</sub> (Fig. C.1A, B) and GABA<sub>B1</sub> (Fig. C.1B, D) subunits are expressed in cells of the stratum spinosum of the epidermis, cells which do not express MAP-2. Both GABA<sub>B</sub> subunits are also expressed in MAP-2 positive neural processes of the stratum basale of the epidermis (Fig. C1C, D; arrowheads).

In summary, there is extensive GABA<sub>B</sub> expression in the epidermis of the mouse hind-paw. The MAP-2 positive processes expressing GABA<sub>B</sub> receptors are likely free nerve endings, which others have shown to be responsible for transmitting nociceptive information (Navarro *et al.*, 2005). The cells in the stratum spinosum are likely all keratinocytes, which have been implicated in pain due to inflammation (Radke *et al.*, 2010).

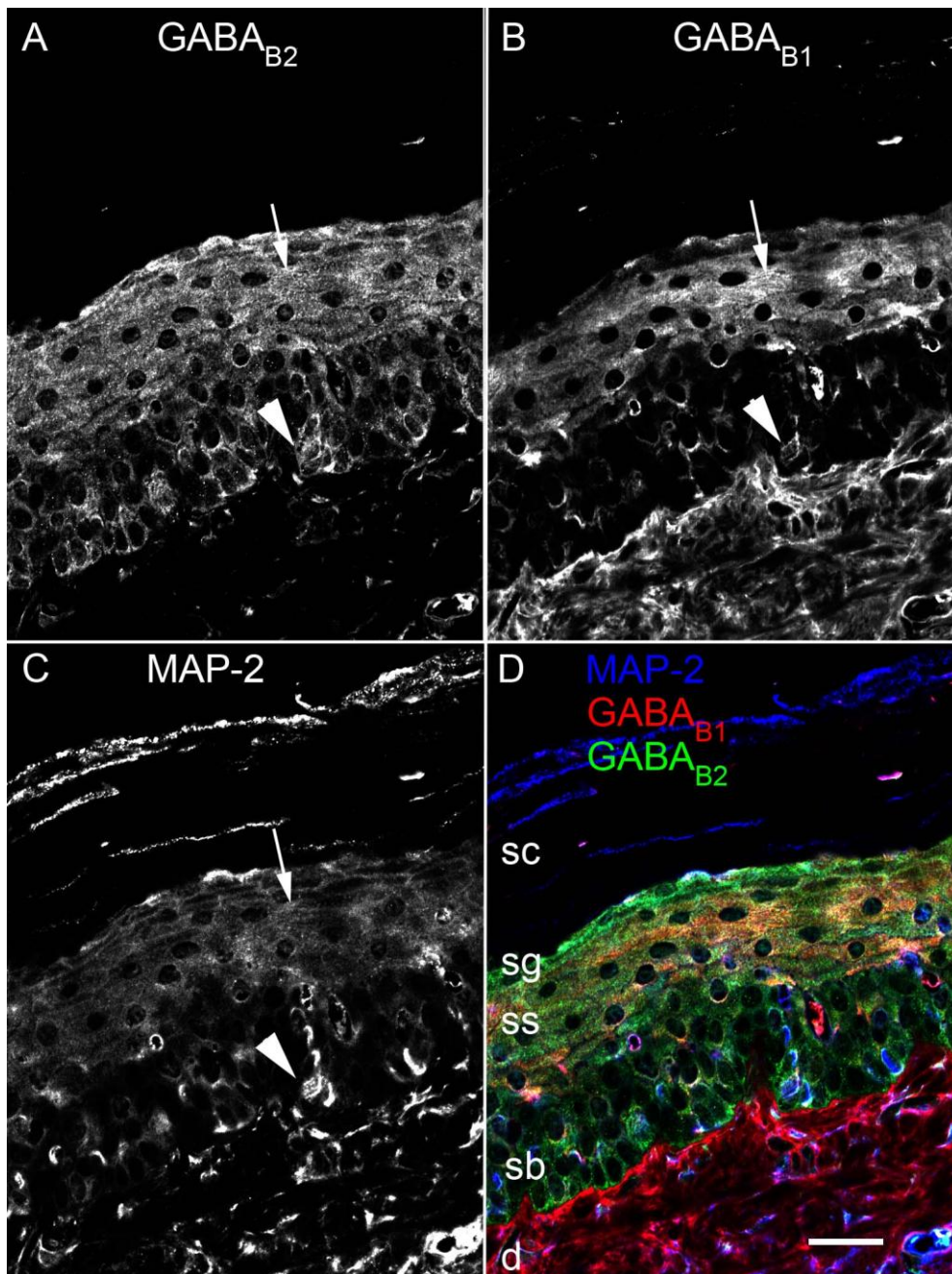


**Figure C.1. GABA<sub>B</sub> receptors are present in the epidermis of the mouse foot pad.**

(A, D) GABA<sub>B2</sub> and (B, D) GABA<sub>B1</sub> subunits are both expressed in cells of the stratum spinosum (ss) of the epidermis (arrows). Both GABA<sub>B</sub> subunits are also expressed in (C, D) MAP-2 positive neural processes of the stratum basale of the epidermis (sb;

arrowheads). Scale bar in (D) is 20  $\mu\text{m}$  and applies to all panels. sc = stratum corneum;  
sg = stratum granulosum; d = dermis.

## References

Reis and Duarte. 2006. Baclofen, an agonist at peripheral GABA<sub>B</sub> receptors, induces antinociception via activation of TEA-sensitive potassium channels. *Br J Pharmacol.* **149**(6):733-9.

**APPENDIX D: ANIMAL CARE CERTIFICATE**

<https://rise.ubc.ca/rise/Doc/0/NM99BB39GEEKRBLVM1CDN9V54...>



**THE UNIVERSITY OF BRITISH COLUMBIA**

**ANIMAL CARE CERTIFICATE**

<b>Application Number:</b> A06-0155			
<b>Investigator or Course Director:</b> <u>Ernest Pui</u>			
<b>Department:</b> Pharmacology & Therapeutics			
<b>Animals:</b>			
<table border="1"><tr><td>Rats SD 520</td></tr><tr><td>Mice CD-1 200</td></tr></table>		Rats SD 520	Mice CD-1 200
Rats SD 520			
Mice CD-1 200			
<b>Start Date:</b> July 16, 2003	<b>Approval Date:</b> July 27, 2007		
<b>Funding Sources:</b>			
<b>Funding Agency:</b>	Canadian Institutes of Health Research (CIHR)		
<b>Funding Title:</b>	Anesthetic actions on currents controlling neuron excitability: resolution using pharmacological and reactive current control approaches		
<b>Unfunded title:</b> N/A			

The Animal Care Committee has examined and approved the use of animals for the above experimental project.

This certificate is valid for one year from the above start or approval date (whichever is later) provided there is no change in the experimental procedures. Annual review is required by the CCAC and some granting agencies.

**A copy of this certificate must be displayed in your animal facility.**